

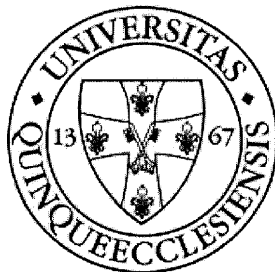
**Doctoral (PhD) dissertation**

**TECHNICAL PITFALLS OF HEART RATE  
VARIABILITY ANALYSIS**

**Laszlo Hejjel, MD**

**University of Pecs, Medical Faculty  
Heart Institute  
Department of Experimental Surgery**

**Program director and supervisor: Elizabeth Roth, MD, DSc**



**Pecs, 2005**

**Table of contents**

**Abbreviations.....4**

**1. Introduction.....5**

1.1. The brief history of HRV analysis.....5

1.2. Anatomical and physiological basis of HRV.....6

1.2.1. Anatomy.....6

1.2.2. The components of HRV.....7

1.2.3. The physiological role of HRV.....9

1.2.4. Behavior of HRV in physiological circumstances.....10

1.3. Clinical significance of HRV analysis.....12

1.3.1. Predicting disease outcome by HRV analysis.....13

1.3.2. Predicting the onset of arrhythmias by HRV changes.....16

1.4. Currently applied techniques, recommendations.....18

1.4.1. The ECG amplifier, analog filters.....18

1.4.2. The analog to digital conversion, interpolation.....19

1.4.3. Digital preprocessing of the ECG signal.....22

1.4.4. Making the heart rate tachogram.....23

1.4.5. Time domain analysis.....25

1.4.6. Frequency domain analysis.....26

1.4.7. Nonlinear analysis.....27

1.5. Current problems in HRV analysis.....29

**2. Objectives.....31**

2.1. Specific aims of the investigation.....31

**3. Methods.....33**

3.1. Computerized system for HRV analysis.....33

3.2. Precisional ECG signal generator and analyzer.....36

3.3. Analog filters.....38

3.4. Software for simulation and evaluation of the digitization error.....40

3.5. The effects of analog corner frequencies on RR-interval detection.....41

3.6. Testing the effects of AC notch filtering on RR-interval detection.....42

3.7. Effects of the sampling rate on the time domain parameters.....43

**4. Results.....44**

4.1. The effects of analog corner frequencies on RR-interval detection.....44

4.1.1. High pass filtering of uncorrupted signal.....44

4.1.2. Low pass filtering of uncorrupted signal.....44

4.1.3. Low pass filtering of AC interference corrupted signal.....44

4.1.4. Low pass filtering of Gaussian noise corrupted signal.....46

4.2. Testing the effects of AC notch filtering on RR-interval detection.....48

4.2.1. Notch filtering the uncorrupted record.....48

4.2.2. Notch filtering the AC interference corrupted record.....48

4.3. Effects of the sampling rate on the time domain parameters.....50

**5. Discussion.....55**

5.1. The effects of analog corner frequencies on RR-interval detection.....55

5.2. Testing the effects of AC notch filtering on RR-interval detection.....56

5.3. Effects of the sampling rate on the time domain parameters.....57

**6. Conclusions.....59**

**7. Novel findings.....59**

**8. References.....60**

**9. Appendix.....71**

**Publications of the author.....89**

**Acknowledgements.....91**

## Abbreviations

AC – alternating current, power line

CV% – coefficient of variation,  $CV\% = SDNN / \text{meanNN} * 100$

DFA – detrended fluctuation analysis

DMA – Direct Memory Access

ECG – electrocardiogram or electrocardiograph

FFT – fast Fourier transformation

HF – high frequency (0.15-0.4 Hz) component of variability

HRV – heart rate variability

LF – low frequency (0.04-0.15 Hz) component of variability

pNN50 – percentage of RR-interval differences greater than 50 ms

RAE – relative accuracy error,  $RAE = (X_{\text{meas}} - X_{\text{true}}) / X_{\text{true}}$

RMS, rms – root mean square

RMSSD – root mean square of successive RR-differences

RPE – relative precision error,  $RPE = SD / X_{\text{mean}}$

SD – standard deviation

SDANN – standard deviation of the averages of 5-minute segments

SDNN – standard deviation of normal-to-normal RR-intervals

SDNNI – SDNN index: mean of the standard deviations of 5-minute segments

SE – sampling error

SI – sampling interval

VLF – very low frequency (0.003-0.04 Hz) component of variability

ULF – ultra low frequency (<0.003 Hz) component of variability

VCD – ventricular complex duration (in ms)

# 1. Introduction

## 1.1. The brief history of heart rate variability analysis

Stephen Hales noted a relationship between the breathing cycles and the arterial blood pressure and interbeat intervals as early as in 1773. Hon and Lee observed that certain heart rate pattern changes were the sign of fetal distress (Hon and Lee 1965). However, quantitative measurements of this variability diffused in the era of the introduction of computerized ECG systems beginning at the early seventies. Automated detection of RR-intervals and their further processing allowed the analysis of longer ECG recordings. Sayers recognized the fluctuations of the heart rate at lower frequencies besides the respiratory arrhythmia by spectral analysis (Sayers 1973). Wolf et al demonstrated the prognostic role of reduced heart rate variability (HRV) in the one-minute ECG segments of 176 AMI-patients (Wolf et al 1978). Akselrod and co-workers revealed the action of the vegetative nervous system in the background of this phenomenon by parasympathetic and sympathetic blockade (Akselrod et al 1981). Nevertheless, it was the publication of Kleiger and colleagues that turned the attention of clinicians to HRV analysis: they proved the decreased HRV in 24-hour Holter tapes in 808 AMI-survivors as a strong predictor of long-term mortality (Kleiger et al 1987).

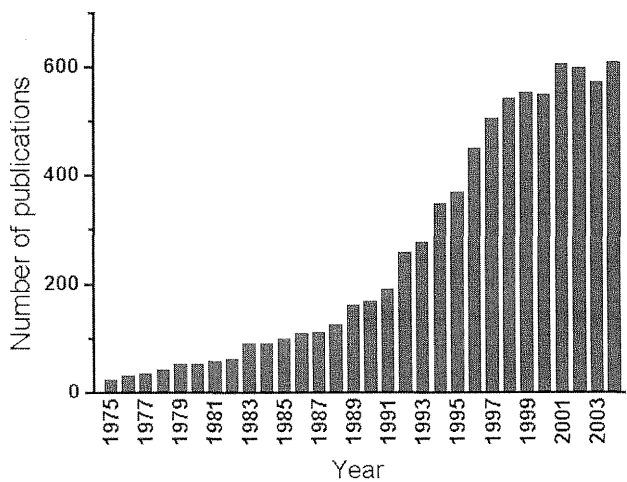


Fig 1.1. Exponentially growing annual number of publications between 1975-2004 found on the Entrez PubMed (<http://www.ncbi.nlm.nih.gov/entrez>) with the term 'heart rate variability'. In the recent years it seems to be saturated around 600/year.

A new and exponentially growing (*Fig. 1.1.*) discipline began to develop: the neurocardiology that investigates the neural control of cardiovascular regulation by statistical, spectral and nonlinear methods. (Appel et al 1989, Aubert and Ramaekers 1999, Berntson et al 1997, Mullen and Cohen 1996, Persson 1997)

## **1.2. Anatomical and physiological basis of HRV**

In physiological circumstances the sinus node controls the actual heart rate as a primary pacemaker. It has both sympathetic and parasympathetic innervations, and several autocrine, paracrine and endocrine effects act on it. The sinus node is the final summing element of sympathetic and parasympathetic stimuli therefore their instantaneous effects are reflected in the actual interbeat interval. The action of these factors show different time-constants which produces certain spectral bands in the beat-to-beat fluctuation (Malik and Camm 1993).

### **1.2.1. Anatomy**

Parasympathetic efferent nerve fibers come through the parasympathetic ganglia positioned in the periaortic and epicardial fat pad. The most part of the efferent vagal pathways to the atria and the sinus and atrioventricular nodes goes across the superior vena cava – aortic root or “third” fat pad in dog (Chiou et al 1997). Efferent sympathetic innervation arrives from superior, middle, and inferior cervical and the upper four or five thoracic ganglia. Medullary nuclei and reticular formation give both excitatory and inhibitory preganglionic efferent fibers as well as accept afferent fibers. Afferent pathways from baroreceptors and so-called cardiopulmonary receptors to the brain stem are closing the loop assuring a feedback mechanism. These baroreceptors are located in the wall of the aortic arch and great arteries arising from it, and in the carotid sinuses. The latter one is considered the most significant in mediating blood pressure changes due to human observations in acute bilateral denervation of carotid sinuses as a result of carotid body tumor extirpation even in long-term periods (Smit et al 2002). The hypothalamus is considered the most important supramedullary compound that integrates autonomic, somatic, mental and emotional information via its extensive associations (*Fig. 1.2.*). (Aubert and Ramaekers 1999, Waller and Schlant 1994)

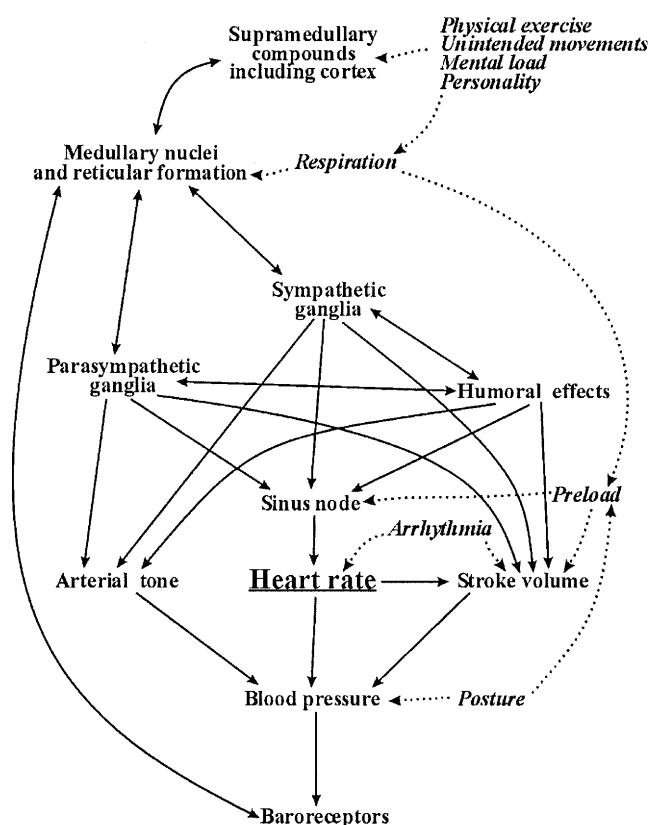


Fig 1.2. Functional block diagram of the control of systemic circulation.

### 1.2.2. The components of HRV

Spectral analysis gets an insight into the composition of HRV. According to several human and animal studies, two clear frequency bands mediated by the autonomic nervous system are present in instantaneous heart rate and blood pressure: a high frequency (HF, 0.15-0.4 Hz) and a low frequency (LF, 0.04-0.15 Hz) component. However, some groups define a third, midfrequency range (e.g.: 0.07-0.13 Hz, Lang et al 1991-1992) that is not generally accepted (in Persson 1997). The HF oscillation is associated to respiration and mediated exclusively by the vagal nerve; the sympathetic nervous system is too sluggish to modulate these HF oscillations (Task Force 1996, Berntson et al 1997). There is a significant central coupling element in the brain stem between respiratory and cardiac vagal neurons (Valentinuzzi and Geddes 1974, Hayano and Yasuma 2003) besides hemodynamic coupling related to preload alterations as a consequence of intrathoracic pressure changes during respiration (West and van Vliet 1983).

The LF part at about 0.1 Hz in human, 0.14 Hz in the dog, 0.3 Hz in the rabbit and 0.4 Hz in the rat, reflects the different conduction times between the receptors, the brain and the effectors due to the size of the organism (Malpas 2002). The origin of these slower oscillations is more obscure: sympathetic and vagal components are present according to chemical or physical denervation and autonomic stimulation studies (Aubert and Ramaekers 1999, Task Force 1996, Berntson et al 1997). There are two hypotheses on the origin of the LF oscillation: The central oscillator theory says that the periodic sympathetic outflow is intrinsically generated by the central nervous system and discharged by the baroreceptor input. In certain conditions the vasculature can have baroreflex-independent resonance at about 0.05 Hz in dog (Grasso et al 1995). The baroreflex feedback loop theory is more popular: the baroreflex takes part in the generation of the autonomic outflow to the sinus node and vasculature. (Malpas 2002)

Is the HRV a reliable measure of the autonomic balance? The amplitude of blood pressure variability not always correlates with the intensity of sympathetic tone reflecting a loose connection or ignored interferences. The endothelium releases the NO as a response to wall stress that dilates the vessel and decreases blood pressure. Considering the NO's half-life of about 6s, it can partially absorb the blood pressure pulsations between 0.1-0.5 Hz. Definitely even more factors or resonant loops can modulate the direct effects of the autonomic nervous system, therefore HRV is not a measure of autonomic balance but a reflection of the sophisticated cardiovascular regulation. Preserved components of HRV mean physiological vagal and sympathetic regulation. The presentation of diminished HRV is more conflicting. Nonetheless, altered HRV has been observed in a range of pathologies, additionally has been found prognostic to disease progression or survival. (Malik and Camm 1993, Malpas 2002)

In the spectrum of HRV there is a very low frequency (VLF) band between 0.04-0.003 Hz, and in long-term (24-hours) HRV analysis an ultra low frequency (ULF) range is identified below 0.003 Hz. Their origin and mechanism are unclear, probably humoral factors (e.g. rennin-angiotensin-aldosteron), vascular autorhythmicity and thermoregulatory cycles, etc. play role (Task Force 1996, Berntson et al 1997). The source of these frequency bands of variability also may be the nonharmonic (fractal) noise due to interaction of different oscillating control mechanisms (Persson 1997). Despite the most fraction of the variability is in the VLF and ULF band (*Fig. 1.3.*), and



it may have significant predictive value in some disease conditions, the HF and LF ranges are more exhaustively investigated (Bigger 1996, Malpas 2002, Persson 1997).

Additionally to neurohormonal actions, also the mechanical stretch of the sinus node (mechanoelectric feedback) can directly modify the instantaneous heart rate period (Horner et al 1996). Within the somewhat independently modulated atrioventricular conduction, a slight modification of sinus node activation also may be picked up (Heneghan et al 2001).

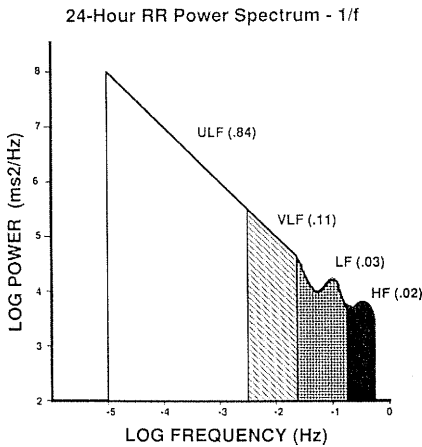


Fig. 1.3. The 24-hour power spectrum of RR-intervals in a double logarithmic scale. ULF-ultra low frequency, VLF-very low frequency, LF-low frequency, HF-high frequency band. The numbers in parentheses show the actual fraction of the given band relative to the total power. (from Bigger 1996)

### 1.2.3. The physiological role of HRV

The HRV and blood pressure fluctuations may be immaterial, as accidental consequences of the regulatory mechanisms. Reduction of midfrequency (0.07-0.13 Hz) peak by mental arithmetic task highly correlated in dizygotic but not monozygotic twins, suggesting a considerable genetic involvement in the control of HRV (Lang et al 1991-1992). According to the kibbutzim family study, the HRV properties are predetermined mainly by genetic and not by environmental factors (Sinnreich et al 1998). Cardiovascular oscillations are universal in the vertebrate as have been preserved during the evolution, suggesting a potential benefit in the natural selection. Though, the respiratory sinus arrhythmia is observed exclusively in mammals, some reptiles may have similar fluctuations related to breathing (Porges et al 2003). The complex systems need rhythmicity to be in working like the microprocessor needs the clock signal (like the

orchestra and the conductor). The respiratory sinus arrhythmia can save breathing and cardiac energy through matching alveolar blood flow to respiratory cycle (Hayano and Yasuma 2003). The nonlinear or chaotic behavior in the cardiovascular system has been known since 1981 (in Denton et al 1990). Chaotic vasomotion more rapidly dissipates transients than sinusoidal vasomotion, assuring greater stability of microvascular flow; and results in more homogenous perfusion (Parthimos et al 1996). Chaotic systems are inherently sensitive to perturbations, which allows large changes with relatively small energy expenditure, resulting in a flexible, dynamically stable system (Denton et al 1990, Goldberger 1999, Wagner and Persson 1998, Lipsitz 2004). Biologically variable extracorporeal circulation more effectively preserves cerebral oxygenation compared to conventional cardiopulmonary bypass as suggested by the better jugular venous oxygen saturation during rewarming (Mutch et al 2000). Biologically variable mechanical ventilation was found to be more effective in a pig model of acute respiratory distress syndrome according to the superior arterial oxygenation and IL-8 concentrations (Boker et al 2002). Diastolic function is better preserved with biologically variable administration of cardioplegia solution during extracorporeal circulation due to enhanced microvascular perfusion that results in more efficient cardioprotection (Graham et al 2002). Thus, cardiovascular variability is considered an advantageous phenomenon, consequently purposive, or at least coincident in the evolutionary process. With other words (from Appel et al 1989): “cardiovascular variability is a music rather than noise”.

#### **1.2.4. Behavior of HRV in physiological circumstances**

The behavior of HRV during certain maneuvers, activities or in different circumstances is widely investigated. Based on the arborescent relations of the neurovegetative regulatory system, countless environmental or intrinsic factors can affect the HRV; therefore each of their influences can be measured.

In 24-h HRV analysis the time domain and spectral indices are growing from childhood (<15 years) to young adulthood (<40 years) and then decline with senescence. Nonlinear measures show gradual reduction in complexity and fractal correlation properties from childhood. They found increased variability at night compared to daytime. The short-term heart rate dynamics of women is closer to 1/f

behavior in detrended fluctuation analysis (DFA); the other indices did not differ from men. (Pikkujämsä et al 1999) The loss of complexity makes the organism more susceptible to external and internal perturbations in seniors (Lipsitz 2004). In another study on healthy adults additionally to prove this trend, the linear regression equations were determined for several measures of 24-hours variability as a function of age (Ziegler et al 1999), e.g.:  $\log \text{RMSSD}(\text{ms}) = -0.008934 \times \text{age}(\text{years}) + 1.446294$  and  $\log \text{HF}(\text{ms}^2) = -0.015942 \times \text{age}(\text{years}) + 2.748431$ .

In a study on 653 patients without known heart disease, an inverse correlation of long-term HRV was proved with the mean heart rate and increasing age. Body mass index did not influence the HRV. Higher functional capacity (exercise tolerance) was coupled to lower heart rate and elevated variability (after normalizing to heart rate there was no difference in HRV). The HF, RMSSD and pNN50 were significantly greater in women, while LF, VLF and SDNNI were higher in men. The SDNN and SDANN did not diverge significantly. (Antelmi et al 2004)

Physical activity abruptly reduces the heart rate interval and short-term time and frequency domain HRV measures those gradually recover after exercise (Javorka et al 2002). Regular aerobic training after six months increased HRV in both young and older persons due to increased parasympathetic activity at rest. This may be an explanation of how the regular physical activity can reduce cardiovascular mortality (Levy et al 1998). In correlation with this study, the cessation of physical training after 4 weeks significantly reduced the maximum oxygen consumption and HRV parameters in young sailors (Hansen et al 2004). In healthy older (60-70 years) men the regular exercise may help to preserve cardiac autonomic regulation that otherwise declines with age (Ueno et al 2002). However, another investigation did not find any correlation of physical fitness and the autonomic cardiac regulation in healthy, young men (Reims et al 2004).

The metronome-breathing increases HF power reflecting elevated parasympathetic flow (Driscoll and DiCicco 2000). Total HRV increases during postural tilt in young but not in old subjects; however excluding the half of the young men who developed vasovagal syncope, there were no significant change in the spectrum. Elevated overall and low frequency variability in young individuals with bias towards syncope probably reflects increased sympathetic activity. (Lipsitz et al 1990)

Spontaneous movements also can increase the overall and LF fluctuations of cardiovascular dynamics (Fortrat et al 1999). Simple mental and verbal activities influence HRV via changes in the respiration rhythm (Bernardi et al 2000); however, mental arithmetic can significantly decrease HRV even with metronome breathing (Hejjel 1999). During mentally demanding computer task the decrease in the HF power and increase of the LF power of variability were influenced mainly by the physical activity (either keyboard or mouse) rather than the mental load (Garde et al 2002). The elevated mental strain of laparoscopic versus conventional surgeries also can be revealed in HRV changes (Böhm et al 2001, Hejjel and Gal 2002). On the other hand, the operative stress influences the autonomic regulation of the patient as well: the circadian variation is ceased after abdominal surgery (Gogenur et al 2002). Anxiety-like and fear-like states increase sympathetic and decrease parasympathetic nervous activity in rats, suggesting a link between psychological stress and cardiovascular disease formation (Inagaki et al 2004).

Particulate air pollution also alters the cardiac autonomic control by a short-acting and a long-acting mechanism via cytokines and the sympathetic stress response, as supposed (Magari et al 2001). Cigarette smoking acutely decreases HRV measures and baroreflex sensitivity in non-smokers (Halmai et al 2003). Half-hour exposures to 50 Hz weak electromagnetic field (20-30  $\mu$ T at the head, 150-200  $\mu$ T at the heart) also influenced the HRV indices in a human study (Tabor et al 2004), opening a new and promising field of research and perhaps therapy. This enumeration could be continued for several more pages...

### **1.3. Clinical significance of HRV analysis**

The number of clinical studies related to HRV analysis is gigantic similarly to physiological investigations, however, with less contradiction. In spite of the imperfect understanding of the fundamental physiopathology, the HRV analysis is increasingly applied in the clinical research for predicting disease progression or mortality, or forecasting the risk or the onset of arrhythmias. Clinical trials have been organized with the use of HRV measurements: the ESVEM (Electrophysiologic Study Versus Electrocardiographic Monitoring), the ATRAMI (Autonomic Tone and Reflexes After

Myocardial Infarction) and a branch of the ARIC (Atherosclerosis Risk in Communities) among others. Recently, depressed HRV and left ventricular function together were used for inclusion and risk stratification of patients participating in ALIVE (AzimiLide post Infarct surVival Evaluation) study (Camm et al 2004). In the not too far future, the real-time analysis of HRV indices may serve as a fine monitoring tool of cardiovascular regulation during surgical or other interventions (Bickel et al 2002, Christ et al 1997).

### 1.3.1. Predicting disease outcome by HRV analysis

*Acute myocardial infarction:* The prognostic role of the reduced 24-hour HRV (SDNN) on mortality after acute myocardial infarction was first published by Kleiger and colleagues based on a multicenter study including 808 patients (Kleiger et al 1987). They found a seriously reduced cumulative survival during the 4-year period in the group with SDNN below 50 ms in the Holter record made 11±3 days after AMI, while higher SDNN correlated with significantly better survival (*Fig. 1.4.*). The decreased HRV was recognized as an independent risk factor for long-term survival after AMI.

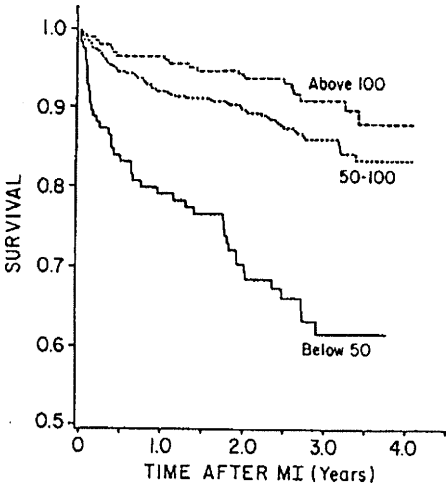


*Fig. 1.4. Cumulative survival rates after acute myocardial infarction stratified by the standard deviation of the RR-intervals from 24-h Holter recording on the 11±3 days after the acute myocardial infarction (from Kleiger et al 1987).*

As the SDNN may be corrupted by noise and artifact due to the unsatisfactory quality of long-term records, Malik and Camm (1991) developed a simple but robust arithmetic method based on a heart rate period histogram. The histogram is

approximated by a triangle, its height is given by the number of intervals in the highest bin (modal bin), therefore the base width or triangular index equals the total number of intervals divided by the modal RR-interval occurrence. The index brings clinically relevant information: the risk of sudden death or symptomatic sustained tachycardia was seven times greater in patients with an index below 25, compared to those with  $\geq 25$ .

Power spectral methods on short-term (2-15 min) records are also bright predictors – similarly to 24-hour studies – of all-cause mortality or sudden cardiac death after an AMI (Bigger et al 1993). ULF ( $< 0.0033$  Hz in this study) power seems to be the strongest predictor of mortality, however estimating this band needs longer records than 15 min. The analysis of short-term HRV together with signal averaged ECG was proved to be a flexible, effective and inexpensive method for risk assessment in coronary heart disease. (Reinhardt et al 1996) recognized the 24-hour time domain HRV and the presence of ventricular late potentials together as the strongest predictors of serious arrhythmias in the first six months following an AMI. Finnish publications (Mäkikallio et al 1999, Huikuri et al 2000) found nonlinear measures of HRV much more powerful predictors of mortality after AMI compared to conventional methods; however they are not popular and generally applied in clinical investigations. The combined use of parameters measuring autonomic imbalance (baroreflex sensitivity, SDNN, heart rate turbulence) can give excellent prediction of mortality in AMI-survivors at low risk (Ghuran et al 2002, from ATRAMI). The low HRV at the early stage of AMI improves during hospitalization period, the LF power was considered as an independent predictor of combined unfavorable short-term events after AMI (Carpeggiani et al 2004). Propranolol therapy versus placebo helps the recovery of HRV after AMI, increases parasympathetic and decreases sympathetic tone, which may explain the mechanism how the beta-blockers improve survival after AMI (Lampert et al 2003). The distribution of low-frequency spectral power (prevalent low-frequency oscillation) is a strong and independent predictor of mortality after AMI (Wichterle et al 2004).

*Coronary heart disease:* The reduced HRV in 2-minute segments of ECG is associated with elevated risk of coronary heart disease and all-cause mortality, additionally, low HRV was hypothesized as a marker of less favorable health (ARIC study, Dekker et al 2000).

*Arrhythmia risk stratification:* Depressed baroreflex sensitivity and HRV can identify patients at risk of malignant arrhythmia or arrhythmic death based on the analysis of 1071 ATRAMI participants (La Rovere et al 2001). The sensitivity of low baroreflex sensitivity was superior to HRV analysis or the presence of non-sustained ventricular tachycardia. However, HRV was not useful for arrhythmia risk stratification in the Marburg Cardiomyopathy Study (Grimm et al 2003).

*Heart failure, dilated cardiomyopathy:* The Poincaré plots of patients with heart failure show different morphology compared to healthy comet-shaped patterns reflecting an altered complexity of HRV (Woo et al 1992). The triangular index (see in 1.4.5.) of the heart rate interval histogram of 24-hour ECG recording correlated with left ventricular ejection fraction and the cardiovascular death or the need for heart transplantation based on a study of 64 patients with congestive heart failure (Wijbenga et al 1998). In postischemic left ventricular dysfunction the HRV is reduced both in symptomatic and symptom-free patients suggested by frequency domain analysis (Scalvini et al 1998). Reduced short-term LF power during controlled respiration (12-15 breath/min) is considered an influential predictor of sudden death in patients with chronic heart failure (La Rovere et al 2003), however, in the above mentioned Marburg Cardiomyopathy Study the HRV was not relevant in risk stratification (Grimm et al 2003).

*Hypertension:* In the ARIC trial the risk of developing hypertension is inversely correlated with the HF power, LF/HF ratio and the SDNN, supposing the importance of autonomic imbalance in the pathogenesis of essential hypertension (Liao et al 1996). Muiesan and coworkers investigated the low frequency peak centered at 0.1 Hz. In normotensives and hypertensives without left ventricular hypertrophy a daytime to nighttime decrease was proved, while hypertensives with left ventricular hypertrophy showed no change of this band. The low-frequency peak was found significantly higher in this latter group, but the reduction of the hypertrophy was associated with the restoration of the low frequency power spectral density and the circadian variation (Muiesan et al 1998). In contrast to the amlodipine, the verapamil significantly increased both time and frequency domain measures of HRV in 24-hour Holter recordings of hypertensive patients, suggesting a supplementary beneficial effect besides decreasing blood pressure (Sahin et al 2004). Ruediger et al (2004) found

significant differences in spectral components of HRV in normal and hypertensive subjects during mental load.

*Multiple metabolic syndrome:* Patients with hypertension, type 2 diabetes and dyslipidemia were included in the study (Liao et al 1998). Adversely affected autonomic regulation of heart rate was recognized by reduced variability that may contribute to the elevated risk of mortality in these patients.

HRV analysis may have prognostic role in several other cardiac and noncardiac diseases. The normalization of the reduced HRV may be a new therapeutic target in the not too distant future (Dekker et al 2000, Lampert et al 2003).

**1.3.2. Predicting the onset of arrhythmias by HRV changes**

Implantable cardioverter defibrillators store the RR-intervals - among other parameters or events - from the intracavitary ECG that can be retrieved from its memory with the programmer. It gives a good chance to investigate the heart rate dynamics right before the onset of the arrhythmic event (*Fig. 1.5.*). Ventricular tachyarrhythmias are preceded by significant reduction of HRV, both HF and LF band, suggesting vagal withdrawal and increased sympathoexcitation (Pruvot et al 2000).

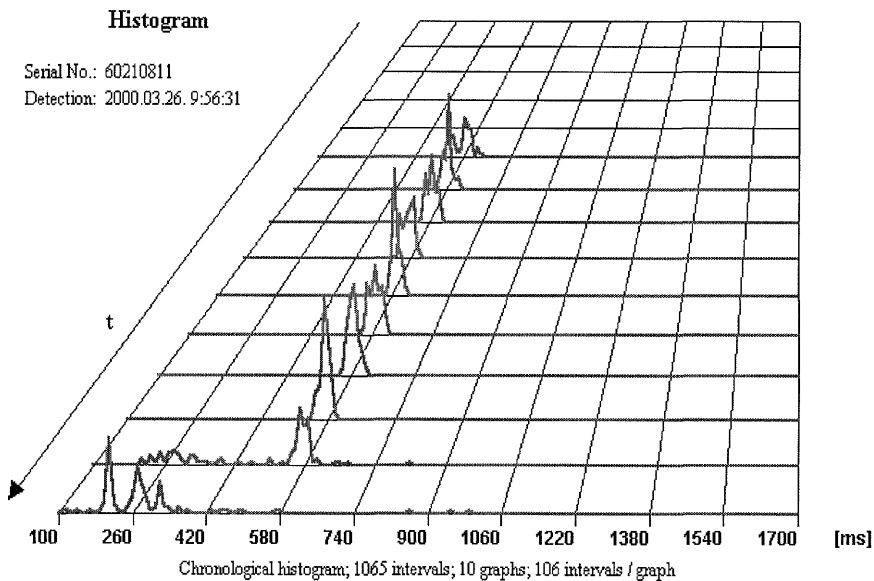


*Fig. 1.5. The chronological histogram before the onset of ventricular tachyarrhythmia as retrieved from the memory of an implantable cardioverter defibrillator. The gradual narrowing (peaking) of the histograms in time (from back to front) represents the reduction of HRV which precedes the occurrence of ventricular premature beats (9<sup>th</sup> histogram) and ventricular tachycardia (last histogram, front). (Thanks to Biotronik Hungary)*



According to long-term Holter observations the reduced HRV is a risk factor for ventricular tachyarrhythmia, during the 1-hour period before the onset of ventricular tachyarrhythmia increased instantaneous RR-interval variability (sinus alternans) appeared as a result of altered vegetative balance that causes electrical instability in the myocardium (Huikuri et al 1996).

In human Holter study the occurrence of paroxysmal atrial fibrillation coincides with autonomic tone variations: a primary increase in sympathetic tone and concomitant abrupt shift toward parasympathetic dominance (Bettoni and Zimmermann 2002). A newer investigation proved that vegetative nervous system acts both in the initiation and termination of the paroxysmal atrial fibrillation, and also the period of the day can influence the LF and HF component changes before and after the atrial fibrillation (Tomita et al 2003). Lombardi and coworkers found that a sympathetic predominance preceded the onset of atrial fibrillation in the majority of the enrolled patients with paroxysmal atrial fibrillation; while in about 30% of enrollees vagal preponderance was observed (Lombardi et al 2004). In patients after non-cardiac thoracic surgery, the postoperative atrial fibrillation was preluded by significant rise in heart rate, both time and frequency domain HRV measures, meaning a sympathetic predominance and consecutive increase in vagal activity (Amar et al 2003). The altered cardiovascular regulation (increased LF band) due to positive pressure pneumoperitoneum during laparoscopic operations may predispose patients with cardiac disease to developing dysrhythmias besides the negative hemodynamic effects of elevated intraabdominal pressure (Bickel et al 2001). After CABG surgery, the decreased complexity measured by approximate entropy in the hour before the onset may predict postoperative atrial fibrillation (Hogue et al 1998). There was no any correlation with traditional measures of HRV. However, CABG patients at risk of postoperative atrial fibrillation can not be identified by preoperative short-term HRV analysis (Hakala et al 2002).

A new research idea: Could the imminent supraventricular or ventricular tachyarrhythmia be prevented by restoring the heart rate dynamics through an intervention into the cardiovascular control loop with a special pacemaker (e.g.: chaotic stimulation – “rechaotization”)?

#### **1.4. Currently applied techniques, recommendations**

The dynamics of the physiological parameters has been ignored for a long time (and typically are overlooked today as well): the heart rate, blood pressure, etc. were evaluated on the spot or in the better case some measurements averaged; or else typical patterns on a short segment of ECG (ischemia, bundle branch block, etc.) or on other graphical representations of the organism's activity were searched (Gleick 1988). All the information borne in the dynamics of their fluctuation was lost. The analysis of long-term ECG in the clinical setting was started when N. J. Holter introduced a radiotelemetric system (1957) designed for recording ECG in active patients. It was surpassed quickly by analog tape-based recorders and later by digital systems those are capable of storing large amount of data and automatic evaluation of the record. The analytic systems also have developed parallel: reliably identify ventricular and supraventricular dysrhythmias, ischemic changes, measure the conventional average parameters of the electric heart cycle. Most of the modern Holter analytic systems include the HRV analysis panel as well. However, the hardware and the digitization interval remained 100-250 Hz that is adequate for rhythm pattern and ischemic event study but may not be sufficient for heart rate dynamics analysis. (in Lombardi 1996, Kennedy 1996, ) To understand the music of the cardiovascular fluctuations, a properly tuned mathematical ear is needed (Appel et al 1989), including also the instrumentation for this measurement.

There are exhaustive recommendations with conditions fulfilled by just the diagnostic equipments (Task Force 1996, Berntson et al 1997, Aubert and Ramaekers 1999, see later); however they are not capable of recording and printing for some 10 seconds or a few minutes. Usually, specially designed equipments are used for short-term (five-minutes as standardized [Task Force 1996]) assessments and commercially available, often ineligible Holter recorders for long-term (24-hours [Task Force 1996]) analysis. Here is a review of currently effective recommendations and applied practice sorted due to the phases of the ECG signal processing.

##### **1.4.1. The ECG amplifier, analog filters**

The ECG signal is a biopotential in the level of 1mV, usually corrupted by high magnitude interference and noise. The selective amplification of the biosignal and rejection of the noise/interference without the influence of the physiological process, are

featured by biopotential amplifiers considering surge protection both of the patient and equipment (Nagel JH 2000). For diagnostic applications a 0.05-200 Hz bandwidth is recommended (Pipberger et al 1975), whereas 0.05-100 Hz for Holter monitors to correctly detect ST-movements, dysrhythmias and morphology changes in the main waves (Bailey et al 1990). The ECG amplifier and its frequency pass band are usually ignored by most papers on HRV analysis (e.g. Aubert and Ramaekers 1999), or stepped over (Berntson et al 1997) by citing old papers from the 70's or 80's, when the accurate evaluation of instantaneous heart rate was not a requisite. The latest Task Force of the European Society of Cardiology and the North American Society of Pacing and Electrophysiology recommends about 200 Hz upper corner frequency without any reference (Task Force 1996); however it is rarely accomplished and mentioned in the publications (a scarce exception: Ziegler et al 1999). Obiter dictum, in the latest reference the applied upper cutoff at 200 Hz is not appropriate for the same 200 Hz sampling frequency per channel according to the Nyquist's law (see in 1.4.2.); actually the real corner frequency of the digitized signal was 100 Hz due to the low rate of analog to digital conversion. On the other hand, 1 ms accuracy heart rate detection can be obtainable at 0.5-35 Hz analog band pass (Ruha et al 1997).

Nowadays, the digital filters are much more popular, in relation to their better performance, but the digitization needs antialiasing filters on the analog side in either way (Bianchi et al 1996, Smith 1999). As a new trend, the high-pass filters used to remove DC or slow components – often in the range of 1V at the input, therefore suppressing the useful signal or saturating the amplifier or the analog to digital converter – are replaced by digital offset subtraction and filtering simplifying the analog front end. However, this needs high-resolution digitization at 19-22 bits. (Carr and Brown 2000)

#### **1.4.2. The analog to digital conversion, interpolation**

The most signals in our macroenvironment are continuous (analog) both in magnitude and time course. However, modern computers can not directly interact with these signals, as the computers' digital operation is discrete. The computers need interpretation: analog-to-digital conversion (digitization) and digital-to-analog conversion. The digitization means discretization both in time (sampling) and amplitude

(quantization), consequently, information is lost during the procedure. The adequate choice of the analog filters, sampling frequency and resolution of quantization preserves the valuable information without attenuating our measurements. (Smith 1999) Similarly to the quantization error, the sampling error (SE) is a uniformly distributed random series in the range of  $-0.5 \cdot SI \leq SE \leq 0.5 \cdot SI$ , where the SI represents the sampling interval (Merri et al 1990). Considering this, the written  $\pm 5$  ms accuracy at 200 Hz sampling is not correct in (Ziegler et al 1999).

According to the Nyquist or Shannon sampling theorem, the sampling frequency must be at least twice the highest frequency of interest in the analog signal. Higher spectral components than the half of the sampling frequency can change their frequency during sampling and can not be reconstructed correctly anymore. The phenomenon is called aliasing: these frequencies appear at lower frequencies in the digital signal, “they change identity”. Therefore analog low pass filters (antialiasing filters) must be used with appropriate corner frequency preceding digitization (Bianchi et al 1996, Smith 1999). Usually Bessel, Butterworth or Chebishev filters are applied depending on the required transfer characteristics (Smith 1999).

The Task Force (1996) recommends a sampling frequency of 250-500 Hz, while advises (parabolic) interpolation at lower rates. Another review (Berntson et al 1997) proposes 500-1000 Hz digitization rate, emphasizing that the 128 Hz digitization rate provided by various Holter monitors is not optimal and suggests interpolation or template matching algorithms in order to improve the temporal accuracy at digitization rates below 250 Hz. Aubert and Ramaekers counsels 250-1000 Hz sampling rate (Aubert and Ramaekers 1999). However, these requirements are often disregarded as seen in *Table 1.1.*, or the sampling frequency is often ignored in the publication. Sampling at 500 Hz with concomitant linear interpolation to 2 kHz and applying matched filtering may provide sufficient timing accuracy of 1 ms as a result of careful analysis by Ruha et al (1997).

There are relatively few articles on the investigation of the optimal sampling rate; those are cited by the above mentioned reviews as well. Barr and Spach (1977) recommended 1500 Hz sampling rate for body surface ECG as early as in 1977.

<b>First author and publication year</b>	<b>Sampling frequency (Hz)</b>	<b>First author and publication year</b>	<b>Sampling frequency (Hz)</b>
Amar 2003	128	Huikuri 2000	128
Antelmi 2004	125	Javorka 2002	1000
Bernardi 2000	250	Kuo 1999	200
Böhm 2001	400	Levy 1998	125
Camman 2002	250	Liao 1998	1000
Carpeggiani 2004	250	Pikkujämsä 1999	256
Christ 1997	128	Pruvot 2000	128
Driscoll 2000	100	Ramaekers 1998	200
Fortrat 1999	1000	Scalvini 1998	1000
Garde 2002	1024	Ziegler 1999	200
Halmi 2003	500		

*Table 1.1. The applied sampling frequencies (Hz) per channel in recent HRV studies listed in alphabetical order by the first author and publication year (as in the References).*

Merri and colleagues (Merri et al 1990) mathematically analyzed the correspondence of the sampling frequency and the error of spectral analysis of HRV, and suggested to compare the magnitude of error power spectra and the HRV, particularly at lower sampling rates. Pinna and coworkers (Pinna et al 1994) evaluated several tape-based and solid state Holter systems, and concluded that there is a significant and unpredictable inter- and intradevice dispersion in spectral parameters, especially in tape-based systems. This error could be improved by higher (250-500 Hz or even more) temporal resolution of digitization. The paper of Riniolo and Porges (1997) suggests rapid sampling rates (1 kHz) and accurate R-wave peak detectors to describe even the smallest oscillations in the heart rate. The article from Friesen et al (1990) is cited by two of above methodical reviews in relation to the accuracy of QRS fiducial point detection, whereas that examined solely the correct recognition of the ventricular complexes by nine QRS detection algorithms, but not their timing accuracy. According to Laguna and Sörnmo's theoretical analysis, a sampling rate of approximately 3 kHz is necessary for accurate ensemble variability measurements of

noise corrupted signals, which was confirmed also by their simulational study based on human ECG database (Laguna and Sörnmo 2000). A newer investigation (Garcia-Gonzalez et al 2004) described theoretically the bias and uncertainty of spectral indices and then computed them via simulation on normal RR-interval recordings from database. The sampling at 125 Hz results in unreliable measures of spectral indices, especially at low-variability signals. The uncertainty is proportional to the inverse of sampling frequency, while the bias is proportional to the inverse of the squared sampling frequency; therefore a higher sampling rate is needed without interpolation.

The time resolution can be enhanced by interpolation or template matching at the fiducial point detection. The cubic interpolation can improve the time-resolution to 1 ms at sampling rates down to 100 Hz (Daskalov and Christov 1997). On the contrary, data compression can introduce further errors in the reconstruction of the digitized signal (Bianchi et al 1996).

A special mathematical process (Barros and Ohnishi 2001) can allow sampling frequency as low as 5 Hz, and it can extract reliable (relative error around 0.03) measures of HRV in the frequency domain without R-wave detection; additionally, the method is exceptionally resistant to white noise. The drawbacks of the method are 1) the lack of visualization of the entire ECG record to allow manual check, and 2) time domain or nonlinear parameters are not available.

#### **1.4.3. Digital preprocessing of the ECG signal**

Digital filtering means a determined mathematical transformation of the digital signal in order to augment/depress some wanted/disturbing characteristics. There is no sharp separation of digital filtering and wave recognition since they are strongly interlaced. The conventional filtering hypothesizes that these wanted (signal) and unwanted (noise) components aligns at different frequency bands, however this is rarely the case as considerable overlapping persists between the ECG signal and power line interference or respiration and motion artifacts (Christov and Daskalov 1999). Therefore the simple band pass, low pass or high pass can not separate them perfectly; instead it may significantly distort the ECG morphology. The AC interference at 50/60 Hz can be removed effectively with notch (band reject) filtering, considering its narrow frequency

band as the harmonics are very small in amplitude (Friesen et al 1990). However, there is no available literature on the action of notch filtering on the accuracy and precision on RR-interval detection. (Bianchi et al 1996, Smith 1999)

Alternative signal processing procedures can be used in separating signal and noise supposing their different statistical properties, their interactions, or other characteristics (Bianchi et al 1996). Moving average filters are simple devices to reduce the random noise (Smith 1999). They operate by averaging a number of adjacent points of the input signal to produce the points of the output signal with improved signal to noise ratio proportional to the square root of the number of averaged points. When the relation of the noise and the signal is nonstationary, adaptive filtering may be applied (Bianchi et al 1996). To preserve the ventricular complex morphology, differential high pass filtering of the ECG was suggested, meaning a different cutoff frequency at different waves of the ECG (Christov et al 1992).

The ubiquitous power line interference is efficiently reduced by a digital subtraction method without adaptation period in any electrical signal by (Dotsinsky and Daskalov 1996, Christov 2000). Combining this method of 50 Hz subtraction and smoothing according to Savitzky-Golay preserved the ECG morphology in QRS boundaries detection by measuring the curvature of the ECG signal (Daskalov and Christov 1999). Further and more sophisticated and reliable processes are assessed in AC interference reduction: nonlinear adaptive filtering (Ziarani and Konrad 2002) or multiscale cross-correlation method (Laciar et al 2003). Electromyogram artifacts may be removed effectively and without significant distortion of the QRS waves by adaptive approximation filtering (Christov and Daskalov 1999).

In spite of efficient filtering techniques, the noise never could be eliminated perfectly without affecting the ECG morphology and potentially the RR-interval timing accuracy, therefore caution must be taken during data acquisition to minimize noise and interference.

#### **1.4.4. Making the heart rate tachogram**

The sequence of the consecutive RR-differences as a function of their serial number is called the tachogram. Therefore, the tachogram is not an evenly sampled series (as the heart rate is not perfectly constant). The first step in generating tachogram

is to detect ventricular complexes and localize stable, constant points in them (fiducial point); the second step is to measure the distance of the consecutive fiducial points.

The recognition of the ventricular complex may occur by (a) structural feature methods (simple threshold, adaptive threshold, first derivative, first derivative + threshold, first and second derivative, digital filters, dual edge detection), (b) contour limiting (or template matching) method, (c) syntactic methods: decomposing the signal to subpatterns and rules, (d) other methods, e.g.: neural networks, etc. Usually the combinations of above methods are applied in commercial ECGs. (Bianchi et al 1996, Friesen et al 1990, Ruha et al 1997). It is important to note that not only the fact of correct ventricular complex recognition, but its accurate timing is of interest in HRV analysis. Template matching methods by interpolation can improve the temporal resolution of inferior quality ECG records due to low sampling frequency; parabolic fitting on the R-wave additionally reduces the effect of the noise on the timing accuracy (Berntson et al 1997).

In spite of the difficult ventricular complex detector algorithms, technical (noises), extracardial (motion artifact, electromyography), or intracardial (premature or missed beats, atypical ECG morphology) artifacts may corrupt the tachogram and consequently HRV indices. Sinus beats usually do not occur out of the interval of about  $\pm 20\%$  of the preceding RR-interval, which assures a possibility of automated filtering. The visual check of the labeled ECG record is recommended anyway in order to verify that exclusively normal sinus beats are enrolled for further analysis (Task Force 1996, Berntson et al 1997). A premature or spuriously detected beat may be simply deleted from the tachogram, however, the extraneous beat may cause a disturbance in the cardiovascular regulation, see heart rate turbulence measures (Schmidt et al 1999), therefore some authors cancels the preceding and 1-3 of the following beats. In the case of missed beats, the options are: (a) measure manually the actual RR-interval if possible, (b) interpolating the missing ventricular complex from neighboring beats, (c) splitting the spuriously long interval to two or more equal intervals, (d) cancel the enormously long RR-interval. Alternatively, the analysis may be limited to segments with normal sinus rhythm and free of any arrhythmias. (Aubert and Ramaekers 1999, Berntson et al 1997, Task Force 1996) A single artifact may be associated with a deviation of the magnitude of the HRV itself or may exceed the variances during



psychophysiological studies in both the time and frequency domain (Berntson and Stowell 1998). The use of simple analog triggering devices needs careful evaluation as they may have considerable number of mistaken RR-intervals and there is no possibility for visual check and manual editing.

#### **1.4.5. Time domain analysis**

Time domain indices are the simplest measures expressing quantitatively the fluctuations of cardiovascular dynamics. This group represents the composition of the tachogram with no regard on the sequence of its elements; therefore these methods are called also statistical techniques. The units of time domain indices are time: s or ms. In the era preceding the automated HRV analysis, the quotient or difference of the shortest and longest RR-interval on a short segment of ECG was used. The spreading of computer-based investigation gave the possibility of recording longer periods of ECG and calculating other statistical parameters. The SDNN represents the standard deviation of normal-to-normal RR-intervals. In long-term records the calculation of the standard deviation of the 5-minute mean RR-interval (SDANN – standard deviation of averaged normal-to normal intervals) or the mean of the standard deviations of 5-minute segments (SDNNI – SDNN index:) may be applied. SDANN measures the variability of cycles longer than 5 minutes, while the SDNNI evaluates the variability of cycles shorter than 5 minutes. The SDNN may be corrected to the mean heart rate interval, resulting in the coefficient of variation:  $CV\% = \frac{SDNN}{\text{mean}} \times 100$ . The RMSSD (root mean square of successive RR-differences) reflects the beat-to-beat (high frequency) variability as it is the square root of the mean of squared differences of neighboring RR-intervals. The pNN50 is the percentage of the successive interval differences above 50 ms. The statistical measures are sensitive to erroneous RR-intervals, especially those reflecting beat-to-beat variability. Geometric methods were introduced to get robust indices of HRV (Cripps et al 1991). They are based on the heart rate interval histogram with conventionally  $1/128 \text{ s} = 7.8125 \text{ ms}$  bins according to the sampling rate (temporal resolution) of older Holter monitors. Modeling the histogram by a triangle, its baseline width can be equal to the quotient of its doubled area and its height. Its height equals to the count in the modal (=highest) bin and the area can be estimated by the total amount of NN-intervals. Thus, the triangular index (TI) can be obtained by the quotient of the

total and modal number of NN-intervals. The triangular interpolation (TINN) equals the baseline-width of a triangle given by its apex as the top of the modal bin and the two sides approximating the two slopes of the histogram by linear regression. The top angle index (TAI) represents the angle in the opposite of the baseline of the fitted triangle in grades. The geometric methods are rarely applied now, probably because they need at least a 20-minute-long record that is too long period for short term analysis regarded to stationarity. The Poincaré plot is discussed in 1.4.7., considering its nonlinear characteristics. (Aubert and Ramaekers 1999, Malik 1996, Task Force 1996, Berntson et al 1997, Ziegler et al 1999)

Due to the physiologic fluctuations at several cycle durations, the values of the time domain indices depend on the length of the tachogram, therefore standard recording times are necessary. The preferred durations are 5 minutes for short- and 24 hours for long-term analysis (Malik 1996, Task Force 1996).

#### **1.4.6. Frequency domain analysis**

Frequency domain analysis decomposes the fluctuating but supposedly stationary time-dependent signal into its spectral constituents, showing the relative [normalized unit –NU,  $HF_{NU} = HF/(HF+LF)$ ,  $LF_{NU} = LF/(HF+LF)$ ] or absolute ( $ms^2/Hz$ ) contributions of certain frequencies to the total variance, or in simple terms: plotting the variance as a function of frequency. Mathematically two main processes are available for spectral analysis: Fast Fourier Transformation (FFT) and autoregressive modeling. The more common FFT requires data series consisting of equidistant points as a function of time; therefore the irregularly time-sampled tachogram must be resampled at a fixed interval of 250-330 ms. In order to avoid the aliasing phenomenon, consecutive low-pass digital filtering is suggested below the half value of the resampling frequency before performing FFT. Removing the ‘DC-component’ of the tachogram is possible by subtracting the mean RR-interval duration, or by subtracting the linear or polynomial trend. Windowing of the resampled tachogram is recommended to prevent the generation of harmonic artifacts resulting from the finite-length tachograms. On the spectral distribution chart of short-term heart rate tachograms high- (HF: 0.4-0.15 Hz), low- (LF: 0.15-0.04 Hz) and very low- (VLF: < 0.04 Hz) frequency bands are distinguished. In the long-term analysis a fourth ultra low frequency band (ULF: <0.003

Hz) is separated, see *Fig. 1.3*. The physiological basis of the above bands is discussed in 1.2.2. Autoregressive modeling by fitting linear predictive models, gives the same, but visually smoother spectra, without the need for resampling the tachogram. The FFT method is much more sensitive to noises. (Bigger 1996, Aubert and Ramaekers 1999, Malik 1996, Task Force 1996, Berntson et al 1997, Persson 1997, Ziegler et al 1999) The trigonometric regressive spectral analysis is free of the need of interpolation of nonequidistant RR-intervals, aliasing, equal length of compared tachograms, and insufficient frequency resolution (Ruediger et al 1999).

The considerable overlapping of the spectral bands due to the interindividual differences in breathing patterns and its coupling to heart rate necessitates the consideration of the mean RR-interval, respiratory rate and tidal volume (Camman and Michel 2002).

The slope of the regression line on the log spectral amplitude against the log frequency (see *Fig. 1.3.*) gives the scaling exponent  $x$  in the  $1/f^x$  plot, which characterizes the contribution of certain frequencies to the overall variability (Lipsitz et al 1990). This exponent opens toward nonlinear (fractal) analysis.

#### **1.4.7. Nonlinear analysis**

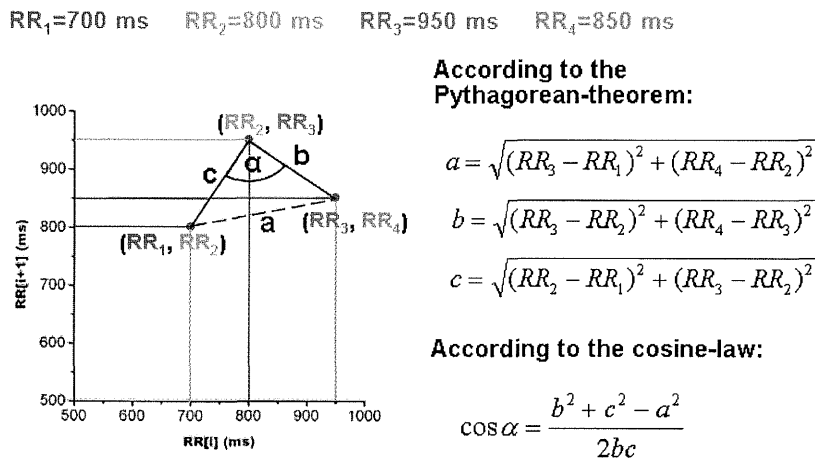
Most of nonlinear methods are still under investigation in spite of some encouraging studies (Christ et al 1997, Pikkujämsä et al 1999, Mäkikallio et al 1999, Voss et al 1995, Huikuri et al 2003).

The Poincaré plot (also return map or Lorentz plot) where the  $(i+1)$ th RR-interval is plotted against the  $(i)$ th RR-interval in Cartesian coordinates consists of a map of dots. Its shape and expansion can be assessed visually. The lesser is the area the smaller is the variability, and on the contrary, greater area corresponds to higher variability. There are three distinct pathological patterns differentiated besides the normal comet-shaped: torpedo-shaped, fan-shaped and complex patterns (Woo et al 1992). The long axis of the plot fits on the unitary slope line passing through the origin, whereas the short axis is perpendicular to that. They cross each other in the center point, which is located at the coordinates of the mean RR-duration. Quantitative analysis can be performed by the calculation of the standard deviation of data points in the direction of the long (SD-LA) or short (SD-SA) axis, the length of both axes equals to the related

standard deviation. The first one represents the short-term, while the last one shows the long-term variability. The return map is originally a non-linear aspect, however, the above mentioned inherited parameters are insensitive to the non-linear characteristics, and practically they are equivalent with the popular time domain methods as has recently been proved by (Brennan et al 2001):

$$SD - SA^2 = \frac{1}{2}RMSSD^2 \text{ and } SD - LA^2 = SDNN^2 - \frac{1}{2}RMSSD^2$$

The angles formed by three consecutive points (see Fig. 1.6.) in an overlapping sliding manner on the map may characterize nonlinear properties; at least these angles are irrespective of the standard deviation and mean heart rate (Hejjel 2002). The mean, standard deviation or the histogram of these angles may be the base of a new index of HRV, however further investigation is needed.



**Alpha independent of the mean and SD of the RR-sequence (similar Δ).**

Fig. 1.6. The calculation of the angle given by three consecutive points on the return map, from the presentation of Hejjel (2002) at the 4th International Congress of Pathophysiology.

Other nonlinear processes are not popular in the clinical or basic medical investigations because their abstract and sophisticated computation, presentation and understanding, although they can give additional information on HRV, therefore they are expected in the arsenal of biomedical sciences. A list of them: fractal dimension, detrended fluctuation analysis, Lyapunov exponents, correlation dimension, and approximate entropy.

### 1.5. Current problems in HRV analysis

As we learned from the 1.2.4. chapter, several concurring biological factors (spontaneous movements, verbalization, breathing rhythm, fitness, etc.) may influence the autonomic nervous system, therefore the indices of HRV. For valid measurements they must be excluded or standardized as much as possible. Special “stress tests” would be composed with reproducible stages or grades considering both physical and mental load, while measuring and comparing (short-term) HRV during the study. The standardization of circumstances in long-term (24-48-h) studies is even more difficult. The second problem is the stationarity (constant mean and variance) of the signal during the measurement. The solution may be the fragmentation of the observation interval into short (presumably stationary) segments of some minutes those are analyzed separately, and/or removing slow nonstationary components by linear or polynomial models (Berntson et al 1997). The third issue is the presentation: several authors misinterpret the results they measured, e.g.: the LF component is thought the measure of purely the sympathetic effects (Garde et al 2002, Bickel et al 2002, Kong et al 2004), however this has been disproved by numerous studies. The HRV is not a measure of autonomic balance but a reflection of the sophisticated cardiovascular regulation. Careful evaluation of the results and their explanation are needed until we do not know more about the underlying physiopathology.

The statistical methods are ideal for random series, the spectral procedures are optimal for periodic and infinite long sequences, whereas the heart rate tachogram shows neither random nor periodic but nonlinear (chaotic) properties (*Fig. 1.7.*). Substantial information on HRV may remain hidden applying the conventional methods (Goldberger 1999). New robust parameters are asked, those inherently characterize nonlinear trait, are easy to be computed and understood in the clinical practice as well.

Cautious revision and consideration of all-inclusive standards of measurement are required as appears from 1.4.1–1.4.7. The effects of intrinsic, environmental and technical interferences or noises must be reappraised in the relation of the accuracy and precision of RR-interval detection that is the base of correct HRV analysis. If necessary, they should be prevented, eliminated or corrected; it may contribute to the liquidation of present misunderstanding in the area of HRV analysis.

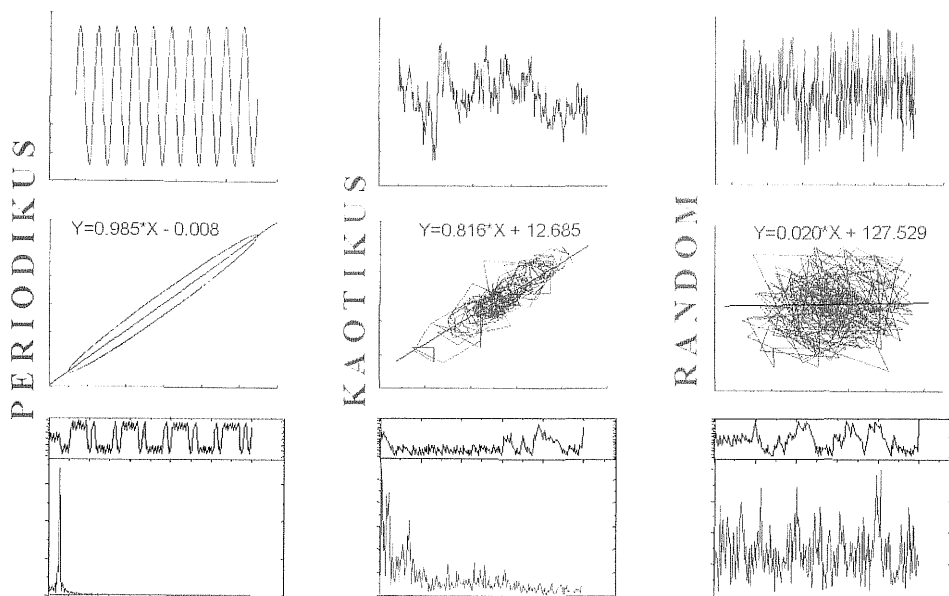


Fig 1.7. Periodic, chaotic and random sequences (upper section), their Poincaré plot (middle section) and Fast Fourier Transformation (bottom section). The different natures of the series are clearly visible (from Hejjel 1999). The slope of the fitted line in the Poincaré plots may be further studied as a new measure of HRV.

## 2. Objectives

### 2.1. Specific aims of the investigation

The latest comprehensive methodical recommendation for HRV analysis was published in 1996 (Task Force of the European Society of Cardiology and the North American Society of Pacing and Electrophysiology, Task Force 1996). Currently this article is respected as one of the most frequently cited paper in Circulation (<http://circ.ahajournals.org/reports/mfc1.dtl>), however, it should be verified in the light of recent technical improvements and the existing ambivalent results in this field. The Task Force precisely covers the duration of the ECG recording, the upper corner frequency of the ECG amplifier, the sampling rate (digitization), validating the equipment with fully reproducible signal with exactly known HRV parameters, standardization of several time and frequency domain measures, and interpretation of the results, besides the underlying physiopathology and possible clinical implications. According to the recommendation, the upper-band frequency cutoff lower than about 200 Hz may create a jitter in the recognition of the QRS fiducial point, causing a measuring error of RR-intervals. However, the main frequency content of the ventricular complex is in the 2-20 Hz range with a maximum at 12 Hz (in Merri et al 1990), therefore lower upper corner frequency may be sufficient for the exact localization of the ventricular complex fiducial point. The unnecessarily higher cutoff may retain more noise in the ECG record also resulting in erroneous RR-interval detection. The ubiquitous power line interference itself or its intended suppression by notch-filters also can flutter the ventricular complex fiducial point.

Poor quality digital records due to low sampling rate also may yield inaccurate measurements, on the other hand, unnecessarily fast sampling results in extreme memory usage, processing time and production costs. There is an inconsistency in the cited (Task Force 1996) suggesting about 200 Hz analog upper cutoff and 250-500 Hz sampling frequency without interpolation considering Nyquist's law.

Present dissertation investigates the actions of different upper and lower corner frequencies of the amplifier, analog power line notch filtering and various sampling rates on the accuracy and precision of RR-interval detection and HRV parameters of

uncorrupted and contaminated ECG signals via computer simulation. The specific stages of the research are enumerated below:

1. Construct an excellent system including hardware and software for sample ECG recording and HRV analysis
2. Develop a precisional ECG signal generator and analyzer for accurate RR-interval measurement to verify the HRV analysis system, the effects of several interferences/noises and their filtering on the accuracy of RR-interval detection
3. Build analog low pass, high pass and notch filters to be evaluated
4. Develop special software for the simulation of digitization of the ECG signals with a range of known variability at different sampling rates, considering the exactness of RR-interval detection
5. Analyze the exactness of RR-interval detection in uncorrupted and noise-contaminated artificial ECG records before and subsequent to high and low pass filtering at different corner frequencies
6. Analyze the exactness of RR-interval detection in uncorrupted and AC interference-contaminated artificial ECG records before and subsequent to notch filtering
7. Investigate the effects of various sampling rates on the accuracy and precision of RR-interval recognition in ECG samples with different variability



### 3. Methods

#### 3.1. Computerized system for HRV analysis

The author's first computer-interfaced,  $\mu$ A741-based ECG amplifier was constructed in 1998. The signal was digitized at 500 Hz with a SoundBlaster-16 sound card programmed in Borland Pascal and Assembly. The need of an easy-handling system was recognized during the initial HRV-measurements, however it was achieved in 2002: a good-quality single-channel amplifier with the INA114 integrated circuit (Burr-Brown Corporation, Tucson, AZ) was born with a frequency transfer of 0.5 to 300 Hz. Digitization occurs at 1 kHz and 12 bit resolution by the ADC-42 analog to digital converter (Pico Technology Ltd., St. Neots, UK) with a notebook computer assuring a portable system (*Fig. 3.1.*). The fully Windows-based ECG-recorder (*Fig. 3.2.*), interactive RR-interval detector (*Fig. 3.3.*) and HRV-analyzer (*Fig. 3.4.* and **Appendix A/1-3**) software were written in Delphi by the author. The equipment showed 1 ms maximal error of RR-interval detection during the test performed with the ECG signal generator, which is comparable to the sampling error at 1 kHz.

Besides acquiring human ECG-samples for further simulation and investigation, there are numerous projects in preliminary stage with the recent ECG-system related to GSM-phone exposition, autonomic assessment of brain injury after extracorporeal circulation, quantifying the operative stress of the surgeon, and track sequential changes following open and laparoscopic abdominal surgeries.

The intelligent RR-interval detector (ECGRdet version 2.0) assures digital filtering (moving average, 50 Hz notch, derivative, and 15-40 Hz band pass); direct ECG-peak recognition, detection of the first zero-crossing after the positive peak, the positive peak, negative peak, or their midpoint in the filtered signal; setting the trigger limits of amplitude or RR-interval ( $\pm 30$ , 25, 20, and 15% of the latest accepted interval); visual check and cutting of the tachogram.

The HRV-analyzer (Varian v. 1.1) gives the mean, minimum and maximum RR-interval, the standard deviation (SDNN), relative mean or coefficient of variation ( $CV = SDNN / \text{mean}$ ), root mean square of successive RR-interval differences (RMSSD), and the percentage of RR-interval differences greater than 50 ms (pNN50) in the time domain; fast Fourier transformation (FFT) and its derived standard parameters; Lorentz-

plot and its derivated parameters; and an RR-interval histogram with its numeric parameters.

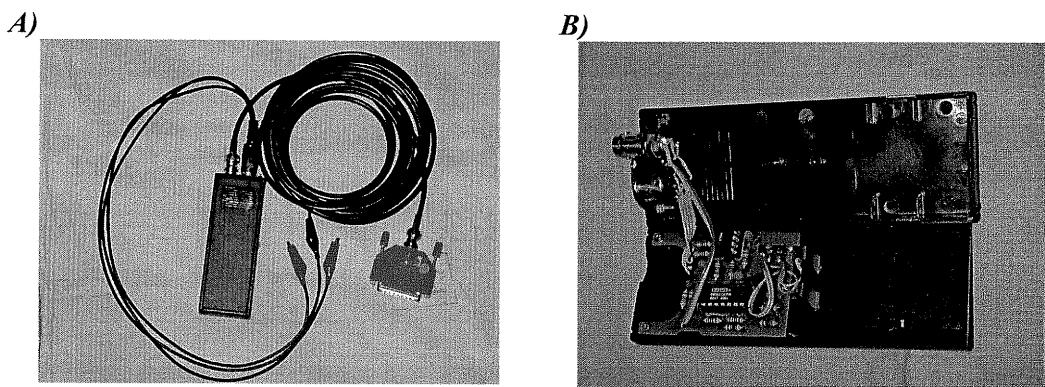


Fig. 3.1. The special hardware for HRV analysis equipped by the author: A) the patient cable, ECG amplifier, data cable and the ADC-42 analog to digital converter, B) the circuitry inside the ECG amplifier and the place for the 9V battery.

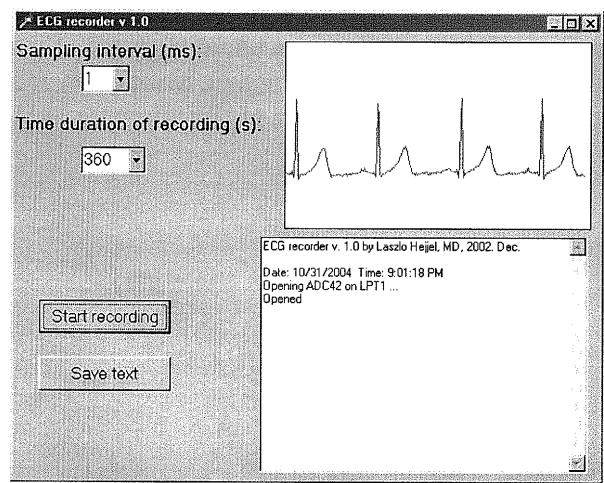


Fig. 3.2. The working window of the ECG recorder v 1.0 software before acquiring 360 s signal at 1 ms sampling interval.

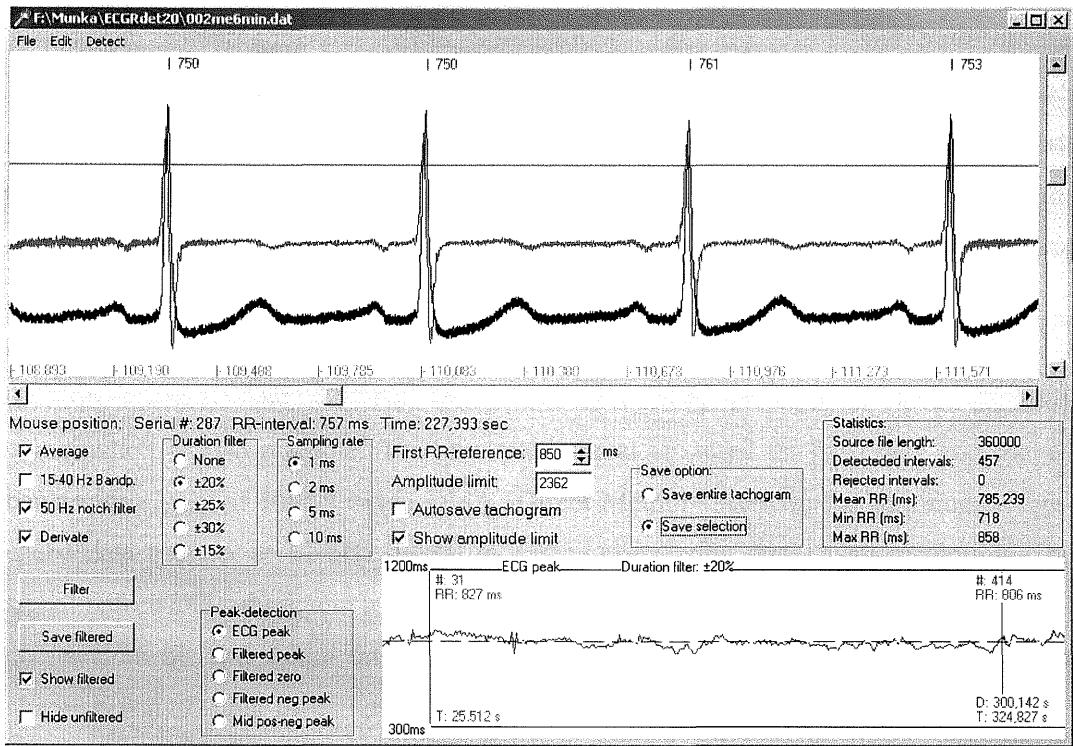


Fig 3.3. The interactive RR-interval detector in work (ECGRdet 2.0). On the upper image the ECG from file 002me6min.dat before (black) and after filtering (moving average, 50 Hz digital notch, derivative) can be seen with the labels of R-detection and the actual RR-interval. The green line is the amplitude threshold, the gray time scale is visible at the bottom. On the right in the middle section there is a statistical chart on the entire tachogram. On the bottom image the resulting tachogram takes place, with a selection of the 31-414<sup>th</sup> intervals giving 300.142 s duration (green verticals and text).

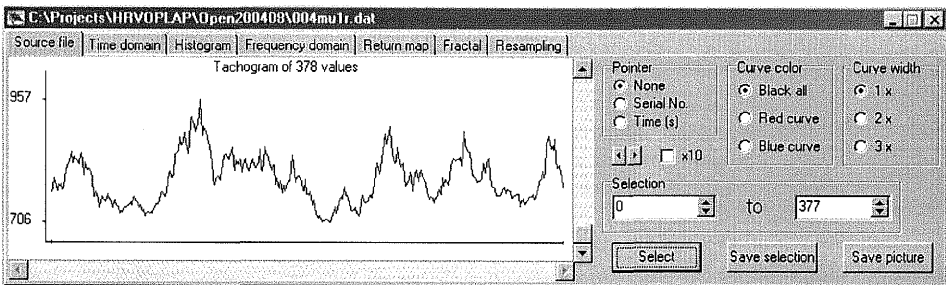


Fig. 3.4. A childwindow of the HRV analyzer software (Varian 1.1) with a tachogram (see more windows in *Appendix A*).

### 3.2. Precisional ECG signal generator and analyzer

The signal generator (ECG Simulator v. 1.0, *Fig. 3.5.*) was built on the DaqBoard2000 factory-calibrated PCI data acquisition card (IOTech Inc., Cleveland, OH). The artificial ECG record is synthesized off-line from a single heart cycle template and a tachogram; both of them can be loaded from existing files or defined in the software considering the recommendations of the Association of the Advancement of Medical Instrumentation (AAMI). Adding a given amplitude of Gaussian (electromyography) noise, 50/60 Hz sine wave (AC interference), sine wave of 5 Hz (motion artifact), and 0.5 Hz sine wave (breathing artifact) or their arbitrary combination is also possible. The generated signal is stored on hard disk and played back with a gain of 1000X using DMA (Direct Memory Access) for continuous high-speed data transfer at 10 kHz digital to analog conversion and 16 bit resolution. The signal before and subsequent to the actual analog filter circuit was digitized at 1 kHz per channel, 16 bit and stored on hard disk by DMA. These latest files containing both channels were further investigated.

The analyzer software (ECGAn v. 1.0, *Fig. 3.6.*) works simultaneously on the two channels: automatically detects the peaks (local maxima), and finds the 2/3, 1/2 and 1/3 height of the peak amplitude on both of the ascending and descending slopes of the ventricular complexes. The distance between these 7 reference points ( $\rightarrow$ RR-intervals, see *Fig. 3.7.*) or their position relative to the equivalent points of the original signal were allocated and visually checked. The results are presented in .text file (**Appendix B/1-2**).

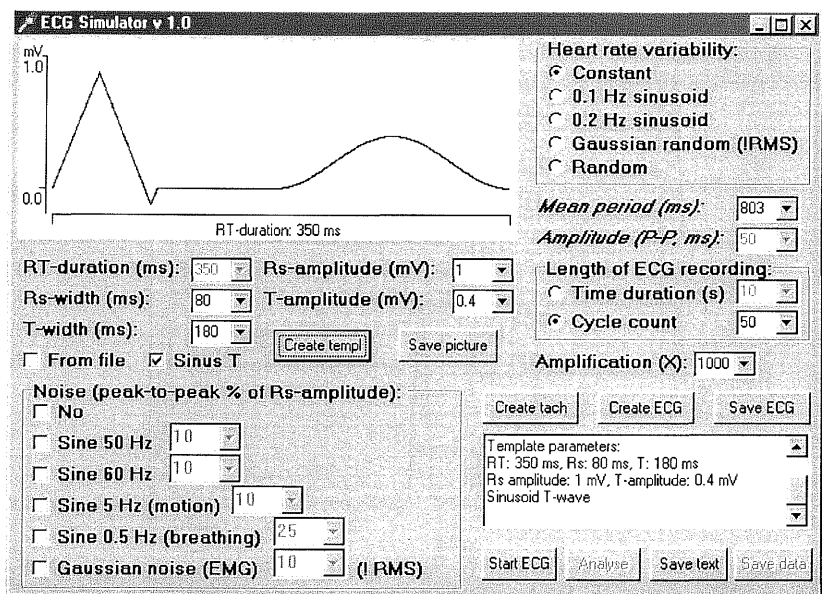


Fig. 3.5. The ECG Simulator v 1.0. software in work.

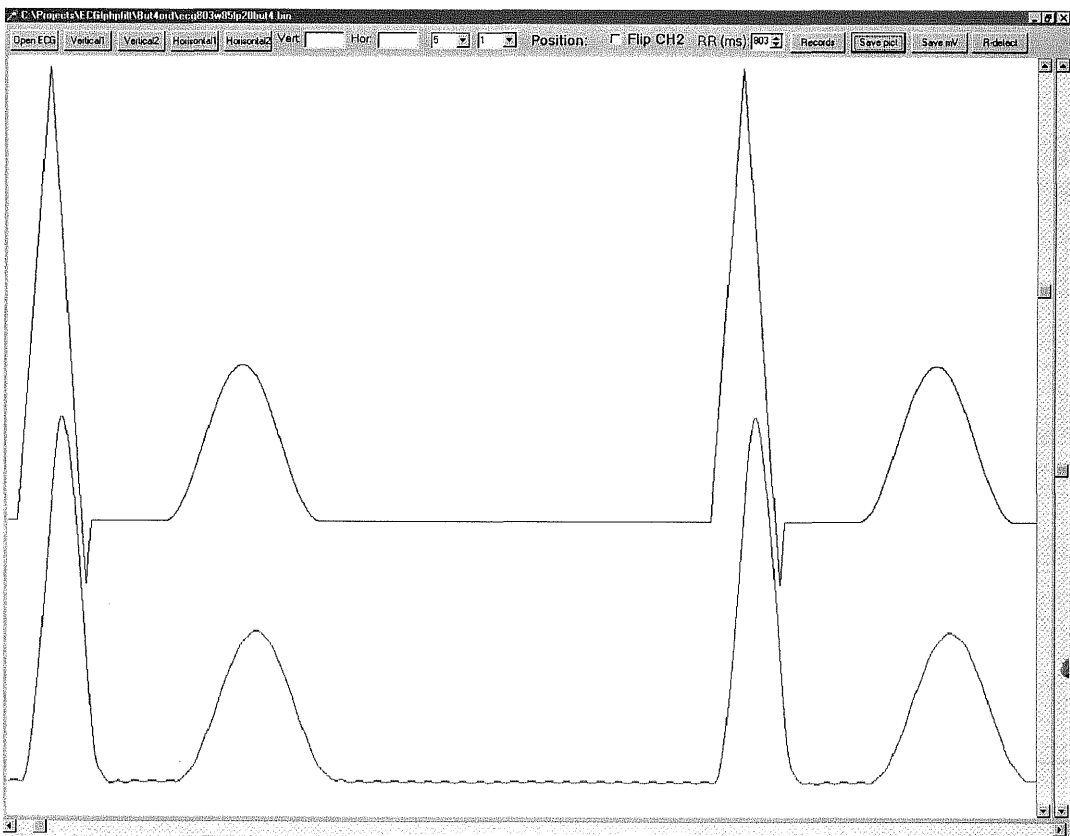


Fig. 3.6. The ECGAn v. 1.0 analyzer software for the ECG Simulator. An uncorrupted ECG before (black) and subsequent to 4<sup>th</sup> order Butterworth low pass filtering at 20 Hz (red) is shown.

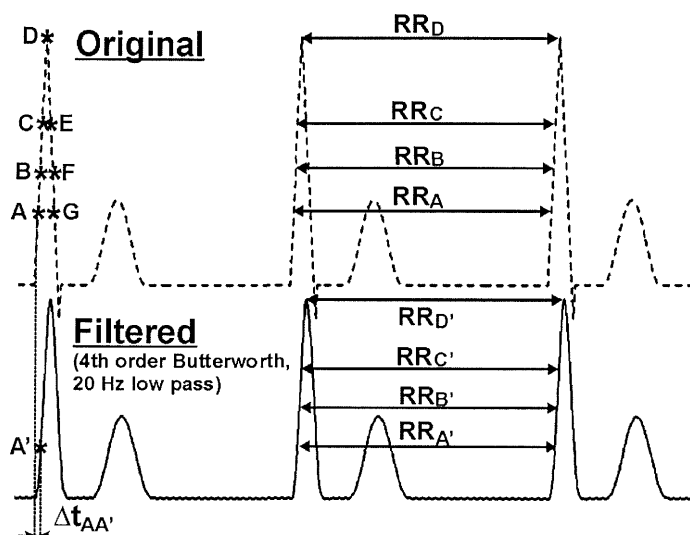


Fig. 3.7. Detecting the 7 reference points by the analyzer (ECGAn 1.0) software: the peak (D) and the 1/3, 1/2, and 2/3 amplitude on both the ascending (A, B, C) and descending (E, F, G) slopes of the ventricular complexes. The RR-intervals given by the distance of the pairs of these 7 points or their timing difference (phase shift) were analyzed.

### 3.3. Analog filters

Analog high pass, low pass and notch filters were assembled using the UAF42 monolithic universal active filter block (Burr-Brown Corporation, Tucson, AZ) tuned by external components calculated by the Filter42 software provided by the manufacturer (available at [www.ti.com](http://www.ti.com)). See frequency responses in Fig. 3.8. measured

A)

B)

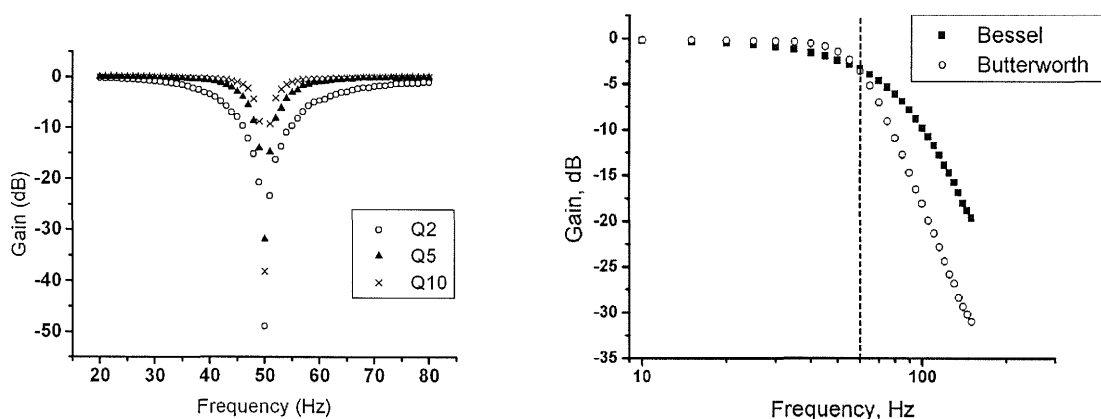


Fig. 3.8. A) Frequency response of the 50 Hz notch filters with  $Q=2, 5$  and  $10$ . B) Frequency response of the 4<sup>th</sup> order Bessel and Butterworth low pass filters at 60 Hz (logarithmic scale)

by the software (Fig. 3.9.) also self-developed around the DaqBoard2000. Filter characteristics are specified in 3.5. and 3.6. sections. The circuit (Fig. 3.10.) was realized on a solderless breadboard (Type 4, Conrad Electronic, Germany). It was shielded by a grounded metal box and powered from the  $\pm 15$  V outputs of the DaqBoard2000 card.

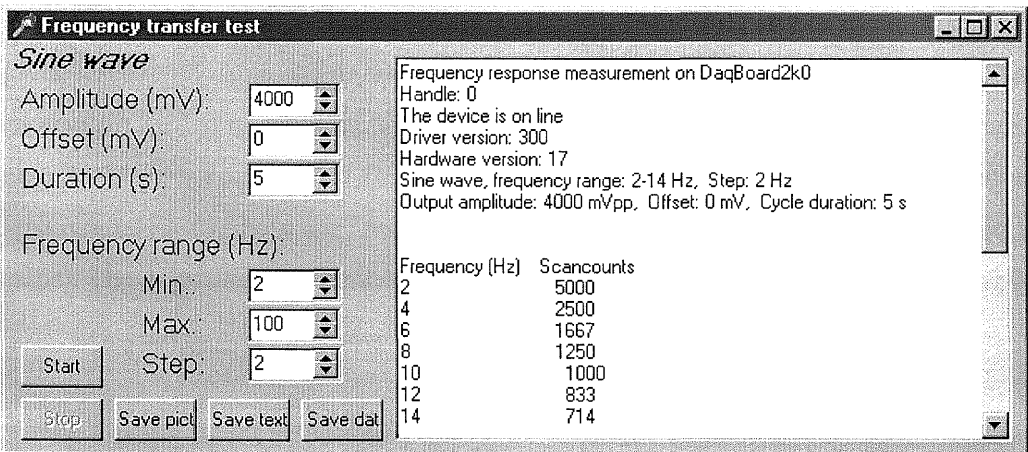


Fig. 3.9. Software for frequency transfer testing. The frequency range, amplitude, offset and the cycle duration of the test sine wave are adjustable.

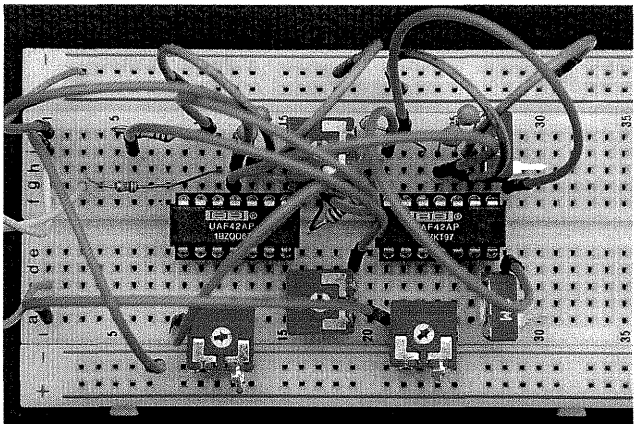


Fig. 3.10. The tunable filter circuit based on UAF42 assembled on a breadboard.

### 3.4. Software for simulation and evaluation of the digitization error

The sampling error (SE) comes from the discretization at finite time resolution (sampling interval – SI) in the digitized signal. This software (Samplerr v. 1.0, *Fig. 3.11.*) – also developed by the author – models the SE by adding a uniformly distributed random series in the range of  $-0.5*SI \leq SE \leq 0.5*SI$  to the supposed R-fiducial point of the “original” tachogram. The original tachogram can be loaded from a .dat file (e.g. real human tachogram) or synthesized in the program (Gaussian random, uniformly distributed random, sinusoid at a given frequency, logistic or any of them mixed with a given frequency sine wave at a certain phase shift and amplitude). The original tachogram shifted to a known mean (e.g. 800 ms), skewed (shrink or stretch) to standard deviations of a given range (e.g. 5-30 ms in steps of 5 ms) are called the adjusted tachograms ( $n=6$ ), those are “resampled” at SI in the chosen range (e.g. 1-10 ms in 1 ms steps). The adjustment by mathematical formula:

$$RR_{s,i}^{ADJ} = \frac{s}{SD} * (RR_i^{ORIG} - \overline{RR}^{ORIG}) + 800 \quad s=5, 10, 15 \dots 30; i=1 \dots 375,$$

where  $s$  is the tuned standard deviation of the adjusted tachograms,  $RR_{s,i}^{ADJ}$  is the  $i$ -th RR-interval in the adjusted tachogram with standard deviation of  $s$ ,  $SD$  represents the standard deviation of the original tachogram from the human objects,  $RR_i^{ORIG}$  is the  $i$ -th RR-interval and  $\overline{RR}^{ORIG}$  represents the mean RR-interval in the original tachogram.

The resampling may be repeated several times resulting in  $6 \times 10 \times 15 = 900$  resampled-adjusted tachograms in our example. Separately for all repetitively resampled group (from each 15-element set), the mean, standard deviation, relative accuracy error ( $RAE = (X_{\text{mean}} - X_{\text{true}}) / X_{\text{true}}$ ) and relative precision error ( $RPE = SD / X_{\text{mean}}$ ), are computed automatically from the mean RR-interval, SDNN, RMSSD and the pNN50 of the resampled-adjusted tachograms and compared to the same parameters of the original, nominally uncorrupted tachograms. The output of the program can be checked in a text box or saved as .dat file for further processing.



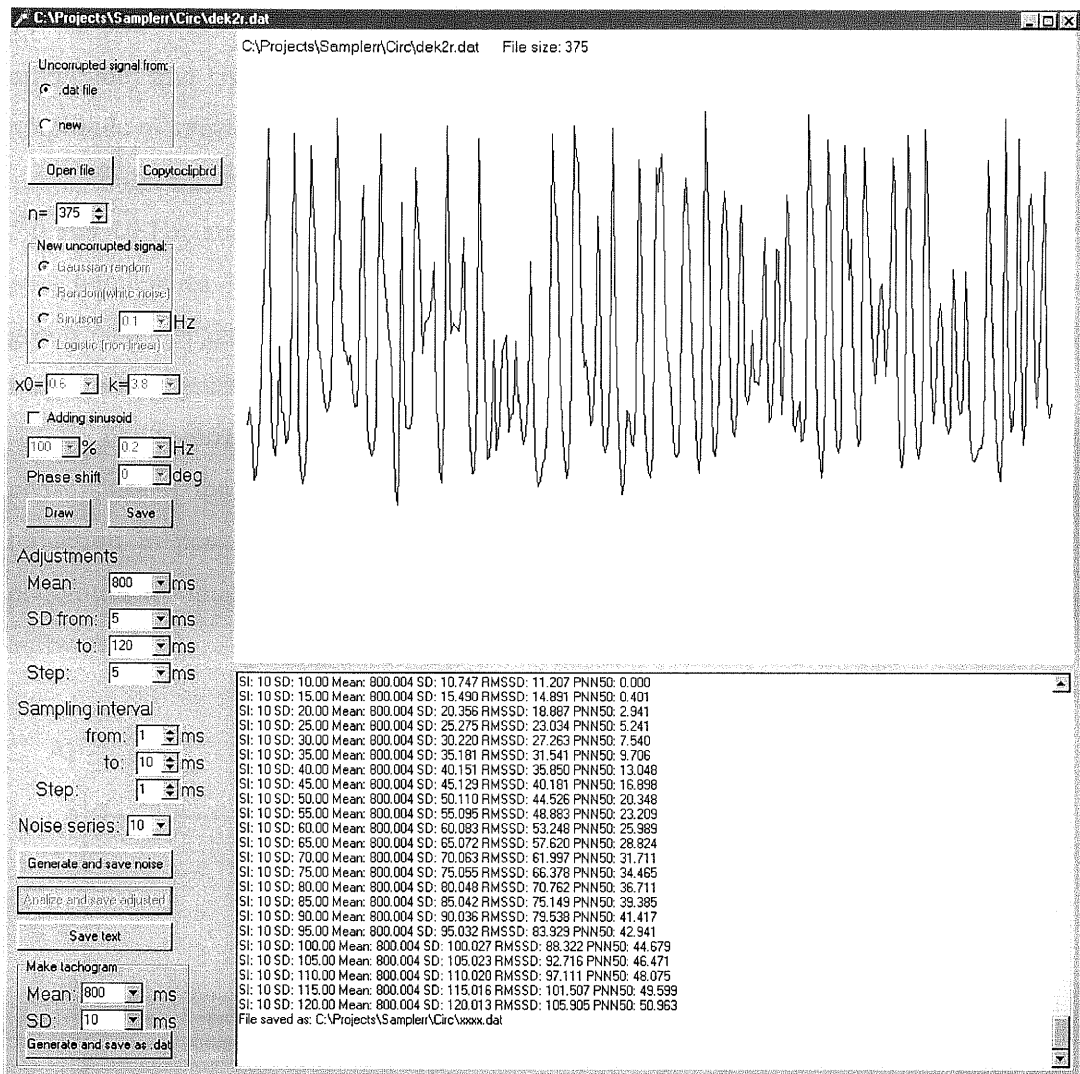


Fig. 3.11. The sampling error simulator software (Samplerr v. 1.0).

### 3.5. The effects of analog corner frequencies on RR-interval detection

The ECG Simulator (3.2.) generated the augmented ECG signal consisting of 21 cycles (giving 20 RR-intervals) with the following parameters: Rs-amplitude=4 V, T-amplitude=1.2 V, RT=350 ms, Rs=65, 85 or 115 ms (ventricular complex duration, VCD), T=180 ms. The T-wave was formed by a sine wave instead of a semi-ellipsoid in order to avoid uncharacteristic abrupt changes at the T-wave boundaries and consecutive spike formation after high pass filtering. The RR-interval was set to 803 ms, in order to prevent synchronization of the ECG signal and AC interference (20 ms period) in the corrupted series. Besides sterile records, power line interference- (added

50 Hz sine wave with 25% or 50% peak-to-peak amplitude of ventricular complex amplitude) and Gaussian noise- (electromyography artifact, 10%, 25%, and 50% rms amplitude of ventricular complex amplitude) corrupted records were investigated.

Filtering was performed by 2<sup>nd</sup> order Butterworth high pass at 0.1, 0.5, 1.0, 2.0, 5.0 and 10 Hz; and 4<sup>th</sup> order Bessel and Butterworth at 20, 40, 60, 80 and 100 Hz low pass frequencies. The Bessel filter has excellent pulse response due to its inherent flat group delay in the pass band, while the Butterworth filter has the flattest pass band magnitude response and steeper attenuation beyond the cutoff frequency (*Fig. 3.12.*).

The mean $\pm$ SD and maxima were calculated individually from the (1) absolute phase shift of the 7 predefined pints of the ventricular complexes, and (2) from the reduction in peak amplitude. The mean $\pm$ SD of the measured RR-intervals and the maximum deviation from the nominal 803 ms were computed also by the ECGAn software (**3.2.**).

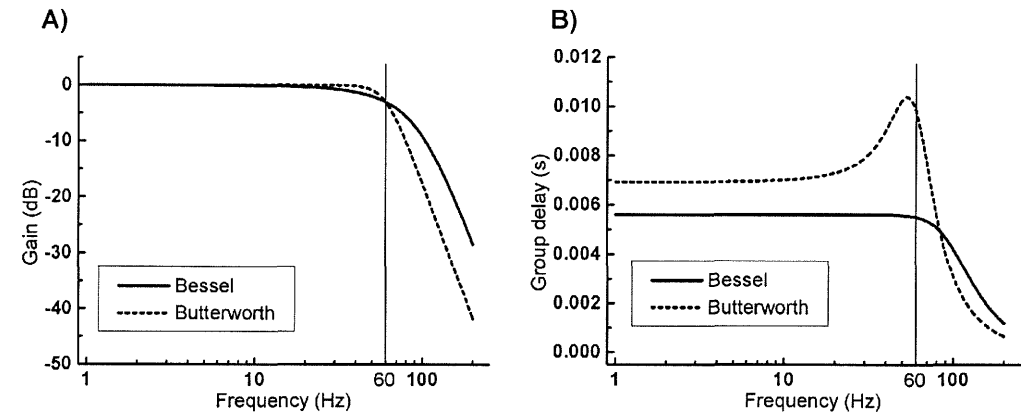


*Fig. 3.12. Calculated gain and group delay responses of the 4<sup>th</sup> order Bessel and Butterworth 60 Hz low pass filters.*

### 3.6. Testing the effects of AC notch filtering on RR-interval detection

Predefined ECG templates (Rs-amplitude=4 V, T-amplitude=1.2 V, RT=350 ms, Rs=65, 85 or 115 ms, T=180 ms) were repeated ten times at 803 ms. AC interference was represented by adding 5%, 10%, 25% and 50% peak-to-peak amplitude 50 Hz sine wave. The above mentioned 7 points of the ventricular complexes were found and manually checked. The mean, SD and maximal deviation from the corresponding point

of the uncorrupted ECG were computed before and subsequent to notch filtering by (3.2.). The 50 Hz band rejection was tuned with filter Q=2, 5 and 10 (Molina 1994).

### 3.7. Effects of the sampling rate on the time domain parameters

Two 375-element high-quality ECG tracings derived from a healthy volunteer and a cardiovascular high-risk, diabetic patient with significantly reduced HRV were shifted to a mean of 800 ms and stretched (or shrunken) to standard deviations of 5-120 ms in 5 ms steps with the Samplerr 1.0 software. All adjusted tachograms were “resampled” at 1-10 ms in 1 ms steps, ten times repetitively at each sampling rate. The mean, standard deviation, RAE and RPE were calculated from the mean RR-interval, SDNN, RMSSD and the pNN50 (*Fig. 3.13.*).

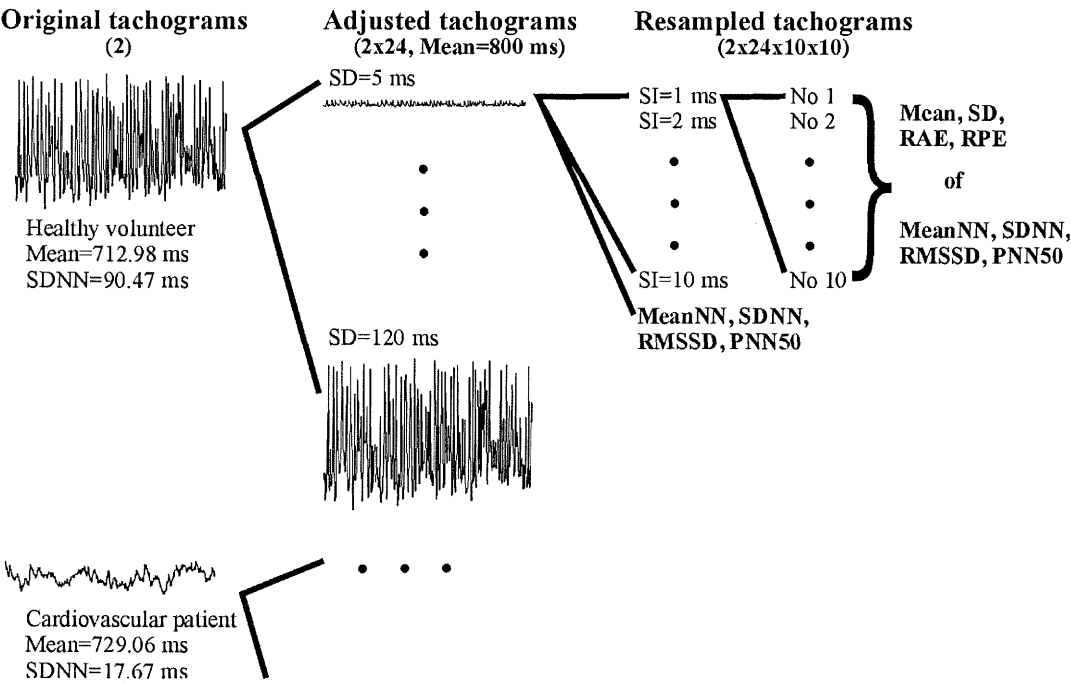


*Fig. 3.13. The scheme of the investigation from the two original tachograms to the analysis of adjusted and resampled tachograms. MeanNN: the mean of normal-to-normal RR-intervals, SDNN: the standard deviation of normal-to-normal RR-intervals, RMSSD: root mean square of successive RR-differences, pNN50: the percentage of consecutive RR-interval differences greater than 50 ms, SD: standard deviation, SI: sampling interval, RAE: relative accuracy error, RPE: relative precision error.*

## 4. Results

### 4.1. Testing the effects of analog corner frequencies on RR-interval detection

#### 4.1.1. High pass filtering of the uncorrupted signal

High pass filtering up to 0.5 Hz of the uncorrupted signal does not result in significant changes in the ECG morphology (*Fig. 4.1.*). At 1 Hz and 2 Hz corner frequencies, considerable alterations befall present, at 5 Hz and 10 Hz cutoff the ECG signal is unrecognizable, however, the error of RR-interval detection remains within 1 ms by the applied algorithm. Results are detailed in **Appendix C/1-2**.

#### 4.1.2. Low pass filtering of uncorrupted signal

Low pass filtering of the uncorrupted ECG signal (*Fig. 4.2.*) causes a slight amplitude reduction and a modest edge-smoothing.

The phase delay depends on the cutoff frequency (20 Hz: 12-19 ms, 100 Hz: 4-5 ms), the reference point of the ventricular complex (ascending slope: 4-14 ms, peak: 5-15 ms, descending slope: 4-20 ms), the type of the filter (on the peak, at 20 Hz, Bessel: 33-34 ms, Butterworth: 14-15 ms), and in a lesser amount on the VCD (65 ms: 4-19 ms, 115 ms: 4-20 ms). Details are in **Appendix D/1-3**. The RR-interval detection remains within 1 ms accuracy error due to the constant phase shift of the ventricular complex at both types of filters.

#### 4.1.3. Low pass filtering of AC interference corrupted signal

Power line interference corruption proportionally alters the reliability of heart rate detection. At 25% or 50% interference, the peak is the most sensitive point (maximum divergence from the nominal 803 ms: 13 ms and 16 ms, respectively), the slopes are somewhat more resistant (maximum difference: 10 ms and 14 ms, respectively). Detailed results are in **Appendix E**.

Bessel or Butterworth filtering at 40 Hz does not considerably recover the accuracy of rate detection. Bessel filtering of the 50% interference series at 20 Hz reduces the maximum error to 7 ms at the peak, whereas down to 2 ms on the slopes.

Butterworth filtering at 20 Hz cutoff decreases the maximum difference to 12 ms at the peak, and 7 ms on the slopes.

Bessel filtering of the 25% interference series at 20 Hz low pass results in a maximum deviation of 3 ms on the peak, and 1 ms on the slopes. Applying a 20 Hz Butterworth filter reduces the error to 8 ms at the peak and 3 ms on the slopes.

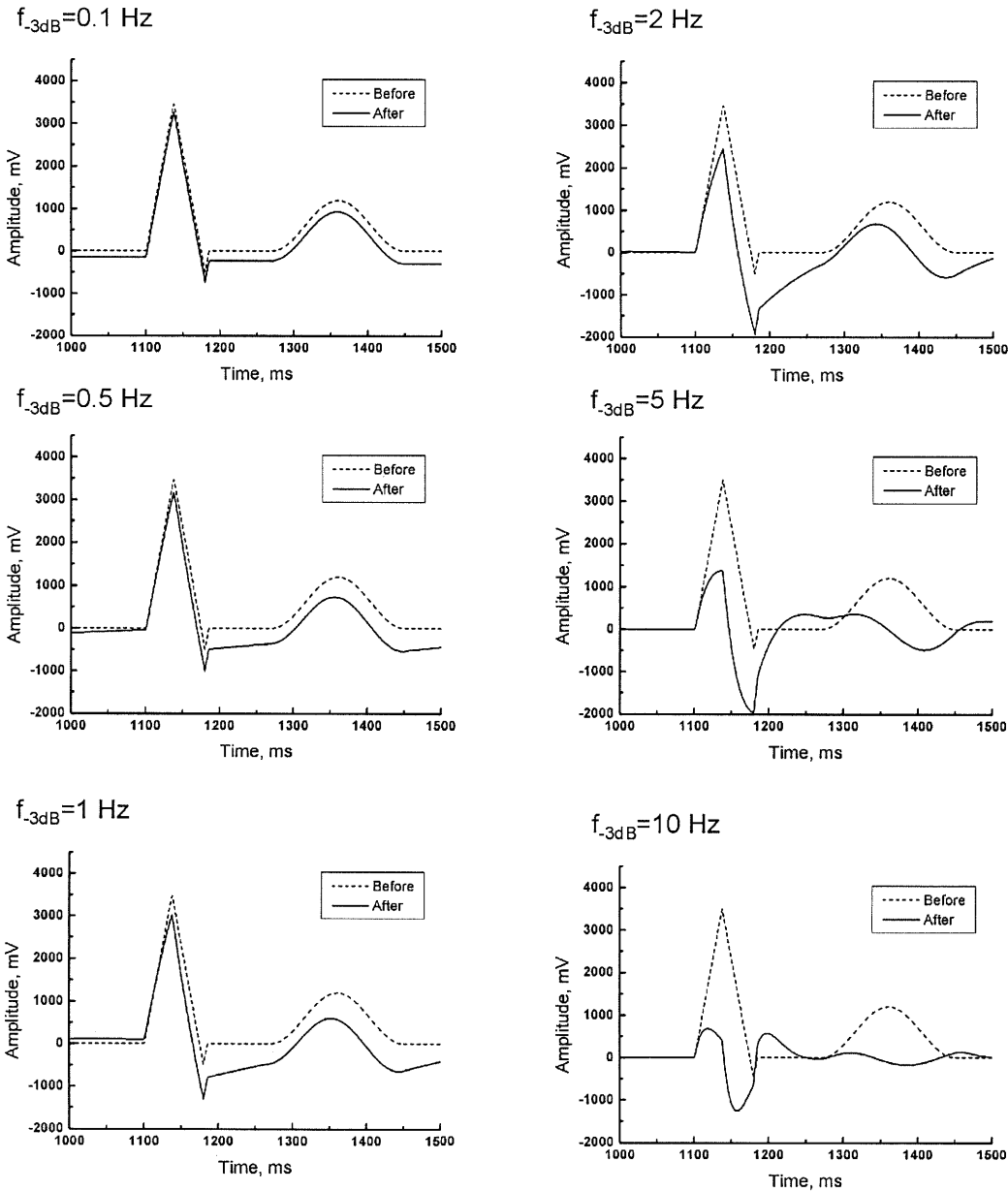


Fig. 4.1. The 2<sup>nd</sup> order Butterworth high pass at different corner frequencies

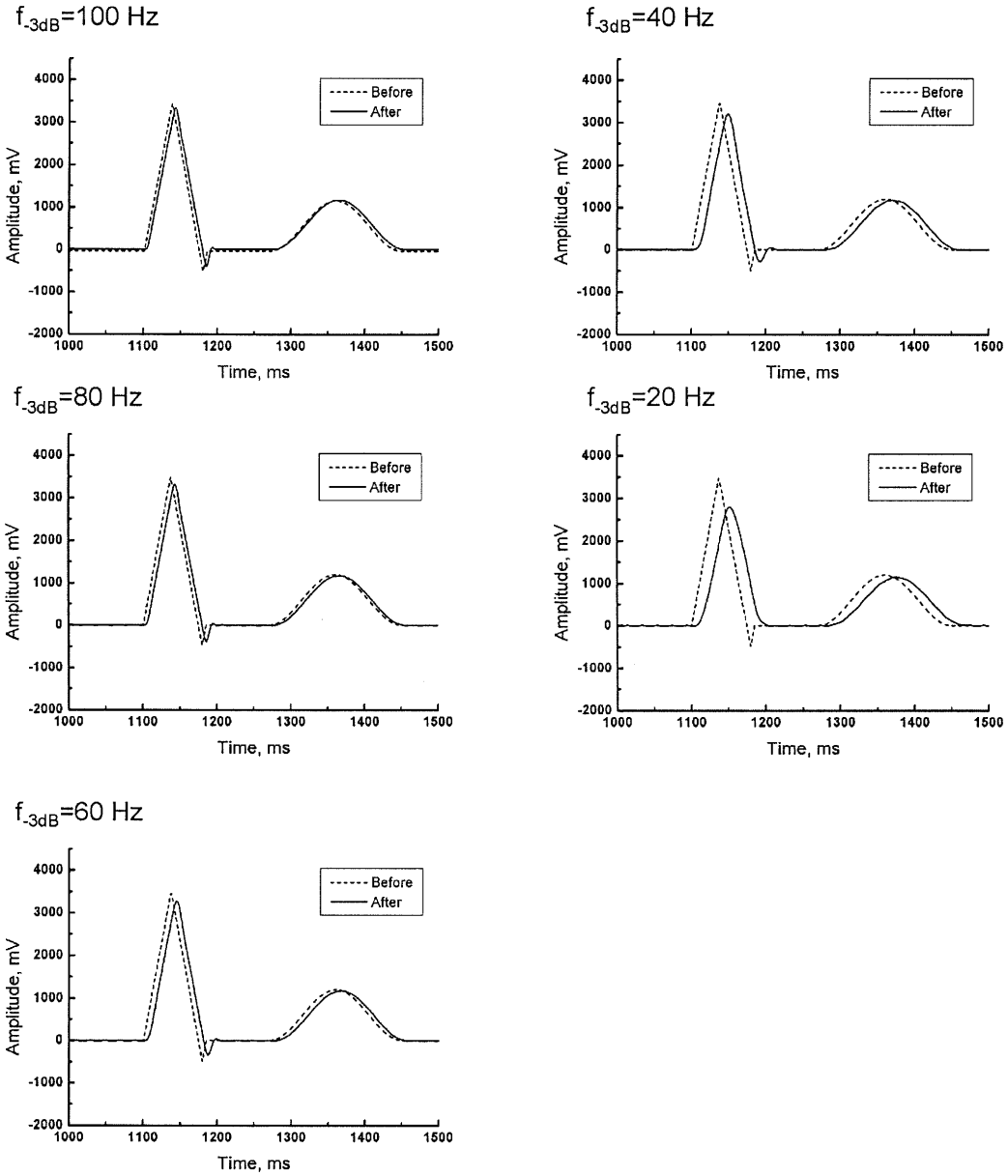


Fig. 4.2. The 4<sup>th</sup> order Butterworth low pass filtering of uncorrupted ECG signal at different corner frequencies.

#### 4.1.4. Low pass filtering of Gaussian noise corrupted signal

Gaussian noise contamination (Fig. 4.3.) causes unpredictable rate detection error independently of the chosen reference point. The 10% noise results in 3-10 ms maximum RR-interval differences from the nominal 803 ms. After passing through the low pass filter, this is reduced to 0-1 ms at every corner frequencies and both type of

filters. The 25% rms amplitude noise causes 6-26 ms error that is reduced to 1-2 ms at 20-40 Hz low pass, while 1-3 ms at 60-100 Hz cutoff. The 50% Gaussian noise gives 10-34 ms deviations. 20-40 Hz low pass is associated with 1-4 ms error, while it is 2-6 ms at 60-100 Hz corner frequency. **Appendix F/1-3** contains the details of measurements.

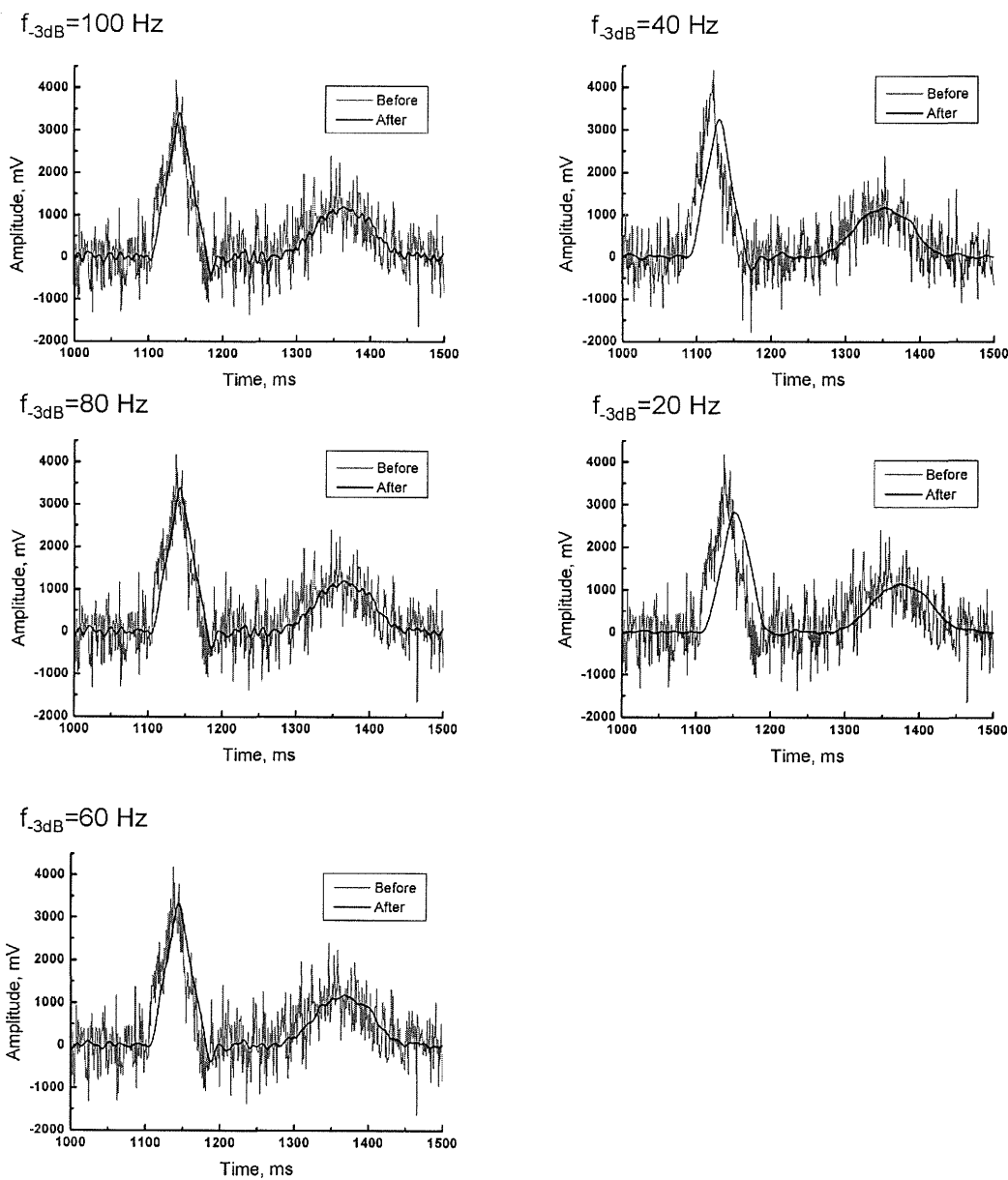


Fig. 4.3. The 4<sup>th</sup> order Butterworth low pass filtering of 25% rms amplitude Gaussian noise corrupted ECG signal at different corner frequencies.

## 4. 2. Testing the effects of AC notch filtering

### 4.2.1. Notch filtering the uncorrupted record

The notch filtering of uncorrupted ECG records does not result in RR-interval detection error greater than 1 ms, which is comparable to the theoretical sampling error at 1 kHz. See the images in **Appendix G** and detailed measurements in **Appendix H**.

### 4.2.2. Notch filtering the AC interference corrupted record

AC interference contamination proportionally to its amplitude distorts the ECG (*Fig. 4.4.*) and alters the accuracy of reference point localization (**Appendix I**): 5% interference amplitude: 2 ms, 10%: 4 ms, 25%: 8 ms, and 50%: 14 ms, which is consistently restored by notch filtering at any filter Q with a minimal error ( $\leq 1$  ms on the ascending slope and peak). The accuracy of peak detection without filtering is maintained up to 10% interference within 1 ms error. The wider the VCD, the more sensitive the RR-interval detection to mains interference; however this is not remarkable (**Appendix J**).



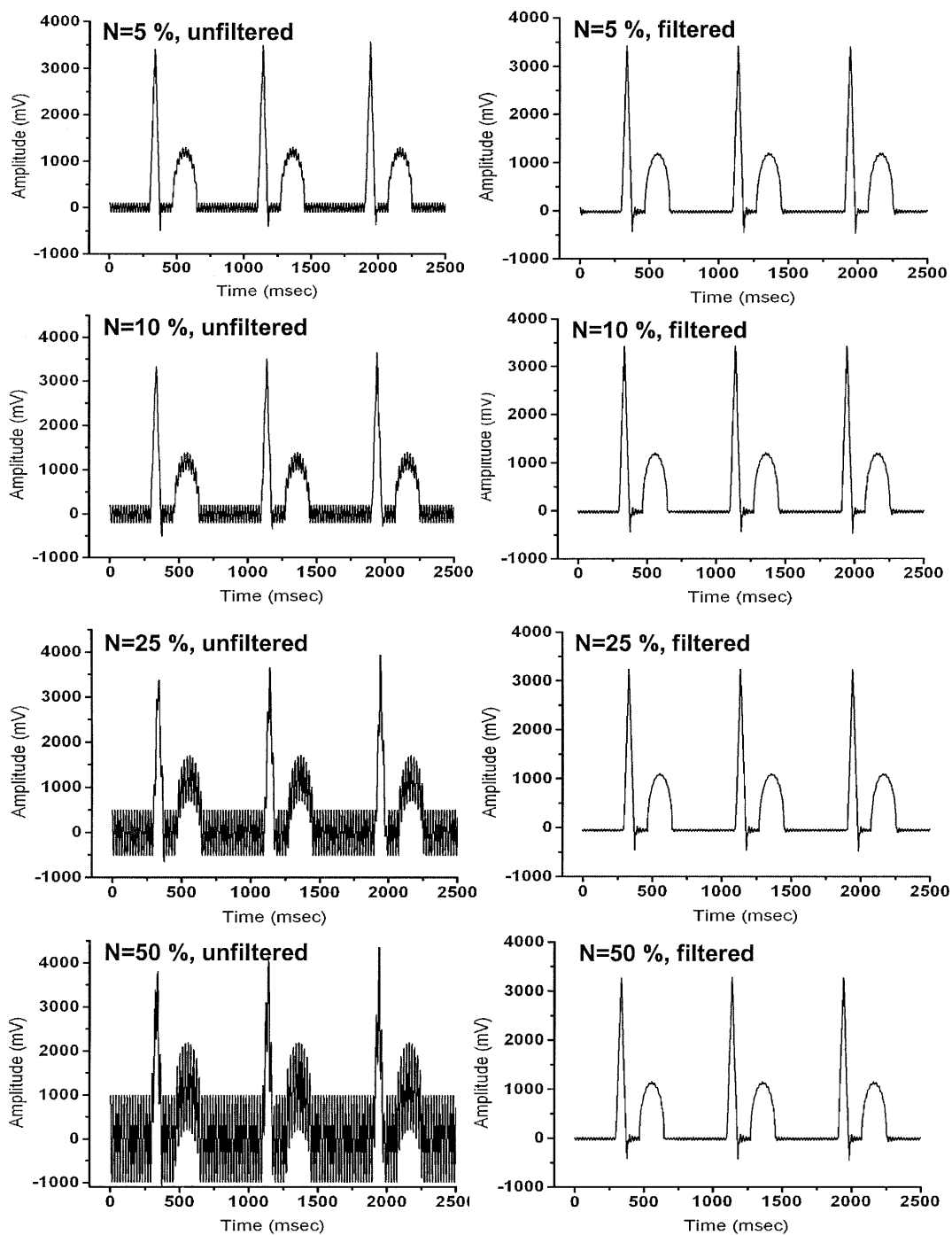


Fig. 4.4. AC notch filtering ( $Q=5$ ) of the 50 Hz interference corrupted ECG signal.

4. 3. Effects of the sampling rate on the time domain parameters

The RAE and RPE of the mean RR-interval were below 0.1% at every sampling interval and in both healthy and high-risk series, as can be seen in Fig. 4.5.

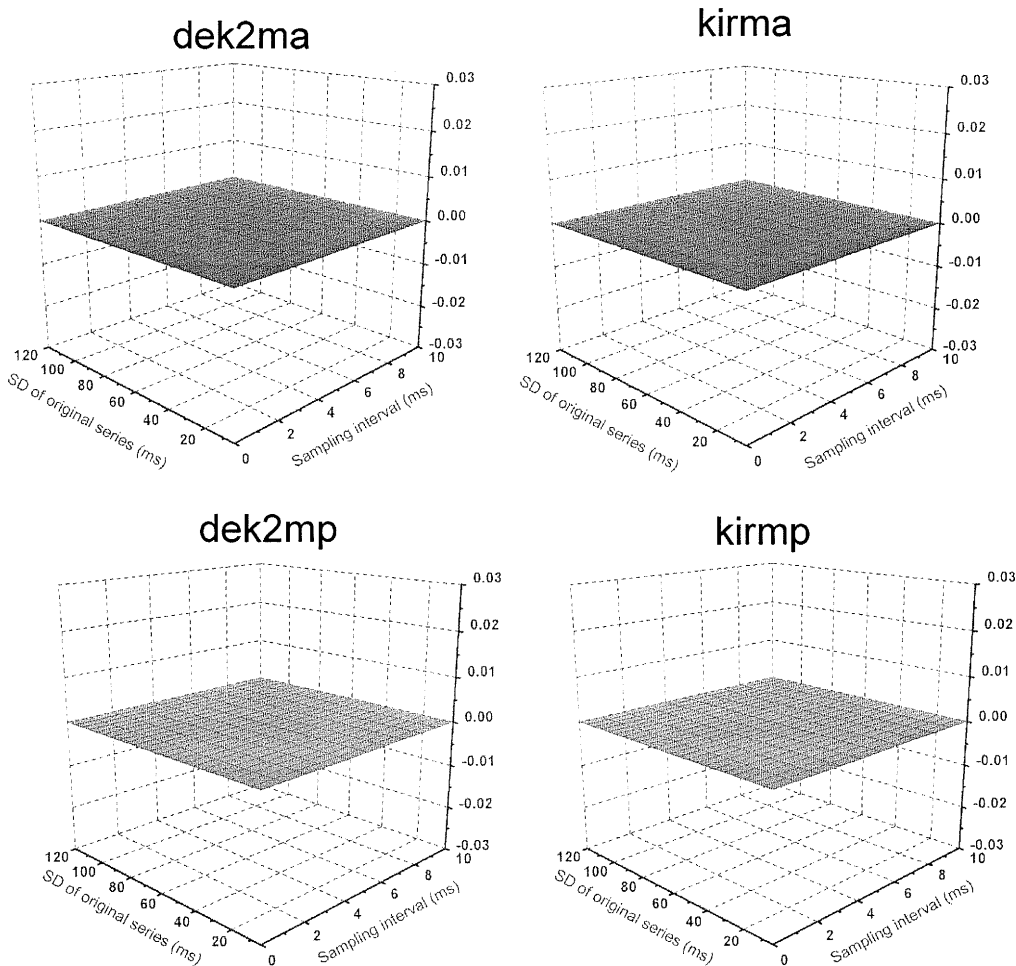


Fig. 4.5. Relative accuracy (a) and precision (p) error of the mean RR-interval (m) of tachograms based on a healthy volunteer (dek2, left column) and a cardiovascular high risk patient (kir, right column).

The RAE of the SDNN for the healthy and high-risk group showed identical trends due to the equal adjustment of this parameter (Fig. 4.6.). The smaller the nominal SD, the higher are the RAE and RPE of SDNN. The RAE exceeded 1% at 2 ms SI, 5% at 4 ms SI, and 30% at 10 ms SI in the series with nominal SD=5 ms. Over 35 ms nominal SD, the RAE remained below 1% even at 10 ms SI. The RPE of SDNN exceeded 1% at SI of 7 ms, and 2% was not reached in the examined range.

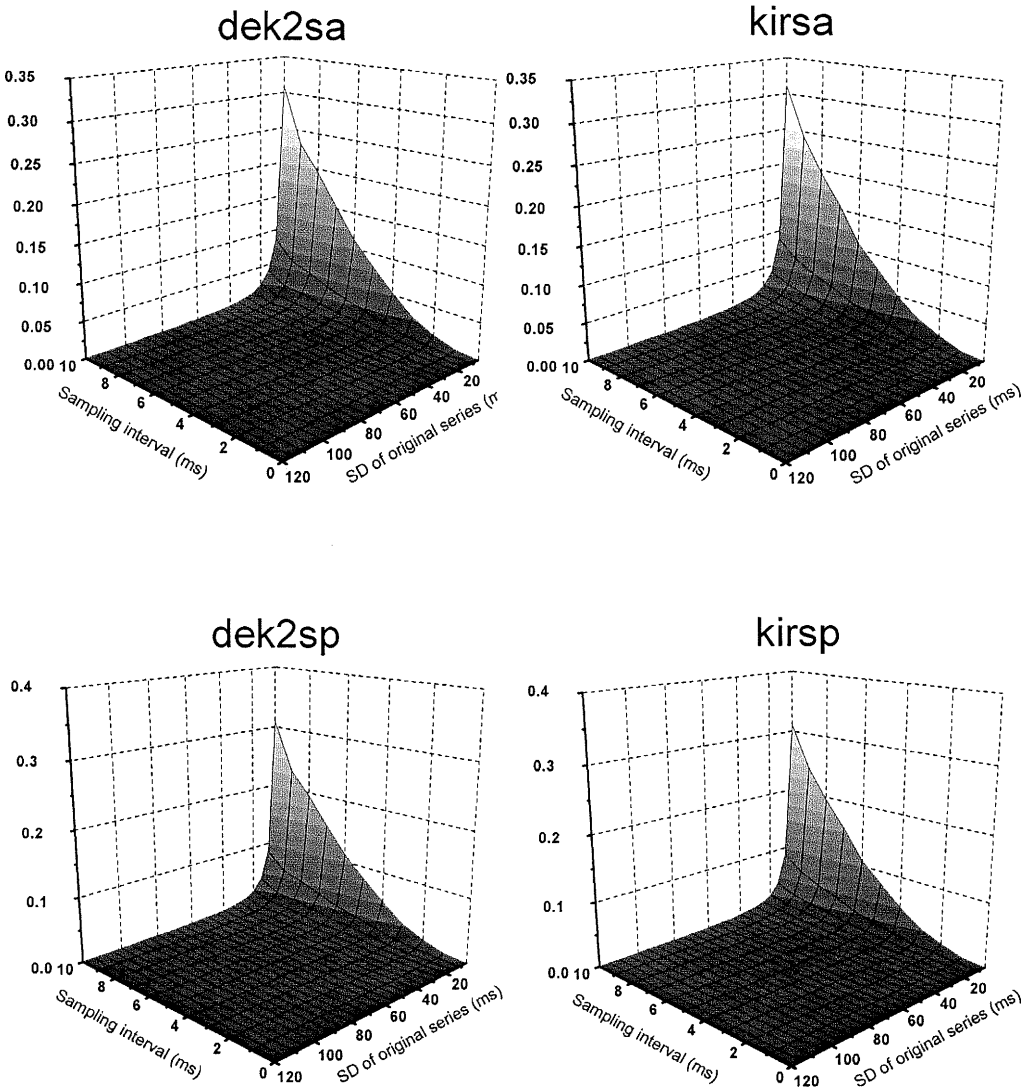


Fig. 4.6. Relative accuracy (a) and precision (p) error of the SDNN (s) of tachograms based on a healthy volunteer (dek2, left column) and a cardiovascular high risk patient (kir, right column).

The RAE of RMSSD (Fig. 4.7.) was as high as 225.2% in the lowest variability tachograms at SI=10 ms. In the 5 ms nominal SD tachogram from the high-risk patient, SI of 1, 2 or 4 ms resulted in RAE of 4.8%, 18.1% and 54.3%, respectively. Resampling the 15 ms adjusted SD series from the high risk patient at 1, 2, 4 or 10 ms SI, the RAE of RMSSD equaled 0.7%, 2.5%, 7.8% and 45.1%, respectively. The RPE of RMSSD was below 5% in the entire observation. The RAE of pNN50 (Fig. 4.8.) was 16% for

the healthy group, and nearly 50% for the high-risk group even at SI of 1 ms. The RPE showed poor precision: it was above 200%.

Table 4.1. demonstrates the inaccuracies of SDNN and RMSSD related to the digitization error through two real human cases. At the healthy volunteer with high HRV the sampling interval of 10 ms may be sufficient to measure these absolute values or changes at similar order of magnitude; however, at the cardiovascular high-risk patient with seriously reduced HRV even the 4 ms (250 Hz) sampling causes 6.5% relative accuracy error of absolute beat-to-beat variability.

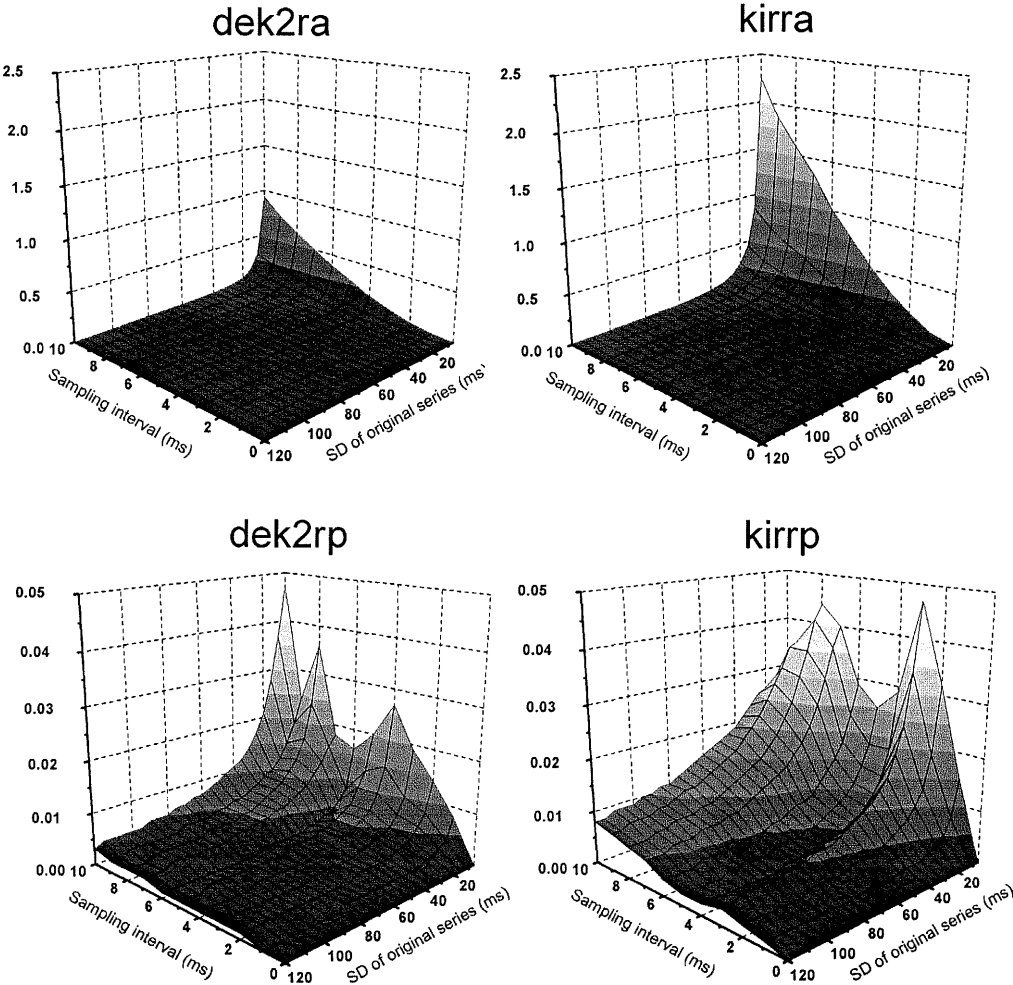


Fig. 4.7. Relative accuracy (a) and precision (p) error of the RMSSD (r) of tachograms based on a healthy volunteer (dek2, left column) and a cardiovascular high risk patient (kir, right column).

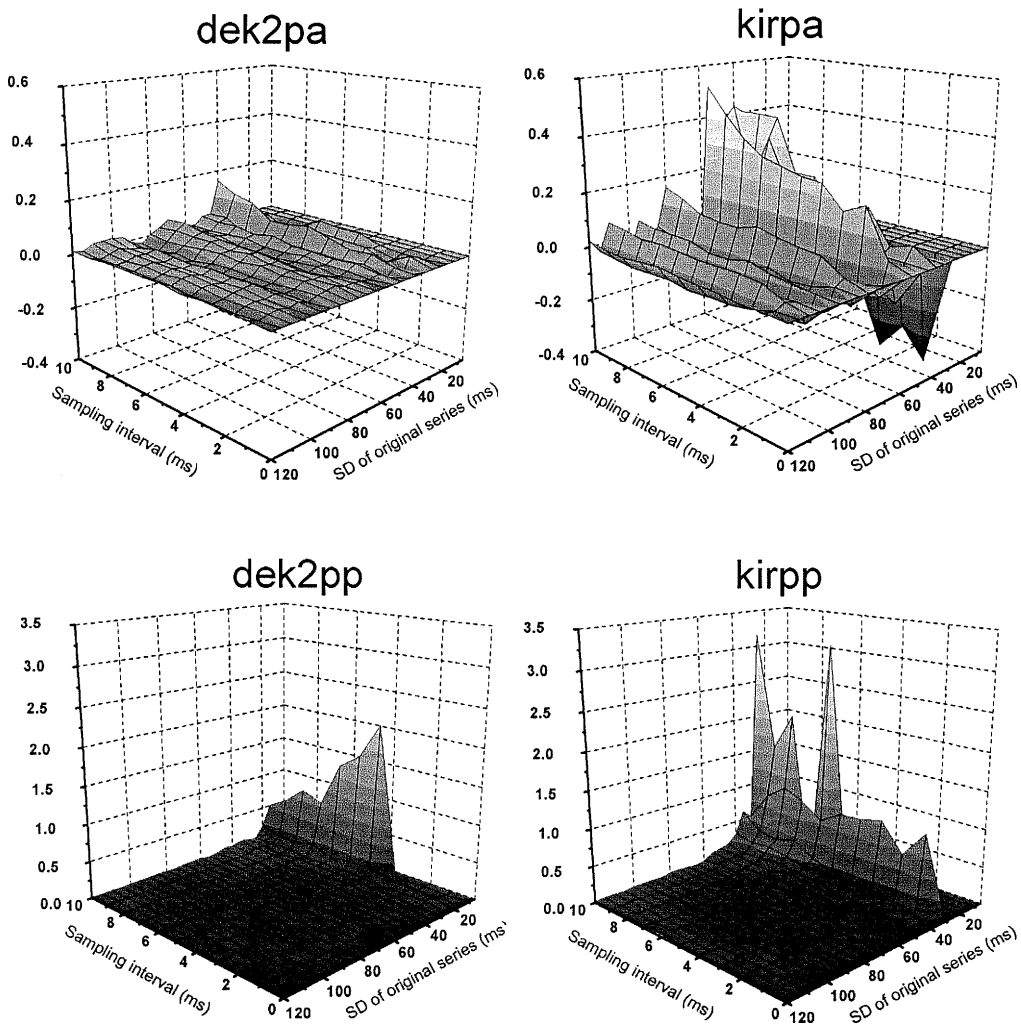


Fig. 4.8. Relative accuracy (a) and precision (p) error of the pNN50 (p) of tachograms based on a healthy volunteer (dek2, left column) and a cardiovascular high risk patient (kir, right column).

SI	Mean of MeanNN	Mean SDNN	RAE of SDNN	RPE of SDNN	Mean RMSSD	RAE of RMSSD	RPE of RMSSD
<b>High-risk patient</b>							
<b>0</b>	<b>729.064</b>	<b>17.673</b>	<b>-</b>	<b>-</b>	<b>8.381</b>	<b>-</b>	<b>-</b>
1	729.064	17.679	0.0%	0.0%	8.423	0.5%	0.7%
2	729.065	17.694	0.1%	0.1%	8.507	1.5%	1.1%
3	729.064	17.722	0.3%	0.2%	8.665	3.4%	1.3%
4	729.064	17.760	0.5%	0.2%	8.929	6.5%	2.1%
5	729.064	17.810	0.8%	0.1%	8.233	10.2%	1.7%
6	729.060	17.835	0.9%	0.2%	9.370	11.8%	2.6%
7	729.065	17.912	1.4%	0.4%	9.772	16.6%	3.6%
8	729.066	17.960	1.6%	0.5%	10.039	19.8%	4.7%
9	729.064	18.033	2.0%	0.3%	10.462	24.8%	3.2%
10	729.068	18.149	2.7%	0.4%	10.963	30.8%	1.9%
<b>Healthy volunteer</b>							
<b>0</b>	<b>712.981</b>	<b>90.466</b>	<b>-</b>	<b>-</b>	<b>79.748</b>	<b>-</b>	<b>-</b>
1	712.981	90.463	0.0%	0.0%	79.758	0.0%	0.0%
2	712.981	90.473	0.0%	0.0%	79.762	0.0%	0.1%
3	712.980	90.468	0.0%	0.0%	79.758	0.0%	0.1%
4	712.979	90.472	0.0%	0.1%	79.733	0.0%	0.2%
5	712.980	90.470	0.0%	0.1%	79.780	0.0%	0.2%
6	712.978	90.523	0.1%	0.1%	79.944	0.2%	0.2%
7	712.980	90.552	0.1%	0.1%	79.964	0.3%	0.3%
8	712.983	90.502	0.0%	0.1%	79.926	0.2%	0.3%
9	712.979	90.500	0.0%	0.2%	79.981	0.3%	0.3%
10	712.979	90.559	0.1%	0.1%	79.958	0.3%	0.4%

Table 4.1. The association of the sampling interval (SI) and time domain parameters of the resampled records from the healthy volunteer and the cardiovascular high-risk patient. Zero sampling interval represents the parameters of the original ECG records with no sampling noise added (nominally uncorrupted). The analysis is based on 10 resampling cycles at each SI.

## 5. Discussion

### 5.1. The effects of analog corner frequencies on RR-interval detection

The RR-interval measurement was reliable at every examined high pass cutoff, however, lower corner frequency below 1 Hz is suggested in order to accurately recognize and exclude non-sinus beats for appropriate HRV measures.

Low pass corner frequency even at 20 Hz results in exact RR-interval detection in the uncorrupted series at every VCD due to the practically constant phase shift of the ventricular complex. The main frequency content of the ventricular complex is in the range of 2-20 Hz with a maximum at 12 Hz (in Merri et al 1990), therefore this lower upper corner frequency can be sufficient for the exact localization of the ventricular complex fiducial point. The phase shift of the ventricular complex correlates with the theoretical group delay of the given filter, with the exception of the 20 Hz low pass 4<sup>th</sup> order Butterworth filter, where the calculated group delay is 20.9-29.0 ms in the band of 2-20 Hz, whereas the measured ventricular complex delay was 12-14 ms on the ascending slope, 14-15 ms on the peak, and 18-20 ms on the descending slope. Normal sinus beats show nearly uniform shape and slew rate of the ventricular complex, therefore filtering does not cause slew rate-dependent jitter in the detection of fiducial point. On the other hand, the maximum phase shift divergence in the range of 65-115 ms VCD is 0 ms on the ascending slope and peak at 100 Hz corner frequency and it remains below or equal to 2 ms even at 20 Hz cutoff. It is important to note that the VCD is slightly broadened due to the larger delay of the descending slopes.

Bessel filter at 20 Hz low pass is superior in the RR-interval detection in power line interference corrupted series, which may be related to its smoother and smaller impulse response. The Butterworth filter or the 40 Hz cutoff seems to be insufficient for power line interference suppression at the examined AC amplitudes. If necessary, power line interference may be managed by notch filtering without compromising the accuracy and precision of heart rate detection (Hejfel 2004).

Gaussian random noise representing EMG artifact may produce significant errors in RR-interval measurement proportionally to its magnitude. Up to 10% rms amplitude it can be prevented by 20-100 Hz low pass filtering within 1 ms maximal deviation, whereas up to 25% amplitude by 20-40 Hz low pass within 2 ms error by

both Bessel and Butterworth type filters. 50% noise causes higher error even at 20 Hz corner frequency.

A corner frequency of 20 Hz for the ECG amplifier is sufficient for accurate HRV measurement with the applied simple peak detecting algorithm; we can increase it for better preservation of the ECG morphology.

Consistently with our observations, Ruha and coworkers constructed a microprocessor-based QRS-detector system with 1 ms timing accuracy using a 0.5-35 Hz analog band pass ECG amplifier (Ruha et al 1997). The limitations of the present investigation may be the strictly uniform ventricular complex morphology, however, VCDs of 65-115 ms show nearly the same phase shift, therefore not affecting RR-measurements. Considering that the errors of the different phases of signal processing are additive, it is suggested to test the entire system with the given frequency response before performing HRV measurements.

## **5.2. Testing the effects of AC notch filtering**

The ventricular complex timing error caused by AC interference can produce a considerable additional fluctuation with a uniformly distributed random noise that results in invalid measures of RR-intervals and consequently heart rate variability either in the frequency domain (Merri et al 1990) or in the time domain, especially in parameters reflecting the beat-to-beat or high frequency variability.

Analog power line interference notch filtering may slightly distort the ventricular complex (*Fig. 5.1.*), however does not cause timing error greater than 1 ms in the R-detection in our study. Ventricular complex detection at the peak is not suggested in spite of its observed relative resistance to the added low-level noise. Most of the structural feature-type R-detectors trigger on the ascending or descending slope (or both) of the ventricular complex in order to avoid inaccurate and imprecise triggering related to split peaks (ventricular asynchrony) those can vary dynamically.



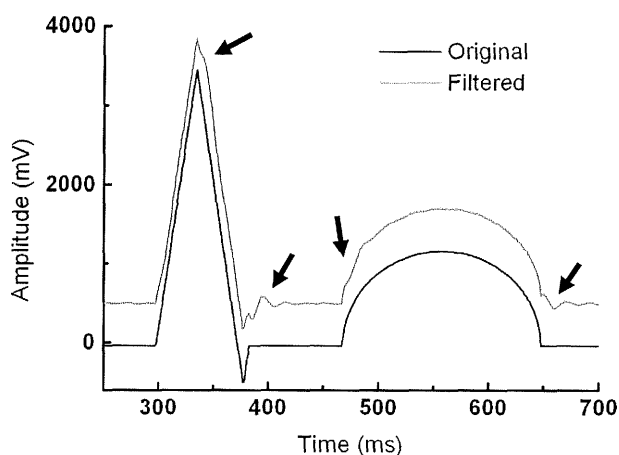


*Fig. 5.1. Detailed view of the distortion caused by the analog power line notch filtering related to its impulse-response (at the arrows). The filtered signal was shifted by 500 mV upward for better separation.  $R_s=85$  ms, filter  $Q=2$ .*

### 5.3. Effects of the sampling rate on the time domain parameters

In this set of model, the mean heart rate was considerably resistant to the sampling error that acts as an added random series with a zero mean. This error is additive to the other parameters resulting in elevated relative accuracy and precision errors, especially in lower-variability tachograms. The similarity of the SDNN-RAE graphs in trend and magnitude between the two main groups was based on the same adjusted SDs. The RMSSD and pNN50 had different trends in the two main groups, reflecting more decreased beat-to-beat (high-frequency) variability in the tachograms based on the high-risk patient's ECG, in spite of the equal adjusted overall variability.

According to the RAE and RPE, the pNN50 was unreliable even at 1 ms SI in the low-variability series; therefore, this measure is not recommended in accordance with the Task Force (Task Force 1996). The applied threshold of 50 ms gives pNN50 a discrete nature, which is the reason for the statistical weakness of this parameter (Malik 1996).

Digitization at a given sampling interval acts as a proportionally additive noise to the extent of the true variability; consequently in smaller variability tachograms (from seriously diseased patients) this process will add greater relative errors, see the analysis of our two original human tachograms in *Table 4.1*. Digitization error may affect the measured HRV on its own or together with other additive technical artifacts. Based on present investigation, a 1 ms sampling interval will minimize digitization-

mediated errors for short-term HRV analysis in the time domain. In case of extremely reduced-variability samples, SIs below 1 ms may be recommended without interpolation; on the other hand, even 5 ms SI can be appropriate for higher-variability series. However, interpolation methods can improve the time-resolution of a poor-quality ECG record, reducing the sampling error (Daskalov and Christov 1997).

Laguna and Sörnmo (2000) found their 3 kHz sampling surprising considering this far higher frequency necessary to the digitization of the ECG signal with 50-200 Hz typical analog upper corner frequency. Our results with the sufficient 20 Hz low pass and the required 1 kHz sampling are similarly unexpected. Considering the information carried in the ECG signal decomposing to frequency and phase constituents, the latter one is proved superior in exact RR-interval detection.

## 6. Conclusions

A frequency band pass of 0.5-20 Hz may be sufficient in the ECG amplifier used for exclusively HRV analysis, which relatively preserves ECG morphology, and improves the accuracy and precision of heart rate detection by reducing AC interference and electromyography noise.

Suppression of the ubiquitous power line interference is recommended in the ECG equipment for HRV analysis, since notch filtering itself does not deteriorate the accuracy of RR-interval detection, rather improves it in cases where significant AC corruption is present.

The mean heart rate interval is extremely resistant to the sampling error. For accurate measurement of SDNN and RMSSD even in patients with seriously reduced variability, 1 ms SI is recommended. However, lower sampling rate may be satisfactory in cases where higher variability or higher changes in variability are expected. The pNN50 is not a reliable measure even at 1 ms SI; therefore its use is not suggested in HRV analysis.

The above investigations expectantly call attention and demand to avoid some ignored technical pitfalls of HRV analysis, which may contribute to elucidate present ambiguous results persisting in this escalating field of cardiology.

## 7. Novel findings

In the available literature there is no similar meticulous investigation on the corner frequencies, AC notch filtering and sampling rate of the ECG for time domain HRV analysis related to the accuracy and precision of heart rate interval detection and the HRV indices. Our examination clearly demonstrates the adverse effects of some inappropriate technical conditions on the accuracy and reliability of HRV measurements. The sampling rate and upper band frequency cutoff suggested by the most comprehensive Task Force for HRV analysis has been obviously refuted by our empirical studies. On the contrary, the 200 Hz upper corner frequency recommended by that paper may retain more high-frequency noise, which can result in considerable errors of RR-interval detection, and consequently false HRV measures.

## 8. References

1. Adamson PB, Smith AL, Abraham WT, Klecker KJ, Stadler RW, Shith A, Rhodes MM: Continuous automatic assessment in patients with symptomatic heart failure. Prognostic value of heart rate variability by an implanted cardiac resynchronization device. *Circulation* 2004, 110(16):2389-2394
2. Akselrod S, Gordon D, Ubel FA, Shannon DC, Barger AC, Cohen RJ: Power spectrum analysis of heart rate fluctuation: a quantitative probe of beat-to-beat cardiovascular control. *Science* 1981, 213: 220-222
3. Amar D, Zhang H, Miodowik S, Kadish AH: Competing autonomic mechanism precede the onset of postoperative atrial fibrillation. *J Am Coll Cardiol* 2003, 42:1262-1268
4. Antelmi I, De Paula RS, Shinzato AR, Peres CA, Mansur AJ, Grupi CJ: Influence of age, gender, body mass index, and functional capacity on heart rate variability in a cohort of subjects without heart disease. *Am J Cardiol* 2004, 93:381-385
5. Appel ML, Berger RD, Saul JP, Smith JM, Cohen RJ: Beat to beat variability in cardiovascular variables: noise or music? *J Am Coll Cardiol* 1989, 14: 1139-1148
6. Aubert AE, Ramaekers D: Neurocardiology: the benefits of irregularity. *Acta Cardiol* 1999, 54: 107-120
7. Bailey JJ, Berson AS, Garson A, Horan LG, Macfarland PW, Mortara DW, Zywertz C: Recommendation for standardization and specification in automated electrocardiography: bandwidth and digital signal processing. A report for health professionals by ad hoc writing group of the committee on electrocardiography and cardiac electrophysiology of the council on clinical cardiology, American Heart Association. *Circulation* 1990, 81(2):730-739
8. Barr RC, Spach MS: Sampling rates required for digital recording of intracellular and extracellular cardiac signals. *Circulation* 1977, 55:40-48
9. Barros AK, Ohnishi N: Heart rate instantaneous frequency (HIF): an alternative approach to extract heart rate variability. *IEEE Trans Biomed Eng* 2001, 48:850-855
10. Bernardi L, Wdowczyk-Szulc J, Valenti C, Castoldi S, Passino C, Spadicini G, Sleight P: Effects of controlled breathing, mental activity and mental stress with or without verbalization on heart rate variability. *J Am Col Cardiol* 2000, 35:1462-1469
11. Berntson GG, Bigger Jr JT, Eckberg DL, Grossman P, Kaufmann PG, Malik M, Nagaraja HN, Porges SW, Saul JP, Stone PH, van der Molen M: Heart rate

- variability: Origins, methods, and interpretive caveats. *Psychophysiology* 1997, 34:623-648
12. Berntson GG, Stowell JR: ECG artifacts and heart period variability: don't miss a beat! *Psychophysiology* 1998, 35:127-132
  13. Bettoni M, Zimmermann M: Autonomic tone variations before the onset of paroxysmal atrial fibrillation. *Circulation* 2002, 105:2753-2759
  14. Bianchi AM, Mainardi LT, Cerutti S: Signal processing. In Moss AJ, Stern S (Ed): *Noninvasive electrocardiology. Clinical aspects of Holter monitoring*. WB Saunders Co Ltd, London, 1996, pp 11-35
  15. Bickel A, Yahalom M, Roguin N, Frankel R, Breslava J, Ivry S, Eitan A: Power spectral analysis of heart rate variability during positive pressure pneumoperitoneum. *Surg Endosc* 2002, 16:1341-1344
  16. Bigger JT, Fleiss JL, Rolnitzky LM, Steinman RC: The ability of several short-term measures of RR variability to predict mortality after myocardial infarction. *Circulation* 1993, 88:927-934
  17. Bigger Jr JT: Heart rate variability: frequency domain. In: Moss AJ, Stern S (eds): *Noninvasive electrocardiology. Clinical aspects of Holter monitoring*. WB Saunders Company Ltd, 1996, London, pp 175-198
  18. Boker A, Graham MR, Walley KR, McManus BM, Girling LG, Walker E, Lefevre GR, Mutch WA: Improved arterial oxygenation with biologically variable or fractal ventilation using low tidal volumes in a porcine model of acute respiratory distress syndrome. *Am J Respir Crit Care Med* 2002, 165(4):456-462
  19. Böhm B, Rötting N, Schwenk W, Grebe S, Mansmann U: A prospective randomized trial on heart rate variability of the surgical team during laparoscopic and conventional sigmoid resection. *Arch Surg* 2001, 136:305-310
  20. Brennan M, Palaniswami M, Kamen P: Do existing measures of Poincaré plot geometry reflect nonlinear features of heart rate variability? *IEEE Trans Biomed Eng* 2001, 48:1343-1347
  21. Camm AJ, Pratt CM, Schwartz PJ, Al-Khalidi HR, Holroyde MJ, Karam R, Sonnenblick EH, Brum JM, ALIVE Investigators: Mortality in patients after a recent myocardial infarction: a randomized, placebo-controlled trial of azimilide using heart rate variability for risk stratification. *Circulation* 2004, 109:990-996
  22. Camman H, Michel J: How to avoid misinterpretation of heart rate variability power spectra? *Comput Method Program Biomed* 2002, 68:15-23
  23. Carpeggiani C, L'Abbate A, Landi P, Michelassi C, Raciti M, Macerata A, Emdin M: Early assessment of heart rate variability is predictive of in-hospital

death and major complications after acute myocardial infarction. *Int J Cardiol* 2004, 96:361-368

24. Carr JJ, Brown J: *Introduction to Biomedical Equipment Technology*. 4<sup>th</sup> edition, Pearson Education, 2000, pp 197-231
25. Chiou CW, Eble JN, Zipes DP: Efferent innervation of the canine atria and sinus and atrioventricular nodes. *Circulation* 1997, 95: 2573-2584
26. Christ F, Abicht JM, Athellogou M, Baschnegger H, Niklas M, Peter K, Messmer K: Cardiovascular monitoring of elective aortic aneurysm repair using methods of chaos analysis. *Int J Microcirc* 1997, 17:374-384
27. Christov II, Dotsinsky IA, Daskalov IK: High-pass filtering of ECG signals using QRS elimination. *Med Biol Eng Comput* 1992, 30:253-256
28. Christov II, Daskalov IK: Filtering of electromyogram artifacts from the electrocardiogram. *Med Eng Phys* 1999, 21:731-736
29. Christov II: Dynamic powerline interference subtraction from biosignals. *J Med Eng Techn* 2000, 24:169-172
30. Cripps TR, Malik M, Farrell TG, Camm AJ: Prognostic value of reduced heart rate variability after myocardial infarction: clinical evaluation of a new analysis method. *Br Heart J* 1991, 65:14-19
31. Daskalov IK, Christov II: Improvement of resolution in measurement of electrocardiogram RR intervals by interpolation *Med Eng Phys* 1997, 19:375-379
32. Daskalov IK, Christov II: Electrocardiogram signal preprocessing for automatic detection of QRS boundaries. *Med Eng Phys* 1999, 21:37-44
33. Dekker JM, Crow RS, Folsom AR, Hannan PJ, Liao D, Swenne CA, Schouten EG: Low heart rate variability in a 2-minute rhythm strip predicts risk of coronary heart disease and mortality from several causes: the ARIC study. *Atherosclerosis Risk in Communities*. *Circulation* 2000, 102:1239-1244
34. Denton TA, diamond GA, Helfant RH, Kham S, Karagueuzian H: Fascinating rhythm: a primer on chaos theory and its application to cardiology. *Am Heart J* 1990, 120:1419-1440
35. Dotsinsky IA, Daskalov IK: Accuracy of 50 Hz interference subtraction from an electrocardiogram. *Med Biol Eng Comp* 1996, 34:489-494
36. Driscoll D, DiCicco G: The effects of metronome breathing on the variability of autonomic activity measurements. *J Manipulative Physiol Ther* 2000, 23:610-614

37. Fortrat JO, Formet C, Frutoso J, Gharib C: Even slight movements disturb analysis of cardiovascular dynamics. *Am J Physiol* 1999, 46:H261-
38. Friesen GM, Janett TC, Jadallah MA, Yates SL, Quint SR, Nagle HT: A comparison of the noise sensitivity of nine QRS detection algorithms. *IEEE Trans Biomed Eng* 1990, 37:85-98
39. Garcia-Gonzalez MA, Fernandez-Chimeno M, Ramos-Castro J: Bias and uncertainty in heart rate variability spectral indices due to the finite ECG sampling frequency. *Physiol Meas* 2004, 25:489-504
40. Garde AH, Laursen B, Jørgensen AH, Jensen BR: Effects of mental and physical demands on heart rate variability during computer work. *Eur J Appl Physiol* 2002, 87:456-461
41. Ghuran A, Reid F, La Rovere MT, Schmidt G, Bigger JT, Camm J, Schwartz PJ, Malik M, ATRAMI Investigators: *Am J Cardiol* 2002, 89:184-190
42. Gleick J: *Chaos. Making a new science.* Penguin Books, 1988, Hungarian Translation: Szegedi P, Göncöl Publishing, Budapest, 1999
43. Gogenur I, Rosenberg-Adamsen S, Rasmussen V, Rosenberg J: Lack of circadian variation in the activity of the autonomic nervous system after major abdominal operations. *Eur J Surg* 2002, 168(4):242-246
44. Goldberger AL: *Physionet. Nonlinear dynamics, fractals, and chaos theory: implications for neuroanatomic heart rate control in health and disease.* <http://www.physionet.org/tutorials/ndc/> (1999)
45. Graham MR, Warrian RK, Girling LG, Doiron L, Lefevre GR, Cheang M, Mutch WA: Fractal or biologically variable delivery of cardioplegic solution prevents diastolic dysfunction after cardiopulmonary bypass. *J Thorac Cardiovasc Surg* 2002, 123(1):63-71
46. Grasso R, Rizzi G, Schena F, Cevese A: Arterial baroreceptors are not essential for low frequency oscillation of arterial pressure. *J Auton Nerv Syst* 1995, 50:323-331
47. Grimm W, Christ M, Bach J, Muller HH, Maisch B: Noninvasive arrhythmia risk stratification in idiopathic dilated cardiomyopathy: results of the Marburg Cardiomyopathy study. *Circulation* 2003, 108:2883-2891
48. Hakala T, Vanninen E, Hedman A, Hippelainen M: Analysis of heart rate variability does not identify the patients at risk of atrial fibrillation after coronary artery bypass grafting. *Scand Cardiovasc J* 2002, 36(3):167-171
49. Halmai L, Rudas M, Makara P, Gingl Z, Rudas L: Immediate effects of smoking on cardiovascular autonomic modulation. *Card Hung* 2003, 33:110-116

50. Hansen AL, Johnsen BH, Sollers JJ, Stenvik K, Thayer JF: Heart rate variability and its relation to prefrontal cognitive function: the effects of training and detraining. *Eur J Appl Physiol* 2004, Aug 25 (Epub)
51. Hayano J, Yasuma F: Hypothesis: respiratory sinus arrhythmia is an intrinsic resting function of cardiopulmonary system. *Cardiovasc res* 2003, 58:1-9
52. Hejmel L: Estimating stress by heart rate variability analysis. XVII Congress on Hungarian Experimental Surgery, Szeged, September 16-18, 1999 (Hungarian)
53. Hejmel L: The Poincaré-plot in heart rate variability analysis. *Acta Physiol Hung* 2002, 89:129 (abstract)
54. Hejmel L, Gal I: Heart rate variability analysis as a tool for quantifying the stress of the surgical team during laparoscopic versus open surgeries. *Eur J Surg Res* 2002, 34(S1):61 (abstract)
55. Heneghan C, Shouldice R, Nolan P, Sheridan E, O'Malley M, Nolan PG, Cullen J, McNicholas W: Independent autonomic modulation of the sinoatrial and atrioventricular nodes assessed through RR and PR interval variation. *Comp Cardiol* 2001, 28:205-208
56. Hogue CW, Domitrovich PP, Stein PK, Despotis GD, Schuessler RB, Kleiger RE, Rottman JN: RR interval dynamics before atrial fibrillation in patients after coronary artery bypass graft surgery. *Circulation* 1998, 98(5):429-434
57. Hon EH, Lee ST: Electronic evaluations of the fetal heart rate patterns preceding fetal death: further observations. *Am J Obstet Gynecol* 1965, 87: 814-826
58. Horner SM, Murphy CF, Coen B, Harrison FG, Vespalcova Z, Lab MJ: Contribution to heart rate variability by mechanoelectric feedback. Stretch of the node reduces heart rate variability. *Circulation* 1996, 94: 1762-1767
59. Huikuri HV, Seppänen T, Koistinen MJ, Airaksinen KEJ, Ikäheimo MJ, Castellanos A, Myerburg RJ: Abnormalities in beat-to-beat dynamics of heart rate before the spontaneous onset of life-threatening ventricular tachyarrhythmias in patients with prior myocardial infarction. *Circulation* 1996, 93:1836-1844
60. Huikuri HV, Mäkitallio TH, Peng CK, Goldberger AL, Hintze U, Møller M, DIAMOND Study Group: Fractal correlation properties of R-R interval dynamics and mortality in patients with depressed left ventricular function after an acute myocardial infarction. *Circulation* 2000, 101:47-53
61. Hukuri HV, Mäkitallio TH, Perkiömäki J: Measurement of heart rate variability by methods based on nonlinear dynamics. *J Electrocard* 2003, 36S:95-99
62. Inagaki H, Kuwahara M, Taubone H: Effects of psychological stress on autonomic control of heart in rats. *Exp Anim* 2004, 53(4):373-378



63. Javorka M, Zila I, Balharek T, Javorka K: Heart rate recovery after exercise: relations to heart rate variability and complexity. *Braz J Med Biol Res* 2002, 35(8):991-1000
64. Kennedy HL: Holter recorders and analytic systems. In Moss AJ, Stern S (Ed): *Noninvasive electrocardiology. Clinical aspects of Holter monitoring*. WB Saunders Co Ltd, London, 1996, pp 5-10
65. Kleiger RE, Miller JP, Bigger JT, Moss AJ, Multicenter Post-infarction Research Group: Decreased heart rate variability and its association with increased mortality after acute myocardial infarction. *Am J Cardiol* 1987, 59: 256-262
66. Kong L, Middleton J, Avolio A: Relation between flight assessment scores and heart rate and blood pressure variability during pursuit tracking tasks in ab-initio student airline pilots. *ESH-BAVAR Congress*, 2004 June 11-12, Angers, France
67. Kuo CD, Chen GY, Lai ST, Wang YY, Shih CC, Wang JH: Sequential changes in heart rate variability after coronary artery bypass grafting. *Am J Cardiol* 1999, 83:776-779
68. Laciár E, Jane R, Brooks DH: Improved alignment method for noisy high-resolution ECG and Holter records using multiscale cross-correlation. *IEEE Trans Biomed Eng* 2003, 50:344-353
69. Lampert R, Ickovics JR, Viscoli CJ, Horwitz RI, Lee FA: Effects of propranolol on recovery of heart rate variability following acute myocardial infarction and relation to outcome in the Beta-blocker Heart Attack Trial. *Am J Cardiol* 2003, 91:137-142
70. Lang E, Szilagyi N, Metneki J, Weisz J: Effects of mental load on the spectral components of heart period variability in twins. *Acta Biochim Biophys Hung* 1991-1992, 26:111-120
71. La Rovere MT, Pinna GD, Hohnloser SH, Marcus FI, Mortara A, Nohara R, Bigger JT, Camm AJ, Schwartz PJ: Baroreflex sensitivity and heart rate variability in the identification of patients at risk for life-threatening arrhythmias. *Circulation* 2001, 103: 2072-2077
72. La Rovere MT, Pinna GD, Maestri R, Mortara A, Capomolla S, Febo O, Ferrari R, Franchini M, Gnemmi M, Opasich C, Riccardi PG, Traversi E, Cobelli F: Short-term heart rate variability strongly predicts sudden cardiac death in chronic heart failure patients. *Circulation* 2003, 107:565-570
73. Levy WC, Cerqueira MD, Harp GD, Johannessen KA, Abrass IB, Schwartz RS, Stratton JR: Effects of endurance exercise training on heart rate variability at rest in healthy young and older men. *Am J Cardiol* 1998, 82:1236-1241

74. Liao D, Cai J, Barnes RW, Tyroler HA, Rautaharju P, Holme I, Heiss G: Association of cardiac autonomic function and the development of hypertension: the ARIC study. *Am J Hypertens* 1996, 9:1147-1156
75. Liao D, Sloan RP, Cascio WE, Folsom AR, Liese AD, Evans GW, Cai J, Sharret AR: Multiple metabolic syndrome is associated with lower heart rate variability. *Diabetes Care* 1998, 21(12):2116-2122
76. Lipsitz LA, Mietus J, Moody GB, Goldberger AL: Spectral characteristics of heart rate variability before and during postural tilt. *Circulation* 1990, 81:1803-1810
77. Lipsitz LA: Physiological complexity, aging and the path to frailty. *Sci Aging Knowledge Environ* 2004, 16:pe16
78. Lombardi F: Technical considerations. In Moss AJ, Stern S (Ed): *Noninvasive electrocardiology. Clinical aspects of Holter monitoring*. WB Saunders Co Ltd, London, 1996, pp 3-4
79. Lombardi F, Tarricone D, Tundo F, Colombo F, Belletti S, Fiorentini C: Autonomic nervous system and paroxysmal atrial fibrillation: a study based on the analysis of RR interval changes before, during and after paroxysmal atrial fibrillation. *Eur Heart J* 2004, 25(14):1242-1248
80. Magari SR, Hauser R, Schwartz J, Williams PL, Smith TJ, Christiani DC: Association of heart rate variability with occupational and environmental exposure to particulate air pollution. *Circulation* 2001, 104:986-991
81. Mäkikallio TH, Høiber S, Køber L, Tarp-Pedersen C, Peng CK, Goldberger AL, Huikuri H, TRACE investigators: Fractal analysis of heart rate dynamics as a predictor of mortality in patients with depressed left ventricular function after myocardial infarction. *Am J Cardiol* 1999, 83:836-839
82. Malik M, Camm AJ: Components of heart rate variability – what they really mean and what we really measure. *Am J Cardiol* 1993, 72: 821-822
83. Malik M: Heart rate variability: time domain. In Moss AJ, Stern S (Ed): *Noninvasive electrocardiology. Clinical aspects of Holter monitoring*. WB Saunders Co Ltd, London, 1996, pp 161-173
84. Malpas SC: Neural influences on cardiovascular variability: possibilities and pitfalls. *Am J Physiol Heart Circ Physiol* 2002, 282:H6-H20
85. Merri M, Farden DC, Mottley JG, Titlebaum EL: Sampling frequency of the electrocardiogram for spectral analysis of the heart rate variability. *IEEE Trans Biomed Eng* 1990, 37:99-106
86. Molina J: Design a 60 Hz notch filter with the UAF42. *Burr-Brown Application Bulletin*, 1994

87. Muiesan ML, Rizzoni D, Zulli R, Castellano M, Bettoni G, Porteri E, Agabiti-Rosei E: Power spectral analysis of the heart rate in hypertensive patients with and without left ventricular hypertrophy: the effect of a left ventricular mass reduction. *J Hypertens* 1998, 16:1641-1650
88. Mullen TJ, Cohen RJ: RR-interval monitoring. In Moss AJ, Stern S (Ed): *Noninvasive electrocardiology. Clinical aspects of Holter monitoring*. WB Saunders Co Ltd, London, 1996, pp 155-160
89. Mutch WAC, Warrian RK, Eschun GM, Girling LG, Doiron L, Cheang MS, Lefevre GR: Biologically variable pulsation improves jugular venous oxygen saturation during rewarming. *Ann Thorac Surg* 2000, 69:491-497
90. Nagel JH: Biopotential amplifiers. In: Bronzino JD: *Biomedical engineering hand book*, 2<sup>nd</sup> edition, Springer-Verlag New York, 2000, pp 70.1-70.14
91. Parthimos D, Edwards DH, Griffith TM: Comparison of chaotic and sinusoid vasomotion in the regulation of microvascular flow. *Cardiovasc Res* 1996, 31:388-399
92. Persson PB: Spectrum analysis of cardiovascular time series. *Am J Physiol* 1997, 273: R1201-R1210
93. Pikkujämsä SM, Mäkikallio TH, Sourander LB, Räihä IJ, Puukka P, Skyttä J, Peng C, Goldberger AL, Huikuri HV: Cardiac interbeat interval dynamics from childhood to senescence. *Circulation* 1999, 100:393-399
94. Pinna GD, Maestri R, Di Cesare A, Colombo R, Minuco G: The accuracy of power spectrum analysis of heart rate variability from annotated RR list generated by Holter systems. *Physiol Meas* 1994, 15:163-179
95. Pipberger HV, Arzbaeher RC, Berson AS, Briller SA, Brody DA, Flowers NC, Geselowitz DB, Lepeschkin E, Oliver GC, Schmitt OH, Spach M: Recommendations for standardization of leads and specification for instruments in electrocardiography and vectorcardiography: report of the Committee of Electrocardiography, American Heart Association. *Circulation* 1975, 52:11-31
96. Porges SW, Riniolo TC, McBride T, Campbell B: Heart rate and respiration in reptiles: contrasts between a sit-and-wait predator and an intensive forager. *Brain Cogn* 2003, 52(1):88-96
97. Pruvot E, Thonet G, Vesin JM, van-Melle G, Seidl K, Schmidinger H, Brachmann J, Jung W, Hoffmann E, Tavernier R, Block M, Podczek A, Fromer M: Heart rate dynamics at the onset of ventricular tachyarrhythmias as retrieved from implantable cardioverter-defibrillators in patients with coronary artery disease. *Circulation* 2000, 101:2398-2404
98. Reims HM, Sevre K, Fossum E, Hoiegggen A, Mellem H, Kjeldsen SE: Relations between insulin sensitivity, fitness and autonomic cardiac regulation in healthy, young men. *J Hypertens* 2004, 22(10):2007-2015

99. Reinhardt L, Mäkijärvi M, Fetsch T, Schulte G, Sierra G, Martinez-Rubio A, Montonen J, Katila T, Borggreffe M, Breithardt G: Noninvasive risk modeling after myocardial infarction. *Am J Cardiol* 1996, 78:627-632
100. Riniolo T, Porges SW: Inferential and descriptive influences on measures of respiratory sinus arrhythmia: sampling rate, R-wave trigger accuracy, and variance estimates. *Psychophysiology* 1997, 34(5):613-621
101. Ruediger H, Klinghammer HL, Scheuch K: The trigonometric regressive spectral analysis a method for mapping of beat-to-beat recorded cardiovascular parameters on to frequency domain in comparison with Fourier transformation. *Comput Methods Programs Biomed* 1999, 58:1-15
102. Ruediger H, Seibt R, Scheuch K, Krause M, Alam S: Sympathetic and parasympathetic activation in heart rate variability in male hypertensive patients under mental stress. *J Hum Hypertens* 2004, 18(5):307-315
103. Ruha A, Sallinen S, Nissilä S: A real-time microprocessor QRS detector system with a 1-ms timing accuracy for the measurement of ambulatory HRV. *IEEE Trans Biomed Eng* 1997, 44:159-167
104. Sahin I, Kosar F, Altunkan S, Günaydin M: Comparison of the effects of amlodipine and verapamil on autonomic activity in hypertensive patients. *Eur J Intern Med* 2004, 15:225-230
105. Sayers BMcA: Analysis of heart rate variability. *Ergonomics* 1973, 16: 17-32
106. Scalvini S, Volterrani M, Zanelli E, Pagani M, Mazzuero G, Coats A, Giordano A: Is heart rate variability a reliable method to assess autonomic modulation in left ventricular dysfunction and heart failure? Assessment of autonomic modulation with heart rate variability. *Int J Cardiol* 1998, 67:9-17
107. Schmidt G, Malik M, Barthel P, Schneider R, Ulm K, Rolnitzky L, Camm AJ, Bigger JT, Schömig A: Heart-rate turbulence after ventricular premature beats as a predictor of mortality after acute myocardial infarction. *Lancet* 1999, 353:1390-1396
108. Sheps DS, McMahon RP, Becker L, Carney RM, Freedland KE, Cohen JD, Sheffels D, Goldberger D, Ketterer MW, Pepine CJ, Raczynski JM, Light K, Krantz DS, Stone PH, Knatterud GL, Kaufmann PG: Mental stress-induced ischemia and all-cause mortality in patients with coronary artery disease. *Circulation* 2002, 105:1780-1784
109. Sinnreich R, Friedlander Y, Sapoznikov D, Kark JD: Familial aggregation of heart rate variability based on short recordings – the kibbutzim family study. *Hum Genet* 1998, 103:34-40
110. Smit AAJ, Timmers HJLM, Wieling W, Wagenaar M, Marres HAM, Lenders JWM, van Montfrans GA, Karemaker JM: Long-term effects of carotid sinus

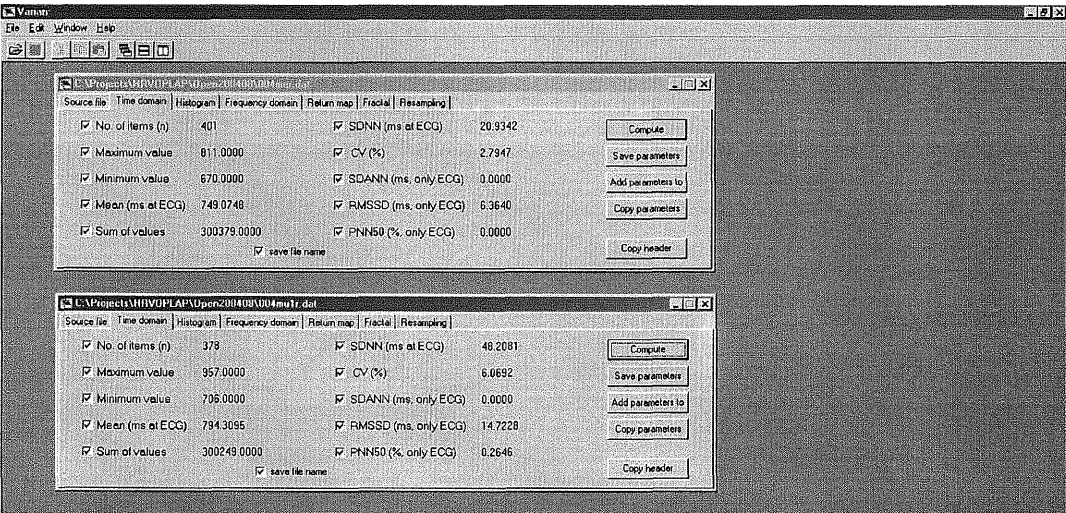
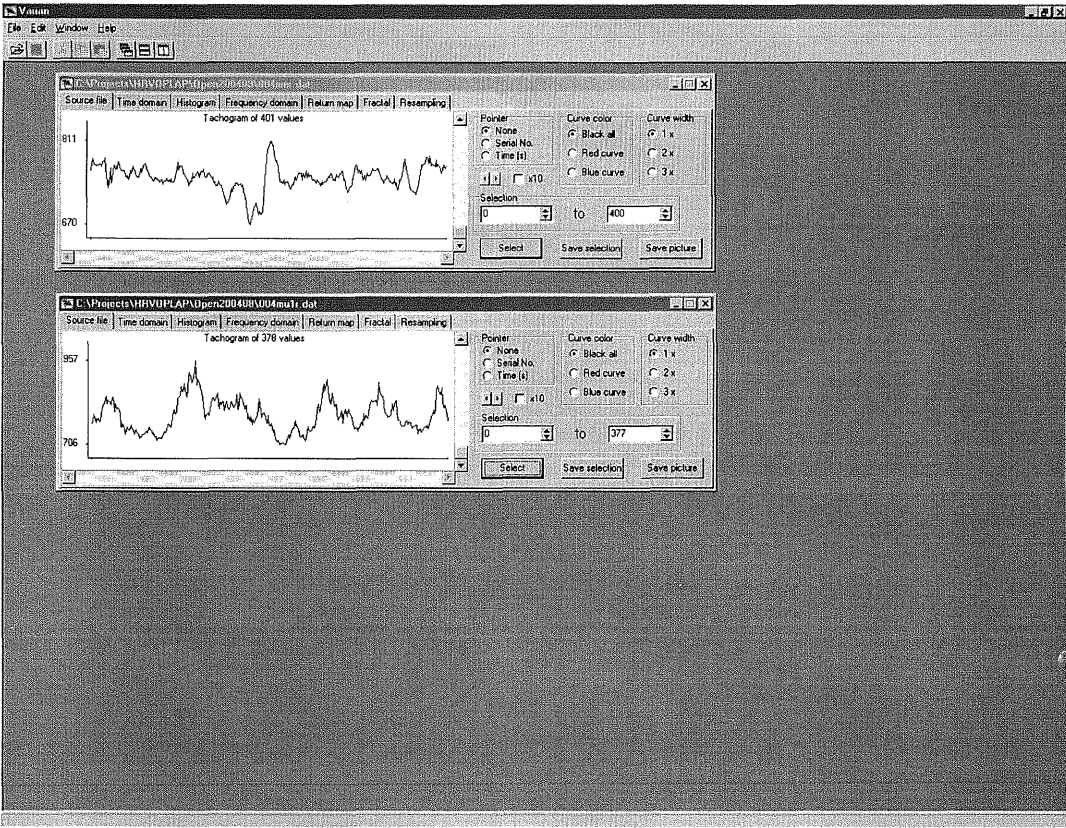
denervation on arterial blood pressure in humans. *Circulation* 2002, 105:1329-1335

111. Smith SW: The scientist and engineer's guide to digital signal processing. 2<sup>nd</sup> ed., San Diego, (CA), California Technical Publishing, 1999, Available at URL: [www.dspguide.com](http://www.dspguide.com)
112. Tabor Z, Michalski J, Rokita E: Influence of 50 Hz magnetic field on human heart rate variability: linear and nonlinear analysis. *Bioelectromagnetics* 2004, 25(6):474-480
113. Task Force of the European Society of Cardiology and the North American Society of Pacing and Electrophysiology: Heart rate variability. Standards of measurement, physiological interpretation, and clinical use. *Circulation* 1996, 93:1043-1065
114. Tomita T, Takei M, Saikawa Y, Hanaoka T, Uchikawa S, Tsutsui H, Aruga M, Miyashita T, Yazaki Y, Imamura H, Kinoshita O, Owa M, Kubo K: Role of autonomic tone in the initiation and termination of paroxysmal atrial fibrillation in patients without structural heart disease. *J Cardiovasc Electrophysiol* 2003, 14(6):559-564
115. Ueno LM, Hamada T, Moritani T: Cardiac autonomic nervous activities and cardiorespiratory fitness in older men. *J Gerontol A Biol Sci Med Sci* 2002, 57(9):M605-M610
116. Valentinuzzi ME, Geddes LA: The central component of the respiratory heart rate response. *Cardiovasc Res Cent Bull* 1974, 12:87-103
117. Voss A, Kurths J, Kleiner HJ, Witt A, Wessel N: Improved analysis of heart rate variability by methods of nonlinear dynamics. *J Electrocardiol* 1995, 28S:81-88
118. Wagner CD, Persson PB: chaos in the cardiovascular system: an update. *Cardiovasc. Res* 1998, 40:257-264
119. Waller BF, Schlant RC: Anatomy of the heart. In Hurst's The heart, Schlant RC, Alexander RC (Eds), McGraw-Hill Inc., New York, 1994, pp 59-112
120. West NH, van Vliet BN: Open-loop analysis of the pulmo-cutaneous baroreflex in the toad *Bufo marinus*. *Am J Physiol* 1983, 245:R642-R650
121. Wichterle D, Simek J, La Rovere MT, Schwartz PJ, Camm AJ, Malik M: Prevalent low-frequency oscillation of heart rate. Novel predictor of mortality after myocardial infarction. *Circulation* 2004, (Epub ahead of print)
122. Wijbenga JAM, Balk AHMM, Meij SH, Simoons ML, Malik M: Heart rate variability index in congestive heart failure: relation to clinical variables and prognosis. *Circulation* 1998, 99:1719-1724

123. Wolf MW, Varigos GA, Hunt D, Sloman JG: Sinus arrhythmia in acute myocardial infarction. *Med J Australia* 1978, 2: 52-53
124. Woo MA, Stevenson WG, Moser DK, Trelease RB, Harper RM: Patterns of beat-to-beat heart rate variability in advanced heart failure. *Am Heart J* 1992, 123:704-710
125. Ziarani AK, Konrad A: A nonlinear adaptive method of elimination of power line interference in ECG signals. *IEEE Trans Biomed Eng* 2002, 49:540-547
126. Ziegler D, Piolot R, Strassburger K, Lambeck H, Dannehl K: Normal ranges and reproducibility of statistical, geometric, frequency domain, and non-linear measures of 24-hour heart rate variability. *Horm metab Res* 1999, 31:672-679

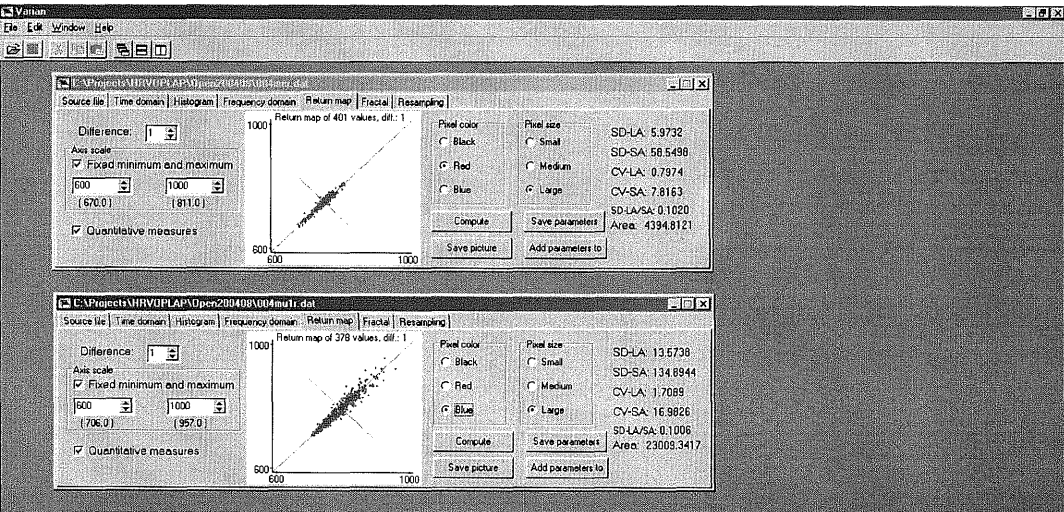
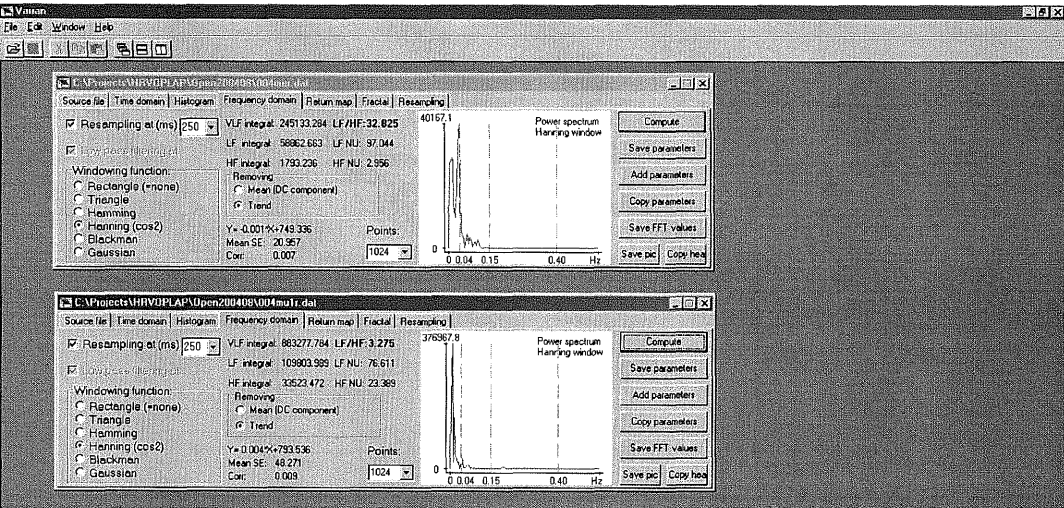
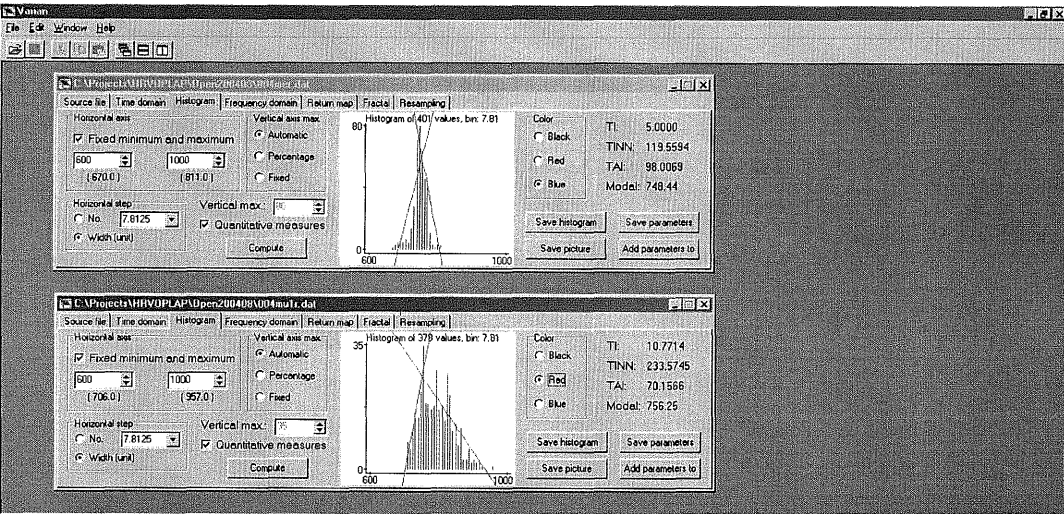
9. Appendix

Appendix A/1) Different windows of the HRV analyzer software.



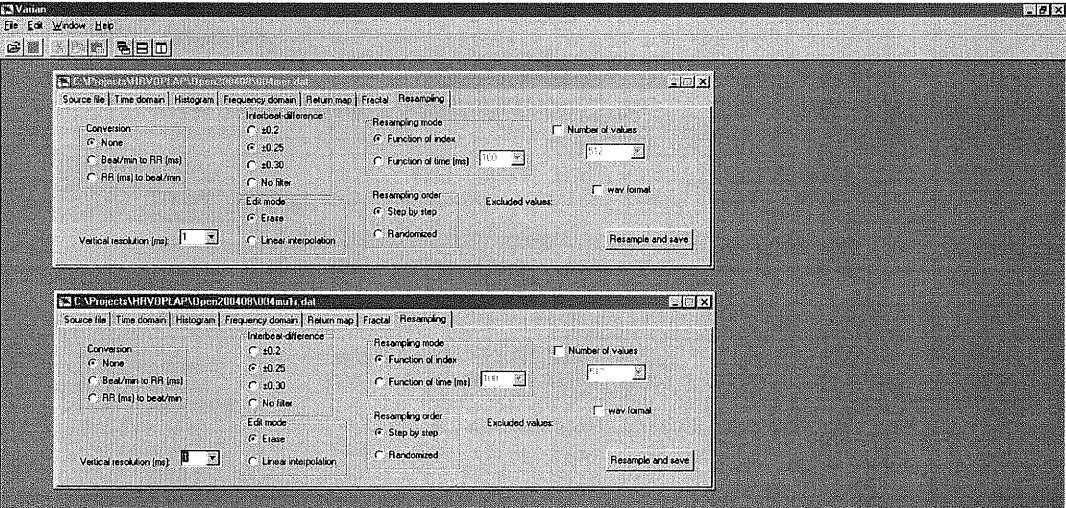
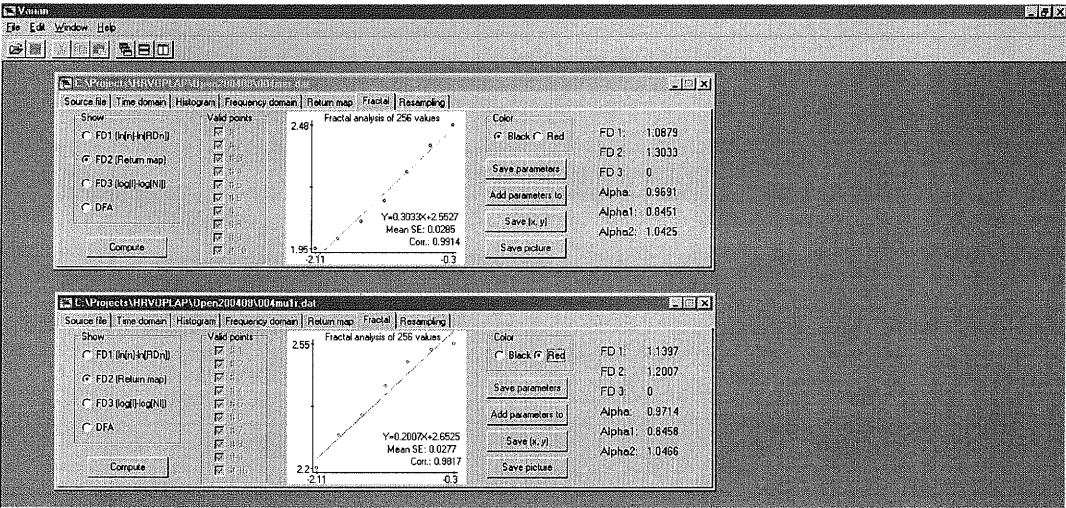


Appendix A/2) Different windows of the HRV analyzer software.





Appendix A/3) Different windows of the HRV analyzer software.



## Appendix B/1) The automatically generated record by the ECGAn 1.0 software.

ECG fiducial point analysis by ECGAn v1.0 (Laszlo Hejjei, MD; 2002 Sep.)								
Date: 12/27/2003 Time: 11:06:35 PM								
File: C:\Projects\ECG\phpfilt\ECG803x85\ecg803x85-400lp.bin								
Number of detected peaks: 21								
Serial#	Asc1/3 (ms)	Asc1/2 (ms)	Asc2/3 (ms)	Peak  (mV)	Ampl (ms)	Desc2/3 (ms)	Desc1/2 (ms)	Desc1/3
1. Original:	310	316	322	335	3496	348	354	360
Filtered:	310	316	322	336	3441	349	355	361
Difference:	0	0	0	1	-55	1	1	1
2. Original:	1113	1119	1125	1138	3496	1151	1157	1163
Filtered:	1113	1119	1125	1139	3441	1152	1158	1164
Difference:	0	0	0	1	-55	1	1	1
3. Original:	1916	1922	1928	1941	3496	1954	1960	1966
Filtered:	1916	1922	1928	1942	3442	1955	1961	1967
Difference:	0	0	0	1	-54	1	1	1
4. Original:	2719	2725	2731	2744	3496	2757	2763	2769
Filtered:	2719	2725	2731	2745	3442	2758	2764	2770
Difference:	0	0	0	1	-54	1	1	1
5. Original:	3522	3528	3534	3547	3496	3560	3566	3572
Filtered:	3522	3528	3534	3548	3442	3561	3567	3573
Difference:	0	0	0	1	-54	1	1	1
6. Original:	4325	4331	4337	4350	3496	4363	4369	4375
Filtered:	4325	4331	4337	4351	3442	4364	4370	4376
Difference:	0	0	0	1	-54	1	1	1
7. Original:	5128	5134	5140	5153	3496	5166	5172	5178
Filtered:	5128	5134	5140	5154	3441	5167	5173	5179
Difference:	0	0	0	1	-55	1	1	1
8. Original:	5931	5937	5943	5956	3496	5969	5975	5981
Filtered:	5931	5937	5943	5957	3441	5970	5976	5982
Difference:	0	0	0	1	-55	1	1	1
9. Original:	6734	6740	6746	6759	3496	6772	6778	6784
Filtered:	6734	6740	6746	6760	3441	6773	6779	6785
Difference:	0	0	0	1	-55	1	1	1
10. Original:	7537	7543	7549	7562	3496	7575	7581	7587
Filtered:	7537	7543	7549	7563	3442	7576	7582	7588
Difference:	0	0	0	1	-54	1	1	1
11. Original:	8340	8346	8352	8365	3496	8378	8384	8390
Filtered:	8340	8346	8352	8366	3442	8379	8385	8391
Difference:	0	0	0	1	-54	1	1	1
12. Original:	9143	9149	9155	9168	3497	9181	9187	9193
Filtered:	9143	9149	9155	9169	3442	9182	9188	9194
Difference:	0	0	0	1	-55	1	1	1
13. Original:	9946	9952	9958	9971	3496	9984	9990	9996
Filtered:	9946	9952	9958	9972	3442	9985	9991	9997
Difference:	0	0	0	1	-54	1	1	1
14. Original:	10749	10755	10761	10774	3496	10787	10793	10799
Filtered:	10749	10755	10761	10775	3440	10788	10794	10800
Difference:	0	0	0	1	-56	1	1	1

Appendix B/2) The automatically generated record by the ECGAn 1.0 software.

15. Original:	11552	11558	11564	11577	3496	11590	11596	11602
Filtered:	11552	11558	11564	11578	3441	11591	11597	11603
Difference:	0	0	0	1	-55	1	1	1
16. Original:	12355	12361	12367	12380	3496	12393	12399	12405
Filtered:	12355	12361	12367	12381	3442	12394	12400	12406
Difference:	0	0	0	1	-54	1	1	1
17. Original:	13158	13164	13170	13183	3495	13196	13202	13208
Filtered:	13158	13164	13170	13184	3442	13197	13203	13209
Difference:	0	0	0	1	-53	1	1	1
18. Original:	13961	13967	13973	13986	3496	13999	14005	14011
Filtered:	13961	13967	13973	13987	3442	14000	14006	14012
Difference:	0	0	0	1	-54	1	1	1
19. Original:	14764	14770	14776	14789	3496	14802	14808	14814
Filtered:	14764	14770	14776	14790	3441	14803	14809	14815
Difference:	0	0	0	1	-55	1	1	1
20. Original:	15567	15573	15579	15592	3496	15605	15611	15617
Filtered:	15567	15573	15579	15593	3441	15606	15612	15618
Difference:	0	0	0	1	-55	1	1	1
21. Original:	16370	16376	16382	16395	3496	16408	16414	16420
Filtered:	16370	16376	16382	16396	3441	16409	16415	16421
Difference:	0	0	0	1	-55	1	1	1
DIFFERENCES:								
Maximum:	0	0	0	1	56	1	1	1
Mean:	0	0	0	1	-54.524	1	1	1
SD:	0	0	0	0	0.663	0	0	0
TACHOGRAM (in ms, Original/Filtered) Number of RR-periods: n=20 ser#=RR(n+1)-RR(n)								
Serial#	Asc1/3	Asc1/2	Asc2/3	Peak	Desc2/3	Desc1/2	Desc1/3	
1.	803/803	803/803	803/803	803/803	803/803	803/803	803/803	
2.	803/803	803/803	803/803	803/803	803/803	803/803	803/803	
3.	803/803	803/803	803/803	803/803	803/803	803/803	803/803	
4.	803/803	803/803	803/803	803/803	803/803	803/803	803/803	
5.	803/803	803/803	803/803	803/803	803/803	803/803	803/803	
6.	803/803	803/803	803/803	803/803	803/803	803/803	803/803	
7.	803/803	803/803	803/803	803/803	803/803	803/803	803/803	
8.	803/803	803/803	803/803	803/803	803/803	803/803	803/803	
9.	803/803	803/803	803/803	803/803	803/803	803/803	803/803	
10.	803/803	803/803	803/803	803/803	803/803	803/803	803/803	
11.	803/803	803/803	803/803	803/803	803/803	803/803	803/803	
12.	803/803	803/803	803/803	803/803	803/803	803/803	803/803	
13.	803/803	803/803	803/803	803/803	803/803	803/803	803/803	
14.	803/803	803/803	803/803	803/803	803/803	803/803	803/803	
15.	803/803	803/803	803/803	803/803	803/803	803/803	803/803	
16.	803/803	803/803	803/803	803/803	803/803	803/803	803/803	
17.	803/803	803/803	803/803	803/803	803/803	803/803	803/803	
18.	803/803	803/803	803/803	803/803	803/803	803/803	803/803	
19.	803/803	803/803	803/803	803/803	803/803	803/803	803/803	
20.	803/803	803/803	803/803	803/803	803/803	803/803	803/803	
Max. Diff.:	0	0	0	0	0	0	0	
Mean:	803/803	803/803	803/803	803/803	803/803	803/803	803/803	
SD:	0/0	0/0	0/0	0/0	0/0	0/0	0/0	

# Appendix C/1)

Timing (position) differences and RR-interval alterations of uncorrupted artificial ECG signal consisting of 21 cycles after 2<sup>nd</sup> order Butterworth high-pass filtering at  $f_{3dB}=0.1...10$  Hz measured at different points of the ventricular complexes, expressed in ms relative to the appropriate point of the uncorrupted series before filtering.

Nominal heart rate period: 803 ms. VCD-ventricular complex duration, Pmaxd – maximal timing difference (positive values represent delay) and Pmean±SD – mean timing difference of the actual filtered record compared to unfiltered one, RRmean±SD – mean RR-interval and RRmaxd – maximal deviation from nominal value after filtering, Asc1/3, Asc1/2, Asc2/3 – relative time points at the actual height of the ascending slope, Peak – relative time points at the peaks of the ventricular complexes, Desc2/3, Desc1/2. Desc1/3 – relative time points at the actual height of the descending slope. Amplitude in mV, time values in ms.

	Asc1/3	Asc1/2	Asc2/3	Peak	Amplitude	Desc2/3	Desc1/2	Desc1/3
VCD=65 ms, $f_{3dB}=0.1$ Hz, 2 <sup>nd</sup> order Butterworth, high-pass								
Pmean±SD	0.86±0.47	0.95±0.21	0.91±0.29	0.00±0.00	-242.47±52.05	-0.95±0.21	-1.29±0.45	-0.95±0.21
Pmaxd	1	1	1	0	-298	1	2	1
RRmean±SD	803.10±0.30	803.05±0.22	803.05±0.22	803.00±0.00	-	802.95±0.22	803.00±0.32	802.95±0.22
RRmaxd	1	1	1	0	-	1	1	1
VCD=65 ms, $f_{3dB}=0.5$ Hz, 2 <sup>nd</sup> order Butterworth, high-pass								
Pmean±SD	-1.00±0.00	0.00±0.00	0.00±0.00	0.00±0.00	-216.43±6.93	-1.00±0.00	-2.00±0.00	-2.00±0.00
Pmaxd	-1	0	0	0	-247	-1	-2	-2
RRmean±SD	803.00±0.00	803.00±0.00	803.00±0.00	803.00±0.00	-	803.00±0.00	803.00±0.00	803.00±0.00
RRmaxd	0	0	0	0	-	0	0	0
VCD=65 ms, $f_{3dB}=1$ Hz, 2 <sup>nd</sup> order Butterworth, high-pass								
Pmean±SD	-0.95±0.21	-1.00±0.00	-1.00±0.00	0.00±0.00	-348.57±17.37	-2.05±0.21	-4.00±0.00	-4.00±0.00
Pmaxd	-1	-1	-1	0	-426	-3	-4	-4
RRmean±SD	802.95±0.22	803.00±0.00	803.00±0.00	803.00±0.00	-	803.00±0.22	803.00±0.00	803.00±0.00
RRmaxd	1	0	0	0	-	1	0	0
VCD=65 ms, $f_{3dB}=2$ Hz, 2 <sup>nd</sup> order Butterworth, high-pass								
Pmean±SD	-2.00±0.00	-2.00±0.00	-2.00±0.00	0.00±0.00	-808.29±1.61	-4.00±0.00	-6.00±0.00	-7.00±0.00
Pmaxd	-2	-2	-2	0	-811	-4	-6	-7
RRmean±SD	803.00±0.00	803.00±0.00	803.00±0.00	803.00±0.00	-	803.00±0.00	803.00±0.00	803.00±0.00
RRmaxd	0	0	0	0	-	0	0	0
VCD=65 ms, $f_{3dB}=5$ Hz, 2 <sup>nd</sup> order Butterworth, high-pass								
Pmean±SD	33.00±0.00	31.00±0.00	30.00±0.00	30.00±0.00	-1286.48±1.33	27.00±0.00	28.00±0.00	30.00±0.00
Pmaxd	33	31	30	32	-1289	27	28	30
RRmean±SD	803.00±0.00	803.00±0.00	803.00±0.00	803.00±0.00	-	803.00±0.00	803.00±0.00	803.00±0.00
RRmaxd	0	0	0	0	-	0	0	0
VCD=65 ms, $f_{3dB}=10$ Hz, 2 <sup>nd</sup> order Butterworth, high-pass								
Pmean±SD	25.00±0.00	22.00±0.00	19.00±0.00	21.00±0.00	-1979.71±1.20	24.00±0.00	20.00±0.00	16.00±0.00
Pmaxd	25	22	19	21	-1982	24	20	16
RRmean±SD	803.00±0.00	803.00±0.00	803.00±0.00	803.00±0.00	-	803.00±0.00	803.00±0.00	803.00±0.00
RRmaxd	0	0	0	0	-	0	0	0

Appendix C/2) Legend in Appendix C/1

VCD=85 ms, f <sub>3dB</sub> =0.1 Hz, 2 <sup>nd</sup> order Butterworth, high-pass								
Pmean±SD	1.86±0.47	1.19±0.50	0.95±0.21	0.00±0.00	-281.10±56.73	-1.33±0.47	-1.95±0.21	-2.24±0.53
Pmaxd	2	2	1	0	-341	-2	-2	-3
RRmean±SD	803.10±0.30	803.05±0.38	803.05±0.22	803.00±0.00	-	803.00±0.32	803.00±0.22	802.95±0.38
RRmaxd	1	1	1	0	-	1	1	1
VCD=85 ms, f <sub>3dB</sub> =0.5 Hz, 2 <sup>nd</sup> order Butterworth, high-pass								
Pmean±SD	-0.95±0.21	-0.95±0.21	0.00±0.00	0.00±0.00	-276.19±7.84	-2.10±0.29	-3.00±0.00	-4.00±0.00
Pmaxd	-1	-1	0	0	-309	-3	-3	-4
RRmean±SD	803.00±0.32	803.00±0.32	803.00±0.00	803.00±0.00	-	803.05±0.22	803.00±0.00	803.00±0.00
RRmaxd	1	1	0	0	-	1	0	0
VCD=85 ms, f <sub>3dB</sub> =1 Hz, 2 <sup>nd</sup> order Butterworth, high-pass								
Pmean±SD	-1.95±0.21	-2.95±0.21	-2.00±0.00	0.00±0.00	-467.38±18.98	-4.00±0.00	-5.05±0.21	-7.00±0.00
Pmaxd	-2	-3	-2	0	-552	-4	-6	-7
RRmean±SD	802.95±0.22	802.95±0.22	803.00±0.00	803.00±0.00	-	803.00±0.00	803.05±0.22	803.00±0.00
RRmaxd	1	1	0	0	-	0	1	0
VCD=85 ms, f <sub>3dB</sub> =2 Hz, 2 <sup>nd</sup> order Butterworth, high-pass								
Pmean±SD	-3.00±0.00	-3.00±0.00	-3.00±0.00	0.00±0.00	-1003.38±1.17	-7.00±0.00	-10.00±0.00	-12.00±0.00
Pmaxd	-3	-3	-3	0	-1005	-7	-10	-12
RRmean±SD	803.00±0.00	803.00±0.00	803.00±0.00	803.00±0.00	-	803.00±0.00	803.00±0.00	803.00±0.00
RRmaxd	0	0	0	0	-	0	0	0
VCD=85 ms, f <sub>3dB</sub> =5 Hz, 2 <sup>nd</sup> order Butterworth, high-pass								
Pmean±SD	38.00±0.00	36.00±0.00	34.00±0.00	42.00±0.00	-1522±1.05	34.00±0.00	31.00±0.00	31.00±0.00
Pmaxd	38	36	34	42	-1524	34	31	31
RRmean±SD	803.00±0.00	803.00±0.00	803.00±0.00	803.00±0.00	-	803.00±0.00	803.00±0.00	803.00±0.00
RRmaxd	0	0	0	0	-	0	0	0
VCD=85 ms, f <sub>3dB</sub> =10 Hz, 2 <sup>nd</sup> order Butterworth, high-pass								
Pmean±SD	29.00±0.00	25.00±0.00	21.00±0.00	19.95±0.21	-2229.10±1.11	24.00±0.00	24.00±0.00	19.00±0.00
Pmaxd	29	25	21	20	-2232	24	24	19
RRmean±SD	803.00±0.00	803.00±0.00	803.00±0.00	803.00±0.32	-	803.00±0.00	803.00±0.00	803.00±0.00
RRmaxd	0	0	0	1	-	0	0	0

	Asc1/3	Asc1/2	Asc2/3	Peak	Amplitude	Desc2/3	Desc1/2	Desc1/3
VCD=115 ms, f <sub>3dB</sub> =0.1 Hz, 2 <sup>nd</sup> order Butterworth, high-pass								
Pmean±SD	2.05±0.84	1.86±0.47	1.43±0.58	0.00±0.00	-336.10±67.24	-1.91±0.29	-3.33±0.56	-4.05±0.65
Pmaxd	3	2	2	0	-411	-2	-4	-5
RRmean±SD	803.15±0.57	803.1±0.30	803.05±0.38	803.00±0.00	-	802.95±0.22	802.95±0.38	802.90±0.43
RRmaxd	2	1	1	0	-	1	1	1
VCD=115 ms, f <sub>3dB</sub> =0.5 Hz, 2 <sup>nd</sup> order Butterworth, high-pass								
Pmean±SD	-1.00±0.00	-1.00±0.00	-1.95±0.21	0.00±0.00	-347.81±9.98	-4.00±0.00	-6.00±0.00	-7.00±0.00
Pmaxd	-1	-1	-2	0	-385	-4	-6	-7
RRmean±SD	803.00±0.00	803.00±0.00	803.00±0.32	803.00±0.00	-	803.00±0.00	803.00±0.00	803.00±0.00
RRmaxd	0	0	1	0	-	0	0	0
VCD=115 ms, f <sub>3dB</sub> =1 Hz, 2 <sup>nd</sup> order Butterworth, high-pass								
Pmean±SD	-3.00±0.31	-3.95±0.21	-3.95±0.21	-1.00±0.00	-613.57±20.71	-6.48±0.50	-9.05±0.21	-12.05±0.21
Pmaxd	-4	-4	-4	-1	-706	-7	-10	-13
RRmean±SD	802.95±0.50	802.95±0.22	802.95±0.22	803.00±0.00	-	803.05±0.22	803.05±0.22	803.05±0.22
RRmaxd	2	1	1	0	-	1	1	1
VCD=115 ms, f <sub>3dB</sub> =2 Hz, 2 <sup>nd</sup> order Butterworth, high-pass								
Pmean±SD	-5.10±0.29	-7.00±0.00	-7.00±0.00	-1.00±0.00	-1332.33±1.45	-10.00±0.00	-16.00±0.00	-20.00±0.00
Pmaxd	-6	-7	-7	-1	-1335	-10	-16	-20
RRmean±SD	803.05±0.38	803.00±0.00	803.00±0.00	803.00±0.00	-	803.00±0.00	803.00±0.00	803.00±0.00
RRmaxd	1	0	0	0	-	0	0	0
VCD=115 ms, f <sub>3dB</sub> =5 Hz, 2 <sup>nd</sup> order Butterworth, high-pass								
Pmean±SD	46.00±0.00	42.00±0.00	37.00±0.00	42.76±0.43	-1866.38±1.13	44.00±0.00	37.00±0.00	31.00±0.00
Pmaxd	46	42	37	43	-1868	44	37	31
RRmean±SD	803.00±0.00	803.00±0.00	803.00±0.00	803.00±0.63	-	803.00±0.00	803.00±0.00	803.00±0.00
RRmaxd	0	0	0	1	-	0	0	0
VCD=115 ms, f <sub>3dB</sub> =10 Hz, 2 <sup>nd</sup> order Butterworth, high-pass								
Pmean±SD	37.00±0.00	31.00±0.00	24.00±0.00	18.76±0.42	-2489.19±1.22	19.00±0.00	16.00±0.00	15.00±0.00
Pmaxd	37	31	24	19	-2492	19	16	15
RRmean±SD	803.00±0.00	803.00±0.00	803.00±0.00	803.00±0.63	-	803.00±0.00	803.00±0.00	803.00±0.00
RRmaxd	0	0	0	1	-	0	0	0

Appendix D/1) Low-pass filtering ECG (VCD=65 ms). Legend in Appendix C/1.

	Asc1/3	Asc1/2	Asc2/3	Peak	Amplitude	Desc2/3	Desc1/2	Desc1/3
VCD=65 ms, f <sub>3dB</sub> =20 Hz, 4 <sup>th</sup> order Butterworth, low-pass								
Pmean±SD	12.00±0.00	12.00±0.00	12.00±0.00	13.10±0.29	-834.14±5.27	19.00±0.00	19.00±0.00	18.00±0.00
Pmaxd	12	12	12	14	-843	19	19	18
RRmean±SD	803.00±0.00	803.00±0.00	803.00±0.00	803.00±0.45	-	803.00±0.00	803.00±0.00	803.00±0.00
RRmaxd	0	0	0	1	-	0	0	0
VCD=65 ms, f <sub>3dB</sub> =40 Hz, 4 <sup>th</sup> order Butterworth, low-pass								
Pmean±SD	11.00±0.00	10.00±0.00	9.00±0.00	11.00±0.00	-331.76±3.69	13.00±0.00	11.00±0.00	11.00±0.00
Pmaxd	11	10	9	11	-337	13	11	11
RRmean±SD	803.00±0.00	803.00±0.00	803.00±0.00	803.00±0.00	-	803.00±0.00	803.00±0.00	803.00±0.00
RRmaxd	0	0	0	0	-	0	0	0
VCD=65 ms, f <sub>3dB</sub> =60 Hz, 4 <sup>th</sup> order Butterworth, low-pass								
Pmean±SD	6.00±0.00	6.00±0.00	6.00±0.00	7.05±0.21	-216.05±3.26	8.00±0.00	7.81±0.39	8.00±0.00
Pmaxd	6	6	6	8	-221	8	8	8
RRmean±SD	803.00±0.00	803.00±0.00	803.00±0.00	803.00±0.32	-	803.00±0.00	803.00±0.00	803.00±0.00
RRmaxd	0	0	0	1	-	0	0	0
VCD=65 ms, f <sub>3dB</sub> =80 Hz, 4 <sup>th</sup> order Butterworth, low-pass								
Pmean±SD	4.00±0.00	5.00±0.00	5.00±0.00	6.00±0.00	-201.52±1.56	6.00±0.00	6.00±0.00	5.00±0.00
Pmaxd	4	5	5	6	-204	6	6	5
RRmean±SD	803.00±0.00	803.00±0.00	803.00±0.00	803.00±0.00	-	803.00±0.00	803.00±0.00	803.00±0.00
RRmaxd	0	0	0	0	-	0	0	0
VCD=65 ms, f <sub>3dB</sub> =100 Hz, 4 <sup>th</sup> order Butterworth, low-pass								
Pmean±SD	4.00±0.00	4.00±0.00	4.00±0.00	5.00±0.00	-154.10±1.19	4.00±0.00	5.00±0.00	4.00±0.00
Pmaxd	4	4	4	5	-156	4	5	4
RRmean±SD	803.00±0.00	803.00±0.00	803.00±0.00	803.00±0.00	-	803.00±0.00	803.00±0.00	803.00±0.00
RRmaxd	0	0	0	0	-	0	0	0

	Asc1/3	Asc1/2	Asc2/3	Peak	Amplitude	Desc2/3	Desc1/2	Desc1/3
VCD=65 ms, f <sub>3dB</sub> =10 Hz, 4 <sup>th</sup> order Bessel, low-pass								
Pmean±SD	26.00±0.00	26.00±0.00	26.00±0.00	32.52±0.50	-1351.29±3.27	40.00±0.00	40.00±0.00	41.86±0.35
Pmaxd	26	26	26	33	-1357	40	40	42
RRmean±SD	803.00±0.00	803.00±0.00	803.00±0.00	803.00±0.55	-	803.00±0.00	803.00±0.00	803.00±0.55
RRmaxd	0	0	0	1	-	0	0	1
VCD=65 ms, f <sub>3dB</sub> =20 Hz, 4 <sup>th</sup> order Bessel, low-pass								
Pmean±SD	14.00±0.00	15.00±0.00	14.00±0.00	17.00±0.00	-673.29±1.61	19.81±0.39	19.00±0.00	18.00±0.00
Pmaxd	14	15	14	17	-676	20	19	18
RRmean±SD	803.00±0.00	803.00±0.00	803.00±0.00	803.00±0.00	-	803.05±0.59	803.00±0.00	803.00±0.00
RRmaxd	0	0	0	0	-	1	0	0
VCD=65 ms, f <sub>3dB</sub> =40 Hz, 4 <sup>th</sup> order Bessel, low-pass								
Pmean±SD	7.19±0.39	7.00±0.00	6.00±0.00	8.00±0.00	-367.71±2.14	10.00±0.00	9.00±0.00	10.00±0.00
Pmaxd	8	7	6	8	-371	10	9	10
RRmean±SD	803.00±0.00	803.00±0.00	803.00±0.00	803.00±0.00	-	803.00±0.00	803.00±0.00	803.00±0.00
RRmaxd	0	0	0	0	-	0	0	0
VCD=65 ms, f <sub>3dB</sub> =60 Hz, 4 <sup>th</sup> order Bessel, low-pass								
Pmean±SD	5.00±0.00	5.00±0.00	4.00±0.00	5.00±0.00	-271.81±1.50	7.00±0.00	6.00±0.00	7.00±0.00
Pmaxd	5	5	4	5	-275	7	6	7
RRmean±SD	803.00±0.00	803.00±0.00	803.00±0.00	803.00±0.00	-	803.00±0.00	803.00±0.00	803.00±0.00
RRmaxd	0	0	0	0	-	0	0	0
VCD=65 ms, f <sub>3dB</sub> =80 Hz, 4 <sup>th</sup> order Bessel, low-pass								
Pmean±SD	4.00±0.00	3.00±0.00	4.00±0.00	4.00±0.00	-179.33±0.78	5.00±0.00	5.00±0.00	5.00±0.00
Pmaxd	4	3	4	4	-181	5	5	5
RRmean±SD	803.00±0.00	803.00±0.00	803.00±0.00	803.00±0.00	-	803.00±0.00	803.00±0.00	803.00±0.00
RRmaxd	0	0	0	0	-	0	0	0
VCD=65 ms, f <sub>3dB</sub> =100 Hz, 4 <sup>th</sup> order Bessel, low-pass								
Pmean±SD	3.00±0.00	3.00±0.00	3.00±0.00	3.00±0.00	-145.76±0.97	4.00±0.00	4.00±0.00	4.00±0.00
Pmaxd	3	3	3	3	-147	4	4	4
RRmean±SD	803.00±0.00	803.00±0.00	803.00±0.00	803.00±0.00	-	803.00±0.00	803.00±0.00	803.00±0.00
RRmaxd	0	0	0	0	-	0	0	0

Appendix D/2) Low-pass filtering ECG (VCD=85 ms). Legend in Appendix C/1.

	Asc1/3	Asc1/2	Asc2/3	Peak	Amplitude	Desc2/3	Desc1/2	Desc1/3
VCD=85 ms, f <sub>3dB</sub> =20 Hz, 4 <sup>th</sup> order Butterworth, low-pass								
Pmean±SD	13.00±0.00	13.00±0.00	12.00±0.00	14.19±0.39	-678.00±5.27	20.00±0.00	19.00±0.00	18.00±0.00
Pmaxd	13	13	12	15	-686	20	19	18
RRmean±SD	803.00±0.00	803.00±0.00	803.00±0.00	803.00±0.45	-	803.00±0.00	803.00±0.00	803.00±0.00
RRmaxd	0	0	0	1	-	0	0	0
VCD=85 ms, f <sub>3dB</sub> =40 Hz, 4 <sup>th</sup> order Butterworth, low-pass								
Pmean±SD	10.00±0.00	10.00±0.00	9.19±0.39	12.00±0.00	-250.71±3.68	12.00±0.00	11.00±0.00	11.00±0.00
Pmaxd	10	10	10	12	-256	12	11	11
RRmean±SD	803.00±0.00	803.00±0.00	803.00±0.55	803.00±0.00	-	803.00±0.00	803.00±0.00	803.00±0.00
RRmaxd	0	0	1	0	-	0	0	0
VCD=85 ms, f <sub>3dB</sub> =60 Hz, 4 <sup>th</sup> order Butterworth, low-pass								
Pmean±SD	7.00±0.00	7.00±0.00	7.00±0.00	7.00±0.00	-182.95±3.40	7.00±0.00	8.00±0.00	7.43±0.50
Pmaxd	7	7	7	7	-189	7	8	8
RRmean±SD	803.00±0.00	803.00±0.00	803.00±0.00	803.00±0.00	-	803.00±0.00	803.00±0.00	803.00±0.00
RRmaxd	0	0	0	0	-	0	0	0
VCD=85 ms, f <sub>3dB</sub> =80 Hz, 4 <sup>th</sup> order Butterworth, low-pass								
Pmean±SD	4.00±0.00	4.00±0.00	4.00±0.00	5.00±0.00	-175.43±1.94	6.00±0.00	6.00±0.00	6.00±0.00
Pmaxd	4	4	4	5	-178	6	6	6
RRmean±SD	803.00±0.00	803.00±0.00	803.00±0.00	803.00±0.00	-	803.00±0.00	803.00±0.00	803.00±0.00
RRmaxd	0	0	0	0	-	0	0	0
VCD=85 ms, f <sub>3dB</sub> =100 Hz, 4 <sup>th</sup> order Butterworth, low-pass								
Pmean±SD	4.00±0.00	4.00±0.00	4.00±0.00	5.00±0.00	-105.71±1.35	5.00±0.00	5.00±0.00	5.00±0.00
Pmaxd	4	4	4	5	-108	5	5	5
RRmean±SD	803.00±0.00	803.00±0.00	803.00±0.00	803.00±0.00	-	803.00±0.00	803.00±0.00	803.00±0.00
RRmaxd	0	0	0	0	-	0	0	0

	Asc1/3	Asc1/2	Asc2/3	Peak	Amplitude	Desc2/3	Desc1/2	Desc1/3
VCD=85 ms, f <sub>3dB</sub> =10 Hz, 4 <sup>th</sup> order Bessel, low-pass								
Pmean±SD	27.00±0.00	27.00±0.00	26.00±0.00	33.50±0.21	-1070.33±3.20	40.00±0.00	40.00±0.00	39.71±0.45
Pmaxd	27	27	26	34	-1074	40	40	40
RRmean±SD	803.00±0.00	803.00±0.00	803.00±0.00	803.05±0.22	-	803.00±0.00	803.00±0.00	803.00±0.55
RRmaxd	0	0	0	1	-	0	0	1
VCD=85 ms, f <sub>3dB</sub> =20 Hz, 4 <sup>th</sup> order Bessel, low-pass								
Pmean±SD	15.00±0.00	14.00±0.00	14.00±0.00	16.62±0.49	-547.19±1.87	20.00±0.00	20.00±0.00	18.00±0.00
Pmaxd	15	14	14	17	-550	20	20	18
RRmean±SD	803.00±0.00	803.00±0.00	803.00±0.00	803.05±0.59	-	803.00±0.00	803.00±0.00	803.00±0.00
RRmaxd	0	0	0	1	-	0	0	0
VCD=85 ms, f <sub>3dB</sub> =40 Hz, 4 <sup>th</sup> order Bessel, low-pass								
Pmean±SD	7.19±0.39	7.00±0.00	7.00±0.00	8.00±0.00	-302.43±2.06	10.00±0.00	10.00±0.00	9.05±0.21
Pmaxd	8	7	7	8	-305	10	10	10
RRmean±SD	803.00±0.00	803.00±0.00	803.00±0.00	803.00±0.00	-	803.00±0.00	803.00±0.00	803.00±0.32
RRmaxd	0	0	0	0	-	0	0	1
VCD=85 ms, f <sub>3dB</sub> =60 Hz, 4 <sup>th</sup> order Bessel, low-pass								
Pmean±SD	5.00±0.00	5.00±0.00	5.00±0.00	6.00±0.00	-148.38±1.46	6.00±0.00	6.00±0.00	6.00±0.00
Pmaxd	5	5	5	6	-151	6	6	6
RRmean±SD	803.00±0.00	803.00±0.00	803.00±0.00	803.00±0.00	-	803.00±0.00	803.00±0.00	803.00±0.00
RRmaxd	0	0	0	0	-	0	0	0
VCD=85 ms, f <sub>3dB</sub> =80 Hz, 4 <sup>th</sup> order Bessel, low-pass								
Pmean±SD	3.00±0.00	3.00±0.00	3.00±0.00	4.00±0.00	-184.19±1.10	5.00±0.00	5.00±0.00	5.00±0.00
Pmaxd	3	3	3	4	-186	5	5	5
RRmean±SD	803.00±0.00	803.00±0.00	803.00±0.00	803.00±0.00	-	803.00±0.00	803.00±0.00	803.00±0.00
RRmaxd	0	0	0	0	-	0	0	0
VCD=85 ms, f <sub>3dB</sub> =100 Hz, 4 <sup>th</sup> order Bessel, low-pass								
Pmean±SD	3.00±0.00	3.00±0.00	3.00±0.00	4.00±0.00	-147.38±0.90	4.00±0.00	3.00±0.00	3.00±0.00
Pmaxd	3	3	3	4	-149	4	3	3
RRmean±SD	803.00±0.00	803.00±0.00	803.00±0.00	803.00±0.00	-	803.00±0.00	803.00±0.00	803.00±0.00
RRmaxd	0	0	0	0	-	0	0	0

Appendix D/3) Low-pass filtering ECG (VCD=115 ms). Legend in Appendix C/1.

	Asc1/3	Asc1/2	Asc2/3	Peak	Amplitude	Desc2/3	Desc1/2	Desc1/3
VCD=115 ms, $f_{3dB}=20$ Hz, 4 <sup>th</sup> order Butterworth, low-pass								
Pmean±SD	14.00±0.00	1.57±0.50	12.00±0.00	14.38±0.49	-511.57±5.46	20.00±0.00	20.00±0.00	18.00±0.00
Pmaxd	14	13	12	15	-520	20	20	18
RRmean±SD	803.00±0.00	803.00±0.55	803.00±0.00	803.00±0.55	-	803.00±0.00	803.00±0.00	803.00±0.00
RRmaxd	0	1	0	1	-	0	0	0
VCD=115 ms, $f_{3dB}=40$ Hz, 4 <sup>th</sup> order Butterworth, low-pass								
Pmean±SD	10.00±0.00	10.00±0.00	9.00±0.00	11.00±0.00	-200.76±4.01	12.00±0.00	12.00±0.00	11.00±0.00
Pmaxd	10	9	9	11	-207	12	12	11
RRmean±SD	803.00±0.00	803.00±0.00	803.00±0.55	803.00±0.00	-	803.00±0.00	803.00±0.00	803.00±0.00
RRmaxd	0	0	0	0	-	0	0	0
VCD=115 ms, $f_{3dB}=60$ Hz, 4 <sup>th</sup> order Butterworth, low-pass								
Pmean±SD	6.00±0.00	6.00±0.00	6.00±0.00	7.00±0.00	-163.86±3.36	7.00±0.00	7.14±0.35	7.43±0.50
Pmaxd	6	6	6	7	-169	8	8	7
RRmean±SD	803.00±0.00	803.00±0.00	803.00±0.00	803.00±0.00	-	803.00±0.00	803.00±0.00	803.00±0.00
RRmaxd	0	0	0	0	-	0	0	0
VCD=115 ms, $f_{3dB}=80$ Hz, 4 <sup>th</sup> order Butterworth, low-pass								
Pmean±SD	5.00±0.00	5.00±0.00	4.00±0.00	5.43±0.50	-150.67±1.55	6.00±0.00	5.00±0.00	6.00±0.00
Pmaxd	5	5	4	6	-153	6	5	6
RRmean±SD	803.00±0.00	803.00±0.00	803.00±0.00	803.00±0.50	-	803.00±0.00	803.00±0.00	803.00±0.00
RRmaxd	0	0	0	1	-	0	0	0
VCD=115 ms, $f_{3dB}=100$ Hz, 4 <sup>th</sup> order Butterworth, low-pass								
Pmean±SD	4.00±0.00	4.00±0.00	3.05±0.21	5.00±0.00	-129.43±1.68	4.00±0.00	5.00±0.00	5.00±0.00
Pmaxd	4	4	4	5	-132	4	5	5
RRmean±SD	803.00±0.00	803.00±0.00	803.00±0.00	803.00±0.00	-	803.00±0.00	803.00±0.00	803.00±0.00
RRmaxd	0	0	0	0	-	0	0	0

	Asc1/3	Asc1/2	Asc2/3	Peak	Amplitude	Desc2/3	Desc1/2	Desc1/3
VCD=115 ms, $f_{3dB}=10$ Hz, 4 <sup>th</sup> order Bessel, low-pass								
Pmean±SD	29.00±0.00	28.38±0.49	26.48±0.50	33.10±0.29	-805.33±3.21	41.00±0.00	39.00±0.00	38.00±0.00
Pmaxd	29	29	27	34	-810	41	39	38
RRmean±SD	803.00±0.00	802.95±0.59	802.95±0.59	803.00±0.45	-	803.00±0.00	803.00±0.00	803.00±0.00
RRmaxd	0	1	1	1	-	0	0	0
VCD=115 ms, $f_{3dB}=20$ Hz, 4 <sup>th</sup> order Bessel, low-pass								
Pmean±SD	15.00±0.00	14.52±0.50	12.00±0.00	16.86±0.35	-415.52±1.59	20.00±0.00	19.00±0.00	19.00±0.00
Pmaxd	15	15	13	17	-419	20	19	19
RRmean±SD	803.00±0.00	803.00±0.00	803.00±0.00	803.00±0.55	-	803.00±0.00	803.00±0.00	803.00±0.00
RRmaxd	0	0	0	1	-	0	0	0
VCD=115 ms, $f_{3dB}=40$ Hz, 4 <sup>th</sup> order Bessel, low-pass								
Pmean±SD	7.19±0.39	7.00±0.00	6.00±0.00	8.00±0.00	-250.43±1.89	10.38±0.49	9.00±0.00	9.00±0.00
Pmaxd	8	7	6	8	-253	11	9	9
RRmean±SD	802.95±0.50	803.00±0.00	803.00±0.00	803.00±0.00	-	803.00±0.55	803.00±0.00	803.00±0.00
RRmaxd	1	0	0	0	-	1	0	0
VCD=115 ms, $f_{3dB}=60$ Hz, 4 <sup>th</sup> order Bessel, low-pass								
Pmean±SD	5.00±0.00	5.00±0.00	5.00±0.00	5.00±0.00	-174.43±1.14	7.00±0.00	6.14±0.35	6.00±0.00
Pmaxd	5	5	5	5	-176	7	7	6
RRmean±SD	803.00±0.00	803.00±0.00	803.00±0.00	803.00±0.00	-	803.00±0.00	803.00±0.00	803.00±0.00
RRmaxd	0	0	0	0	-	0	0	0
VCD=115 ms, $f_{3dB}=80$ Hz, 4 <sup>th</sup> order Bessel, low-pass								
Pmean±SD	4.00±0.00	3.67±0.47	3.00±0.00	4.00±0.00	-142.67±0.94	5.00±0.00	5.00±0.00	5.00±0.00
Pmaxd	4	4	3	4	-145	5	5	5
RRmean±SD	803.00±0.00	803.00±0.00	803.00±0.00	803.00±0.00	-	803.00±0.00	803.00±0.00	803.00±0.00
RRmaxd	0	0	0	0	-	0	0	0
VCD=115 ms, $f_{3dB}=100$ Hz, 4 <sup>th</sup> order Bessel, low-pass								
Pmean±SD	3.00±0.00	3.00±0.00	3.00±0.00	4.00±0.00	-117.05±0.65	4.00±0.00	4.00±0.00	3.00±0.00
Pmaxd	3	3	3	4	-118	4	4	3
RRmean±SD	803.00±0.00	803.00±0.00	803.00±0.00	803.00±0.00	-	803.00±0.00	803.00±0.00	803.00±0.00
RRmaxd	0	0	0	0	-	0	0	0



**Appendix E) Butterworth and Bessel low-pass filtering 25 and 50% peak-to-peak amplitude AC interference corrupted ECG.**

VCD-ventricular complex duration, U – unfiltered i.e. before filtering, F – filtered, Mean±SD – mean RR-interval, and MaxD – maximal deviation from nominal value before and after filtering, Asc1/3, Asc1/2, Asc2/3 –at the actual height of the ascending slope, Peak –on the peaks of the ventricular complexes, Desc2/3, Desc1/2, Desc1/3 –at the actual height of the descending slope. Amplitude in mV, time values in ms.

	Asc1/3	Asc1/2	Asc2/3	Peak	Desc2/3	Desc1/2	Desc1/3
<b>VCD=85 ms, N=25%, <math>f_{3dB}=20</math> Hz, 4<sup>th</sup> order Butterworth, low-pass</b>							
Mean±SD U	803.00±3.98	803.00±3.98	803.00±4.34	803.00±5.53	803.00±4.67	803.00±3.85	803.00±3.87
Mean±SD F	803.00±1.18	803.00±0.55	803.00±1.10	803.00±3.27	803.00±0.78	803.00±1.00	803.00±1.10
MaxD U/F	10/3	10/1	11/2	13/8	11/1	9/2	10/2
<b>VCD=85 ms, N=25%, <math>f_{3dB}=40</math> Hz, 4<sup>th</sup> order Butterworth, low-pass</b>							
Mean±SD U	803.00±3.98	803.00±3.96	803.00±4.20	803.00±5.53	803.00±4.68	803.00±3.82	803.00±3.83
Mean±SD F	803.00±1.55	803.00±0.95	803.00±1.67	803.00±2.81	803.00±1.52	803.00±1.18	803.00±1.58
MaxD U/F	10/4	10/2	10/4	13/7	11/3	9/3	10/4
<b>VCD=85 ms, N=25%, <math>f_{3dB}=20</math> Hz, 4<sup>th</sup> order Bessel, low-pass</b>							
Mean±SD U	803.00±3.98	803.00±4.11	803.00±4.31	803.00±5.55	803.00±4.68	803.00±3.99	803.00±3.87
Mean±SD F	803.00±0.55	803.00±0.00	803.00±0.55	803.00±1.18	803.00±0.55	803.00±0.55	803.00±0.55
MaxD U/F	10/1	10/0	11/1	13/3	11/1	10/1	10/1
<b>VCD=85 ms, N=25%, <math>f_{3dB}=40</math> Hz, 4<sup>th</sup> order Bessel, low-pass</b>							
Mean±SD U	803.00±3.98	803.00±3.96	803.00±4.45	803.00±5.13	803.00±4.42	803.00±3.96	803.00±3.86
Mean±SD F	803.00±2.43	803.00±1.95	803.00±2.57	803.00±4.09	803.00±2.74	803.00±1.79	803.00±2.59
MaxD U/F	10/6	10/5	11/6	12/10	11/7	10/5	10/6
<b>VCD=85 ms, N=50%, <math>f_{3dB}=20</math> Hz, 4<sup>th</sup> order Butterworth, low-pass</b>							
Mean±SD U	803.00±4.92	803.00±5.35	803.00±5.51	803.00±6.33	803.00±5.37	803.00±5.24	803.00±4.93
Mean±SD F	803.00±2.74	803.00±1.92	803.00±2.05	803.00±5.06	803.00±2.35	803.00±1.87	803.00±2.21
MaxD U/F	12/7	13/5	14/5	15/12	13/6	13/4	12/5
<b>VCD=85 ms, N=50%, <math>f_{3dB}=40</math> Hz, 4<sup>th</sup> order Butterworth, low-pass</b>							
Mean±SD U	803.00±5.05	803.00±5.36	803.00±5.37	803.00±6.33	803.00±5.36	803.00±5.22	803.00±4.92
Mean±SD F	803.00±3.46	803.00±2.70	803.00±3.73	803.00±4.91	803.00±3.18	803.00±2.99	3.54
MaxD U/F	12/8	13/7	13/9	15/12	13/8	13/7	12/9
<b>VCD=85 ms, N=50%, <math>f_{3dB}=20</math> Hz, 4<sup>th</sup> order Bessel, low-pass</b>							
Mean±SD U	803.00±5.05	803.00±5.36	803.00±5.37	803.00±6.33	803.00±5.51	803.00±5.24	803.00±5.05
Mean±SD F	803.00±1.10	803.00±0.63	803.00±0.89	803.00±2.57	803.00±0.84	803.00±0.55	803.00±1.05
MaxD U/F	12/2	13/1	13/2	15/7	14/2	13/1	12/2
<b>VCD=85 ms, N=50%, <math>f_{3dB}=40</math> Hz, 4<sup>th</sup> order Bessel, low-pass</b>							
Mean±SD U	803.00±5.05	803.00±5.36	803.00±5.23	802.95±6.63	803.00±5.10	803.00±5.36	803.00±5.10
Mean±SD F	803.00±4.24	803.00±4.11	803.00±4.55	803.00±5.48	803.00±4.66	803.00±4.09	803.00±3.96
MaxD U/F	12/11	13/10	13/11	16/13	13/11	13/10	12/10

20 Hz 4<sup>th</sup> order Bessel calculated gain and phase at 50 Hz: -19.47 dB, -607.83°  
40 Hz 4<sup>th</sup> order Bessel calculated gain and phase at 50 Hz: -4.92 dB, -509.69°  
20 Hz 4<sup>th</sup> order Butterworth calculated gain and phase at 50 Hz: -31.84 dB, -658.63°  
40 Hz 4<sup>th</sup> order Butterworth calculated gain and phase at 50 Hz: -8.43 dB, -584.14°

**Appendix F/1) Butterworth and Bessel low-pass filtering 10% rms amplitude Gaussian noise corrupted ECG. RR-interval alterations of corrupted ECG signal consisting of 20 intervals after 4th order Butterworth or Bessel low pass filtering, measured at different points of the ventricular complexes.**

Nominal heart rate period: 803 ms. VCD – ventricular complex duration, U – unfiltered i.e. before filtering, F – filtered, Mean±SD – mean RR-interval, and MaxD – maximal deviation from nominal value before and after filtering, Asc1/3, Asc1/2, Asc2/3 –at the actual height of the ascending slope, Peak –on the peaks of the ventricular complexes, Desc2/3, Desc1/2. Desc1/3 – at the actual height of the descending slope. Amplitude in mV, time values in ms.

	Asc1/3	Asc1/2	Asc2/3	Peak	Desc2/3	Desc1/2	Desc1/3
VCD=85 ms, N=10%, f <sub>3dB</sub> =20 Hz, 4 <sup>th</sup> order Butterworth, low-pass							
Mean±SD U	803.05±1.60	802.90±2.05	803.00±2.10	802.90±2.10	803.10±2.84	803.05±2.44	802.90±1.58
Mean±SD F	803.00±0.45	803.00±0.67	803.00±0.00	803.00±0.45	803.00±0.32	803.00±0.45	803.00±0.00
MaxD U/F	3/1	4/1	4/0	5/1	7/1	5/1	3/0
VCD=85 ms, N=10%, f <sub>3dB</sub> =40 Hz, 4 <sup>th</sup> order Butterworth, low-pass							
Mean±SD U	803.15±2.01	803.00±2.88	802.90±1.45	803.05±1.96	803.00±3.47	803.00±2.12	803.00±2.12
Mean±SD F	803.00±0.00	803.00±0.78	803.05±0.59	802.95±0.50	802.95±0.59	803.00±0.32	803.00±0.45
MaxD U/F	3/0	6/1	3/1	6/1	10/1	4/1	4/1
VCD=85 ms, N=10%, f <sub>3dB</sub> =60 Hz, 4 <sup>th</sup> order Butterworth, low-pass							
Mean±SD U	803.10±2.30	803.05±2.56	803.00±2.78	803.00±2.28	803.10±3.00	803.00±1.84	802.90±2.05
Mean±SD F	803.00±0.55	803.00±0.45	803.00±0.71	803.00±0.00	803.00±0.63	803.00±0.55	802.95±0.59
MaxD U/F	5/1	5/1	6/1	5/0	6/1	4/1	4/1
VCD=85 ms, N=10%, f <sub>3dB</sub> =80 Hz, 4 <sup>th</sup> order Butterworth, low-pass							
Mean±SD U	803.15±2.20	803.05±2.80	803.10±3.19	803.20±2.29	802.95±2.16	802.95±2.44	803.00±2.07
Mean±SD F	803.00±0.55	803.05±0.50	803.05±0.67	803.00±0.55	802.95±0.59	803.00±0.63	802.95±0.50
MaxD U/F	6/1	5/1	6/1	6/1	5/1	5/1	6/1
VCD=85 ms, N=10%, f <sub>3dB</sub> =100 Hz, 4 <sup>th</sup> order Butterworth, low-pass							
Mean±SD U	803.10±2.30	803.05±2.22	803.00±2.78	803.00±2.28	803.10±3.00	803.00±1.84	802.95±2.36
Mean±SD F	803.00±0.71	803.05±0.50	803.05±0.67	803.00±0.55	803.00±0.71	803.00±0.55	802.95±0.67
MaxD U/F	5/1	5/1	6/1	5/1	6/1	4/1	5/1

VCD=85 ms, N=10%, f <sub>3dB</sub> =20 Hz, 4 <sup>th</sup> order Bessel, low-pass							
Mean±SD U	802.90±1.61	802.90±2.70	803.10±2.45	802.95±1.66	802.85±3.32	802.75±2.07	803.00±1.87
Mean±SD F	803.00±0.45	803.00±0.32	803.05±0.74	802.95±0.59	803.00±0.45	802.95±0.50	803.00±0.00
MaxD U/F	3/1	6/1	6/1	4/1	6/1	4/1	3/0
VCD=85 ms, N=10%, f <sub>3dB</sub> =40 Hz, 4 <sup>th</sup> order Bessel, low-pass							
Mean±SD U	803.10±1.00	803.20±2.29	802.80±3.17	802.90±2.97	803.10±2.77	803.05±2.01	803.20±2.69
Mean±SD F	803.00±0.00	803.00±0.45	803.00±0.84	803.00±0.00	803.00±0.00	803.00±0.55	802.95±0.67
MaxD U/F	2/0	5/1	7/1	6/0	6/0	4/1	5/1
VCD=85 ms, N=10%, f <sub>3dB</sub> =60 Hz, 4 <sup>th</sup> order Bessel, low-pass							
Mean±SD U	803.10±2.30	803.05±2.56	803.00±2.78	803.00±2.28	803.10±3.00	803.00±1.84	802.90±2.05
Mean±SD F	803.00±0.71	803.05±0.50	803.00±0.55	803.00±0.32	803.00±0.63	802.95±0.59	802.95±0.22
MaxD U/F	5/1	5/1	6/1	5/1	6/1	4/1	4/1
VCD=85 ms, N=10%, f <sub>3dB</sub> =80 Hz, 4 <sup>th</sup> order Bessel, low-pass							
Mean±SD U	802.90±1.61	802.90±2.70	803.10±2.45	802.95±1.66	802.85±3.32	802.75±2.07	803.00±1.97
Mean±SD F	803.00±0.84	803.00±0.63	803.05±0.74	803.00±0.55	803.00±0.45	803.00±0.55	802.95±0.22
MaxD U/F	3/1	6/1	6/1	4/1	6/1	4/1	3/1
VCD=85 ms, N=10%, f <sub>3dB</sub> =100 Hz, 4 <sup>th</sup> order Bessel, low-pass							
Mean±SD U	803.15±2.07	803.00±2.88	802.90±1.45	803.05±1.96	803.00±3.48	803.00±2.12	803.00±2.12
Mean±SD F	803.00±0.45	803.05±0.38	803.05±0.74	803.00±0.63	803.00±0.63	803.00±0.45	802.95±0.50
MaxD U/F	3/1	6/1	3/1	6/1	10/1	4/1	4/1

Appendix F/2) Butterworth and Bessel low-pass filtering 25% rms amplitude Gaussian noise corrupted ECG. Legend in Appendix E/1.

	Asc1/3	Asc1/2	Asc2/3	Peak	Desc2/3	Desc1/2	Desc1/3
VCD=85 ms, N=25%, f <sub>3dB</sub> =20 Hz, 4 <sup>th</sup> order Butterworth, low-pass							
Mean±SD U	803.05±5.96	802.90±3.36	803.10±3.56	803.35±3.32	803.20±6.28	803.15±4.08	803.10±5.77
Mean±SD F	802.95±0.59	802.05±0.81	802.95±0.50	803.00±0.71	803.05±0.67	803.00±0.71	803.00±0.78
MaxD U/F	10/1	9/1	9/1	7/2	13/2	11/1	10/2
VCD=85 ms, N=25%, f <sub>3dB</sub> =40 Hz, 4 <sup>th</sup> order Butterworth, low-pass							
Mean±SD U	802.85±5.03	803.15±3.12	802.80±3.46	802.95±4.35	803.25±5.33	802.95±4.87	803.15±4.23
Mean±SD F	803.00±0.63	802.95±0.87	802.95±1.02	803.00±0.71	803.00±1.00	803.05±1.07	803.05±1.02
MaxD U/F	9/1	8/2	8/2	10/1	10/2	10/2	10/2
VCD=85 ms, N=25%, f <sub>3dB</sub> =60 Hz, 4 <sup>th</sup> order Butterworth, low-pass							
Mean±SD U	803.15±5.23	803.00±4.52	803.45±5.06	803.55±6.99	803.30±7.96	803.40±9.52	803.00±4.46
Mean±SD F	803.00±0.84	802.95±0.97	802.95±1.02	802.95±0.87	802.95±1.32	803.00±1.14	803.00±0.89
MaxD U/F	12/2	13/2	11/2	20/2	20/3	26/2	10/2
VCD=85 ms, N=25%, f <sub>3dB</sub> =80 Hz, 4 <sup>th</sup> order Butterworth, low-pass							
Mean±SD U	803.15±5.23	803.00±4.52	803.45±5.06	803.55±6.99	803.30±7.96	803.40±9.52	803.00±4.46
Mean±SD F	803.05±1.07	802.95±0.97	803.00±1.05	803.00±0.95	803.00±1.52	803.00±1.00	803.00±0.95
MaxD U/F	12/2	13/2	11/2	20/2	20/3	26/2	10/2
VCD=85 ms, N=25%, f <sub>3dB</sub> =100 Hz, 4 <sup>th</sup> order Butterworth, low-pass							
Mean±SD U	802.65±4.46	802.80±6.19	802.70±5.92	802.75±4.01	802.80±4.64	802.90±3.30	802.80±3.14
Mean±SD F	803.00±1.23	802.90±0.94	803.00±0.95	802.95±1.07	803.00±1.55	803.05±1.20	803.00±1.05
MaxD U/F	9/2	18/2	16/2	13/3	12/3	8/3	9/2

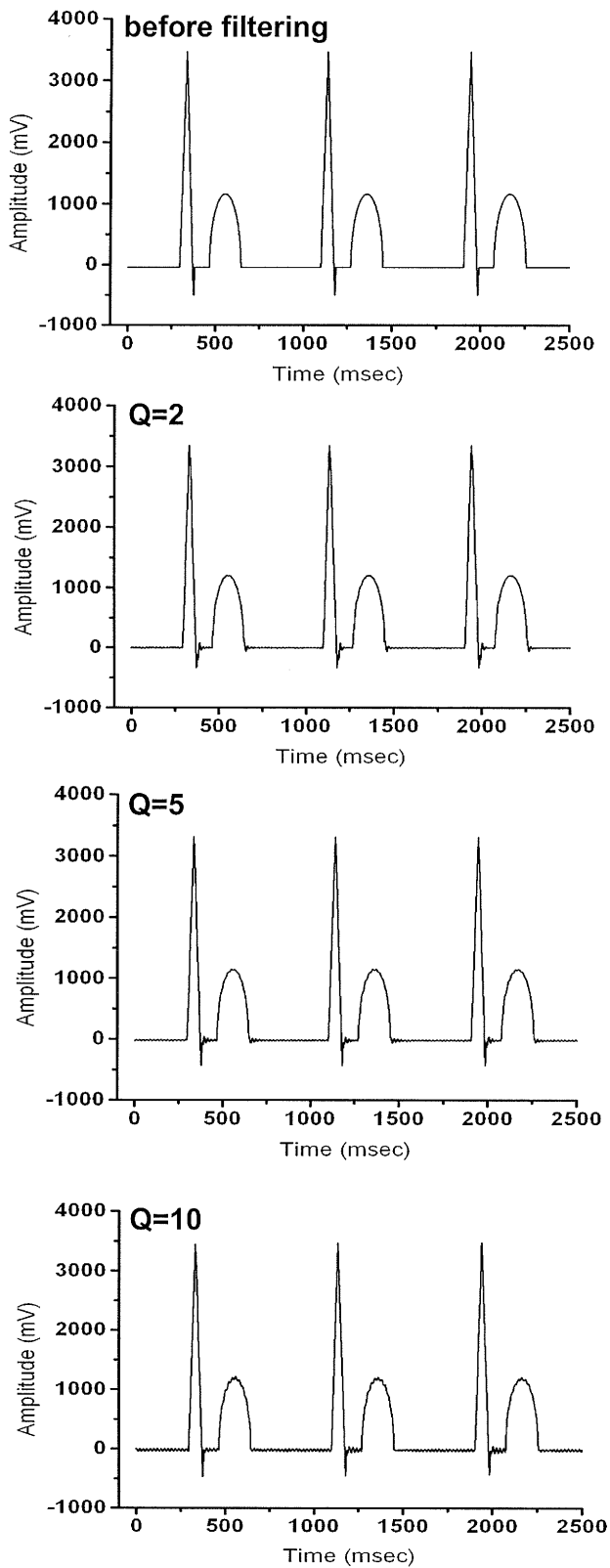
VCD=85 ms, N=25%, f <sub>3dB</sub> =20 Hz, 4 <sup>th</sup> order Bessel, low-pass							
Mean±SD U	802.65±3.97	802.80±6.09	802.70±5.49	802.75±4.01	802.80±4.64	802.95±3.31	802.80±3.96
Mean±SD F	802.95±0.67	803.00±0.45	802.95±0.74	803.00±0.95	803.05±0.67	803.00±0.78	803.00±0.63
MaxD U/F	6/1	18/1	16/1	13/2	12/1	8/1	11/1
VCD=85 ms, N=25%, f <sub>3dB</sub> =40 Hz, 4 <sup>th</sup> order Bessel, low-pass							
Mean±SD U	802.85±5.32	803.15±3.35	802.80±3.46	802.95±4.35	803.25±5.33	802.95±5.62	803.15±4.23
Mean±SD F	803.00±0.78	802.90±0.83	803.00±0.78	803.00±0.71	802.95±1.02	803.05±0.97	803.05±0.81
MaxD U/F	9/2	9/2	8/2	10/2	10/2	12/2	10/2
VCD=85 ms, N=25%, f <sub>3dB</sub> =60 Hz, 4 <sup>th</sup> order Bessel, low-pass							
Mean±SD U	802.70±7.19	802.60±4.27	802.70±4.71	802.65±3.72	802.65±4.77	803.25±4.29	803.15±4.65
Mean±SD F	803.00±1.14	802.90±1.00	803.00±0.84	803.00±0.55	802.95±1.56	803.05±0.81	803.00±1.18
MaxD U/F	19/2	10/2	11/1	9/1	9/3	10/1	9/3
VCD=85 ms, N=25%, f <sub>3dB</sub> =80 Hz, 4 <sup>th</sup> order Bessel, low-pass							
Mean±SD U	802.90±5.37	802.80±5.44	802.90±4.39	803.00±3.98	803.20±5.37	802.95±5.72	802.55±4.83
Mean±SD F	803.00±1.27	802.90±0.70	802.95±0.97	803.00±1.14	802.95±1.69	803.05±1.02	803.00±1.00
MaxD U/F	10/2	10/2	11/2	9/2	12/3	14/2	11/2
VCD=85 ms, N=25%, f <sub>3dB</sub> =100 Hz, 4 <sup>th</sup> order Bessel, low-pass							
Mean±SD U	802.65±4.64	802.80±6.09	802.70±5.63	802.75±4.01	802.80±4.64	802.90±3.30	802.80±3.14
Mean±SD F	803.00±1.27	802.85±1.06	803.00±1.00	802.95±1.24	802.90±1.61	803.05±1.07	803.00±1.05
MaxD U/F	9/3	18/2	16/2	13/3	12/3	8/2	9/2

Appendix F/3) Butterworth and Bessel low-pass filtering 50% rms amplitude Gaussian noise corrupted ECG. Legend in Appendix E/1.

	Asc1/3	Asc1/2	Asc2/3	Peak	Desc2/3	Desc1/2	Desc1/3
VCD=85 ms, N=50%, f <sub>3dB</sub> =20 Hz, 4 <sup>th</sup> order Butterworth, low-pass							
Mean±SD U	802.70±5.90	802.90±7.96	802.95±7.95	803.00±8.31	802.90±8.41	802.95±9.39	802.60±7.45
Mean±SD F	803.00±1.64	803.00±1.23	802.95±0.92	802.95±1.16	803.00±0.95	803.05±0.92	803.15±1.01
MaxD U/F	10/3	14/2	16/2	17/3	17/2	18/2	19/2
VCD=85 ms, N=50%, f <sub>3dB</sub> =40 Hz, 4 <sup>th</sup> order Butterworth, low-pass							
Mean±SD U	802.65±10.11	802.75±9.92	802.75±10.94	802.75±11.19	802.85±10.93	802.90±11.88	802.45±11.21
Mean±SD F	803.00±1.82	803.05±1.72	803.05±1.56	802.90±1.30	802.95±1.43	803.00±1.30	803.10±1.22
MaxD U/F	24/4	28/4	30/3	30/3	30/4	31/3	34/2
VCD=85 ms, N=50%, f <sub>3dB</sub> =60 Hz, 4 <sup>th</sup> order Butterworth, low-pass							
Mean±SD U	802.65±10.11	802.75±9.92	802.75±10.94	802.75±11.19	802.85±10.93	802.90±11.88	802.45±11.21
Mean±SD F	803.00±2.00	803.05±2.24	803.00±1.95	802.90±1.95	803.00±1.84	803.00±1.64	803.05±1.36
MaxD U/F	24/4	28/4	30/4	30/4	30/5	31/3	34/2
VCD=85 ms, N=50%, f <sub>3dB</sub> =80 Hz, 4 <sup>th</sup> order Butterworth, low-pass							
Mean±SD U	802.75±7.91	802.55±7.91	802.50±7.49	802.35±7.88	802.45±8.05	802.55±7.91	802.50±8.82
Mean±SD F	802.95±2.44	803.05±2.69	803.00±1.90	802.95±1.99	802.95±2.25	803.00±2.05	803.00±2.07
MaxD U/F	17/4	14/5	14/4	13/5	14/6	16/4	19/3
VCD=85 ms, N=50%, f <sub>3dB</sub> =100 Hz, 4 <sup>th</sup> order Butterworth, low-pass							
Mean±SD U	802.80±9.89	802.95±9.08	802.85±8.88	803.10±8.85	803.10±8.43	803.10±8.34	803.40±7.51
Mean±SD F	803.00±2.57	803.05±3.07	803.00±1.92	802.95±2.00	802.95±2.38	802.95±2.52	803.00±2.17
MaxD U/F	28/5	21/6	20/4	19/5	18/6	17/5	17/4

VCD=85 ms, N=50%, f <sub>3dB</sub> =20 Hz, 4 <sup>th</sup> order Bessel, low-pass							
Mean±SD U	803.03±6.45	802.90±8.53	803.15±8.09	803.15±7.81	803.15±7.57	803.20±7.62	803.05±5.47
Mean±SD F	803.00±1.55	803.00±1.00	803.00±0.84	802.90±1.18	803.00±0.95	803.05±1.02	803.05±1.02
MaxD U/F	14/3	22/2	22/1	21/3	21/2	22/2	13/2
VCD=85 ms, N=50%, f <sub>3dB</sub> =40 Hz, 4 <sup>th</sup> order Bessel, low-pass							
Mean±SD U	803.35±9.39	803.45±9.31	803.50±9.26	803.55±9.34	803.60±9.18	803.70±8.75	803.35±6.60
Mean±SD F	802.95±1.94	803.05±1.94	803.00±1.30	803.00±1.55	803.00±1.84	803.00±1.23	803.05±1.40
MaxD U/F	26/3	26/4	25/3	25/3	22/4	17/3	11/3
VCD=85 ms, N=50%, f <sub>3dB</sub> =60 Hz, 4 <sup>th</sup> order Bessel, low-pass							
Mean±SD U	802.65±10.11	802.75±9.92	802.75±10.94	802.75±11.19	802.85±10.93	802.90±11.88	802.45±11.21
Mean±SD F	803.00±2.03	803.05±2.36	803.00±1.58	802.95±1.88	803.00±1.82	802.95±1.63	803.05±2.00
MaxD U/F	24/4	28/5	30/3	30/4	30/4	31/4	34/3
VCD=85 ms, N=50%, f <sub>3dB</sub> =80 Hz, 4 <sup>th</sup> order Bessel, low-pass							
Mean±SD U	803.20±6.00	803.20±8.27	802.95±8.68	802.85±10.07	802.85±10.74	803.00±11.36	803.20±11.00
Mean±SD F	802.90±2.23	803.05±2.85	803.00±1.70	803.00±1.84	802.90±2.47	802.95±2.20	803.00±1.98
MaxD U/F	13/4	18/5	21/3	26/4	27/6	28/5	27/3
VCD=85 ms, N=50%, f <sub>3dB</sub> =100 Hz, 4 <sup>th</sup> order Bessel, low-pass							
Mean±SD U	803.35±9.39	803.45±9.31	803.50±9.26	803.55±9.34	803.60±9.18	803.70±8.75	803.35±6.60
Mean±SD F	803.05±2.29	803.15±3.12	803.00±1.84	803.00±2.26	802.90±2.51	802.95±2.38	803.00±1.90
MaxD U/F	26/5	26/6	25/4	25/5	22/6	17/5	11/3

Appendix G) AC notch filtering of the uncorrupted ECG signal.



**Appendix H)** Timing differences of uncorrupted artificial ECG signal consisting of 10 cycles after  $f=50$  Hz notch filtering ( $Q=2, 5, 10$ ) measured at different points of the ventricular complexes, expressed in ms relative to the appropriate point of the uncorrupted series.

HRP-heart rate period, VCD-ventricular complex duration, MaxD – maximal timing difference of the actual unfiltered and filtered records compared to uncorrupted records ( $n=10$  cycles), Asc1/3, Asc1/2, Asc2/3 – relative time points at the actual height of the ascending slope, Peak – relative time points at the peaks of the ventricular complexes, Desc2/3, Desc1/2, Desc1/3 – relative time points at the actual height of the descending slope.

	Asc1/3	Asc1/2	Asc2/3	Peak	Desc2/3	Desc1/2	Desc1/3
HRP=803 ms, VCD=65 ms, Q=2							
Mean±SD	1±0	1±0	0±0	0±0	4±0	2±0	1±0
MaxD	1	1	0	0	4	2	1
Q=5							
Mean±SD	1±0	1±0	0±0	0±0	2.2±0.422	1±0	0±0
MaxD	1	1	0	0	3	1	0
Q=10							
Mean±SD	0±0	0.2±0.422	0±0	0±0	1.3±0.483	0±0	-1±0
MaxD	0	1	0	0	2	0	-1
HRP=803 ms, VCD=85 ms, Q=2							
Mean±SD	1±0	0±0	0±0	0±0	3±0	2±0	2±0
MaxD	1	0	0	0	3	2	2
Q=5							
Mean±SD	0.7±0.483	0±0	0.4±0.516	0±0	1±0	0.6±0.516	1±0
MaxD	1	0	1	0	1	1	1
Q=10							
Mean±SD	0±0	0±0	0±0	0±0	0.2±0.422	0±0	0.7±0.483
MaxD	0	0	0	0	1	0	1
HRP=803 ms, VCD=115 ms, Q=2							
Mean±SD	1±0	1±0	0±0	0±0	2±0	2±0	2±0
MaxD	1	1	0	0	2	2	2
Q=5							
Mean±SD	0±0	0.9±0.316	0±0	0±0	1±0	1±0	1±0
MaxD	0	1	0	0	1	1	1
Q=10							
Mean±SD	0.7±0.483	1±0	0±0	0±0	0.2±0.422	-0.2±0.422	0±0
MaxD	1	1	0	0	1	-1	0

**Appendix I)** The influence of power line interference (N=5%, 10%, 25%, 50% peak-to-peak of maximal ventricular complex amplitude) and consecutive notch filtering on the accuracy and precision of ventricular complex detection.

Values are expressed in ms relative to the appropriate point of the uncorrupted series. HRP-heart rate period, VCD-ventricular complex duration, U – unfiltered, F – filtered, MaxD – maximal timing difference of the actual unfiltered/filtered records compared to uncorrupted records (n=10 cycles), Asc1/3, Asc1/2, Asc2/3 – relative time points at the actual height of the ascending slope, Peak – relative time points at the peaks of the ventricular complexes, Desc2/3, Desc1/2, Desc1/3 – relative time points at the actual height of the descending slope.

	Asc1/3	Asc1/2	Asc2/3	Peak	Desc2/3	Desc1/2	Desc1/3
<b>HRP=803 ms, VCD=85 ms, N=5%, Q=2</b>							
Mean±SD U	-0.6±0.843	-0.5±0.527	-0.3±1.252	0±0	-0.6±1.174	-0.2±0.632	0.3±0.823
Mean±SD F	1±0	0±0	0±0	0±0	3±0	2±0	2±0
MaxD U/F	-2/1	-1/0	-2/0	0/0	-2/3	-1/2	1/2
<b>Q=5</b>							
Mean±SD U	-0.4±0.843	-0.5±0.527	0.1±1.37	0±0	-0.6±1.174	-0.2±0.632	0.3±0.823
Mean±SD F	0±0	0±0	0±0	0±0	1±0	0±0	1±0
MaxD U/F	-2/0	-1/0	-2/0	0/0	-2/1	-1/0	1/1
<b>Q=10</b>							
Mean±SD U	0.2±0.789	0±0.667	0.2±1.229	0±0	0.2±1.135	0.5±0.527	1±0.816
Mean±SD F	0.5±0.527	0±0	0.4±0.516	0±0	0±0	0.5±0.527	1±0
MaxD U/F	-1/0	-1/0	-1/0	0/0	-1/1	0/0	2/1
<b>HRP=803 ms, VCD=85 ms, N=10%, Q=2</b>							
Mean±SD U	-0.3±1.567	-0.3±0.823	-0.2±2.486	0±0	-0.7±2.214	-0.3±1.252	1±1.633
Mean±SD F	1±0	0±0	0±0	0±0	3±0	2±0	2±0
MaxD U/F	-3/1	-1/0	-3/0	0/0	-4/3	-2/2	3/2
<b>Q=5</b>							
Mean±SD U	0.4±1.578	0±1.274	0.4±2.413	0±0	-0.7±2.214	-0.5±1.269	0.9±1.792
Mean±SD F	0.3±0.483	0±0	0.2±0.422	0±0	1±0	0±0	1±0
MaxD U/F	2/1	2/0	4/1	0/0	-4/1	-2/0	3/1
<b>Q=10</b>							
Mean±SD U	-0.3±1.567	-0.3±0.823	-0.2±2.486	0±0	-0.7±2.214	-0.3±1.252	1±1.633
Mean±SD F	0±0	0±0	0.1±0.316	0±0	0.4±0.516	0±0	0.7±0.483
MaxD U/F	-3/0	-1/0	-3/1	0/0	-4/1	-2/0	3/1
<b>HRP=803 ms, VCD=85 ms, N=25%, Q=2</b>							
Mean±SD U	0.6±2.875	0.9±3.178	1.3±4.668	1.6±3.921	-2.6±3.627	-3.3±3.561	0.4±3.134
Mean±SD F	1±0	0±0	0±0	0±0	3±0	2±0	2±0
MaxD U/F	-5/1	7/0	7/0	8/0	-7/3	-8/2	5/2
<b>Q=5</b>							
Mean±SD U	0.5±2.759	0.8±3.259	2±4.422	0.9±3.843	-2.6±3.627	-3.5±3.536	0.3±3.268
Mean±SD F	0±0	-1±0	0±0	0±0	1±0	0±0	1±0
MaxD U/F	-5/0	7/-1	7/0	7/0	-7/1	-8/0	5/1
<b>Q=10</b>							
Mean±SD U	0.9±3.035	1.1±3.213	2.4±4.477	1.7±3.917	-2.5±3.689	-3.2±3.425	0.3±3.268
Mean±SD F	0±0	0±0	0.1±0.316	0±0	0.7±0.483	0±0	0.5±0.527
MaxD U/F	-5/0	7/0	7/1	8/0	-7/1	-8/0	5/1
<b>HRP=803 ms, VCD=85 ms, N=50%, Q=2</b>							
Mean±SD U	6.2±4.077	7.8±4.917	6.8±4.566	2±4.69	-5±4.346	-7.7±4.111	-8.5±4.378
Mean±SD F	1±0	0±0	0±0	0±0	3±0	2±0	2±0
MaxD U/F	13/1	13/0	12/0	9/0	-12/3	-14/2	-14/2
<b>Q=5</b>							
Mean±SD U	5.8±4.131	7.5±5.191	6.4±4.6	1.2±4.59	-5.3±4.218	-8±4.243	-9.1±4.122
Mean±SD F	0±0	-1±0	-0.1±0.316	0±0	1±0	0±0	1±0
MaxD U/F	13/0	13/-1	11/-1	8/0	-12/1	-14/0	-14/1
<b>Q=10</b>							
Mean±SD U	6.2±4.077	7.9±5.043	6.8±4.566	2±4.69	-5±4.346	-7.7±4.111	-8.5±4.378
Mean±SD F	0±0	0±0	0±0	0±0	0.6±0.516	0±0	0.8±0.422
MaxD U/F	13/0	14/0	12/0	9/0	-12/1	-14/0	-14/1

**Appendix J)** The influence of ventricular complex duration (VCD=65 ms, 86 ms, and 115 ms) and power line interference (N=5%, 10%, 25%, and 50% peak-to-peak of maximal ventricular complex amplitude) on the accuracy and precision of ventricular complex detection. Filter Q=5 in all runs.

Values are expressed in ms relative to uncorrupted series. HRP-heart rate period, VCD-ventricular complex duration, U – unfiltered, F – filtered, MaxD – maximal difference between the actual unfiltered and filtered RR-series (n=9), Asc1/3, Asc1/2, Asc2/3 – relative time points at the actual height of the ascending slope, Peak – relative time points at the peaks of the ventricular complexes, Desc2/3, Desc1/2. Desc1/3 – relative time points at the actual height of the descending slope.

	Asc1/3	Asc1/2	Asc2/3	Peak	Desc2/3	Desc1/2	Desc1/3
HRP=803 ms, VCD=65 ms, Q=5, N=5%							
Mean±SD U	-0.3±0.483	0.6±0.516	-0.1±0.876	0±0	0.4±1.174	0.3±0.823	-0.3±0.483
Mean±SD F	0.9±0.316	1±0	0±0	0±0	2.6±0.516	1±0	0±0
MaxD U/F	-1/1	1/1	1/0	0/0	2/3	1/1	-1/0
N=10%							
Mean±SD U	0±0.816	0.7±1.418	-0.1±1.792	0±0	0.7±2.111	0.3±1.252	-0.2±0.789
Mean±SD F	1±0	1±0	0±0	0±0	2.8±0.422	1±0	0±0
MaxD U/F	1/1	3/1	3/0	0/0	3/3	2/1	-1/0
N=25%							
Mean±SD U	1.1±2.514	1.5±2.953	-0.1±3.695	0±3.944	0.7±4.165	0±3.432	-0.7±2.406
Mean±SD F	0.9±0.316	1±0	0±0	0±0	2.6±0.516	1±0	0±0
MaxD U/F	4/1	6/1	-5/0	7/0	-5/3	-6/1	-5/0
N=50%							
Mean±SD U	4.7±3.561	3.7±4.111	1.6±4.402	-0.7±5.187	-3.1±4.932	-3.7±4.968	-4.3±4.165
Mean±SD F	0±0	0.6±0.516	0±0	0±0	2±0	1±0	0±0
MaxD U/F	10/0	10/1	8/0	-8/0	-8/2	-10/1	-11/0
HRP=803 ms, VCD=85 ms, Q=5, N=5%							
Mean±SD U	-0.4±0.843	-0.5±0.527	0.1±1.37	0±0	-0.6±1.174	-0.2±0.632	0.3±0.823
Mean±SD F	0±0	0±0	0±0	0±0	1±0	0±0	1±0
MaxD U/F	-2/0	-1/0	-2/0	0/0	-2/1	-1/0	1/1
N=10%							
Mean±SD U	0.4±1.578	0±1.247	0.4±2.413	0±0	-0.7±2.214	-0.5±1.269	0.9±1.792
Mean±SD F	0.3±0.483	0±0	0.2±0.422	0±0	1±0	0±0	1±0
MaxD U/F	2/1	2/0	4/1	0/0	-4/1	-2/0	3/1
N=25%							
Mean±SD U	0.5±2.759	0.8±3.259	2±4.422	0.9±3.843	-2.6±3.627	-3.5±3.536	0.3±3.268
Mean±SD F	0±0	-1±0	0±0	0±0	1±0	0±0	1±0
MaxD U/F	-5/0	7/-1	7/0	7/0	-7/1	-8/0	5/1
N=50%							
Mean±SD U	5.8±4.131	7.5±5.191	6.4±4.6	1.2±4.59	-5.3±4.218	-8±4.243	-9.1±4.122
Mean±SD F	0±0	-1±0	-0.1±0.316	0±0	1±0	0±0	1±0
MaxD U/F	13/0	13/-1	11/-1	8/0	-12/1	-14/0	-14/1
HRP=803 ms, VCD=115 ms, Q=5, N=5%							
Mean±SD U	0.2±1.229	0.1±1.37	-0.1±0.876	0±0	0.3±0.823	0.1±1.37	0.4±1.35
Mean±SD F	0±0	1±0	0±0	0±0	1±0	1±0	1±0
MaxD U/F	2/0	-2/1	1/0	0/0	1/1	-2/1	2/1
N=10%							
Mean±SD U	0±2.404	-0.8±2.616	0.6±2.271	0.1±0.316	0.1±1.969	0.5±2.759	0.5±2.461
Mean±SD F	0±0	1±0	0±0	0±0	1±0	1±0	1±0
MaxD U/F	4/0	-4/1	4/0	1/0	-4/1	4/1	-4/1
N=25%							
Mean±SD U	1.3±3.974	2.8±4.022	3.6±4.061	-0.8±5.308	-3.1±4.254	-3.6±3.406	-1±4.163
Mean±SD F	0±0	1±0	0±0	0±0	1±0	1±0	1±0
MaxD U/F	8/0	7/1	10/0	-8/0	-10/1	-7/1	-8/1
N=50%							
Mean±SD U	11.3±4.715	12±4.619	9.6±5.542	-0.9±6.226	-11±5.292	-11.7±4.923	-11±4.472
Mean±SD F	0±0	1±0	0±0	0±0	1±0	1±0	1±0
MaxD U/F	17/0	20/1	17/0	-9/0	-18/1	-20/1	-16/1



## **Publications of the author**

### **Related articles of the author**

**Hejjel L**, Gal I: Heart rate variability analysis. *Acta Physiol Hung* 2001 (2002), 88:219-230

**Hejjel L**: Suppression of power-line interference by analog notch filtering in the ECG signal for heart rate variability analysis. To do or not to do? *Med Sci Monit* 2004, 10:MT6-MT13

**Hejjel L**, Roth E: What is the adequate sampling interval of the ECG signal for heart rate variability analysis in the time domain? *Physiol Meas* 2004, 25:1405-1411 (*IF*: 1.159)

**Hejjel L**, Kellenyi L: The corner frequencies of the ECG amplifier for heart rate variability analysis. *Physiol Meas* 2005, 26:39-47 (*IF*: 1.159)

### **Related citable abstracts of the author**

**Hejjel L**, Roth E: Chaos theory and its application to cardiology. *Perfusion* 2000, 8:360-361 (*IF*: 0.167)

**Hejjel L**: Impact of sampling frequency of the ECG on heart rate variability parameters in the time domain. *Cardiol Hung* 2002, S1:87 (*Hungarian*)

**Hejjel L**: The Poincaré-plot in heart rate variability analysis. *Acta Physiol Hung* 2002, 89:129

**Hejjel L**, Gal I: Heart rate variability analysis as a tool for quantifying the stress of the surgical team during laparoscopic versus open surgeries. *Eur J Surg Res* 2002, 34(S1):61 (*IF*: 0.706)

**Hejjel L**: Reappraising technical aspects of the ECG recording for HRV analysis. *ESH-BAVAR Congress Book*, 2004, 37

### **Related presentations of the author**

**Hejjel L**: Estimating stress by heart rate variability analysis. *XVII. Congress on Hungarian Experimental Surgery*, Szeged, September 16-18, 1999 (*Hungarian*)

**Hejjel L**: Chaos theory and its possible application in cardiology and cardiac surgery. *Danubian Forum of Cardiac Surgery*, Ostrawa, June 9-10, 2000

**Hejjel L**: Chaos theory and its application to cardiology. *III. International Symposium on Myocardial Cytoprotection*, Pecs, September 26-28, 2000 (*poster*)

**Hejjel L:** Impact of sampling frequency of the ECG on Heart rate variability parameters in the time domain. *Annual Meeting of the Hungarian Society of Cardiology*, Balatonfüred, Hungary, April 30-May 3, 2002 (Hungarian)

**Hejjel L, Gal I:** Heart rate variability analysis as a tool for quantifying the stress of the surgical team during laparoscopic versus open surgeries. *European Society for Surgical Research Congress*, Szeged, Hungary, May 23-25, 2002

**Hejjel L:** The Poincaré-plot in heart rate variability analysis. *4th International Congress of Pathophysiology*, Budapest, Hungary, June 29-July 5, 2002

**Hejjel L:** Reappraising technical aspects of the ECG recording for HRV analysis. *European Society of Hypertension, Meeting of the Working Group of Blood Pressure and Heart Rate Variability*, Angers, France, June 11-12, 2004 (poster)

**Hejjel L:** Technical pitfalls of heart rate variability analysis. *XI. Congress of the Hungarian Society of Cardiac Surgery*, Pécs, Hungary, November 4-6, 2004

### Other articles from the author

**Hejjel L, Vaszily M, Szabo Z, Peterffy A:** Alternatives to cardiac transplantation. *Orv Hetil* 1997, 138:1107-1111 (Hungarian)

Vaszily M, **Hejjel L, Peterffy A:** Dynamic cardiomyoplasty I. Theoretical background. *Cardiol Hung* 1997, 26(3):109-12 (Hungarian)

Vaszily M, **Hejjel L, Szeráfin T, Bodi A, Hermann K, Peterffy A:** Dynamic cardiomyoplasty II. Our experiences. *Cardiol Hung* 1997, 26(3):115-19 (Hungarian)

Gal I, Szivos J, Balint A, **Hejjel L, Györy I, Nagy B:** Laparoscopic gastric surgery. Early experiences. *Acta Chir Hung* 1999, 38(2):163-5

Gal I, Szivos J, **Hejjel L:** Laparoscopic truncal vagotomy, antrectomy, and Billroth-II reconstruction for complicated duodenal ulcer (case report and review of the literature). *Magy Seb* 1999, 52:81-84 (Hungarian)

**Hejjel L, Mecsek L, Szabo Z, Gal I:** Fatal mediastinitis following routine laparoscopic cholecystectomy. *Surg Endosc* 2000, 14(3):296, Epub.: 2000, February 12 (IF: 2.122)

**Hejjel L, Roth E:** Molecular, cellular and clinical aspects of myocardial ischaemia. *Orv Hetil* 2000, 141:539-546 (Hungarian, Lajos Markusovszky award of year 2000)

**Hejjel L, Kónyi A, Horváth I, Papp L:** Complex treatment of ischemic heart disease. *Cardiol Hung* 2001, 4:265-68 (Hungarian)

**Hejjel L, Roth E:** Myocardial preconditioning. Review. *Orv Hetil* 2002, 143:587-594 (Hungarian)

**Hejjel L, Donauer E, Lenárd L, Imre J, Simor T:** Treatment of atrial fibrillation with intraoperative radiofrequency ablation in one stage with valve surgery. *Magy Seb* 2004, 57:225-228 (Hungarian)

**Hejjel L, Komocsi A, Kónyi A, Lenárd L, Imre J, Papp L:** About the acute coronary syndrome in 2004. *Cardiol Hung* 2004, 34:194-200 (Hungarian)

Roth E, **Hejjel L**, Jaberansari MT, Jancso G: The role of free radicals in endogenous adaptation and intracellular signals. *Exp Clin Cardiol* 2004, 9:13-16

### **Other citable abstracts from the author**

**Hejjel L**, Roth E: Endogen adaptation mechanisms to ischaemia in the heart. *J Mol Cell Cardiol* 1999, 31:A97 (IF: 4.954)

**Hejjel L**, Roth E: Myocardial cytoprotection contra preconditioning. Clinical aspects. *Exp Clin Cardiol* 2003, 8:40

**Hejjel L**, Kellenyi L, Ajtay Z, Bartfai I, Solymos A, Jakab A, Stefanics G, Kovacs P, Bauer M, Nemeth A, Faludi B, Thuroczy G, Papp L: Assessment of open heart surgery-related brain injury by event-dependent evoked responses (reaction time). *Cardiol Hung* 2004, 34:D6 (Hungarian)

### **Book chapter**

Roth E, **Hejjel L**: Oxygen free radicals in heart disease. Novel therapies. In: Pugsley MK (Ed): Cardiac drug development guide, Humana Press, CA, 2003, 47-66

### **Acknowledgements**

I am grateful to my former chief, Istvan Gal, MD, PhD, who inspired and allowed me to start PhD education in Pecs as a corresponding student. I express my sincere thanks to Elizabeth Roth, MD, DSc for her attentive tutorship. She assured me freedom to investigate my own ideas. Special thanks to Lorand Kellenyi, MSc, PhD qualified electrical engineer for his practical advices and for the overnight professional conversations. I am beholden to my present chief, Lajos Papp, MD, DSc for supporting my ambitions and scientific work. I am thankful to my family for their solicitude and encouragement. Thanks to my friend, Zoltan Kovacs for his assistance at the initial stages of my research and to the Burr-Brown Corporation for the sample electronic parts.